### TWO PARTNERS OF THE RIBOSOME, EF-TU AND LEPA

### **EVELINA INES DE LAURENTIIS**

B.Sc. University of Lethbridge, 2007

### A Thesis

Submitted to the School of Graduate Studies

of the University of Lethbridge

in Partial Fulfilment of the

Requirements for the Degree

## **MASTER OF SCIENCE**

Department of Chemistry and Biochemistry

University of Lethbridge

LETHBRIDGE, ALBERTA, CANADA

© Evelina I. De Laurentiis, 2009

#### Abstract

The translational GTPases elongation factor Tu (EF-Tu) and LepA modulate the dynamics of tRNA on the ribosome. EF-Tu facilitates the delivery of aminoacyl-tRNA (aa-tRNA) to the translating ribosome and LepA catalyzes the retro-translocation of tRNA•mRNA from the E- and P-sites of the ribosome back to the P- and A-sites. Although an increasing body of structural and biochemical information is available, little is known about the functional cycle of LepA during retro-translocation, the kinetics of EF-Tu dissociation from the ribosome and the rate of EF-Tu conformational change during aa-tRNA delivery. This thesis reports the successful construction and biochemical characterisation of a mutant form of EF-Tu from *Escherichia coli* ideal for the specific incorporation of fluorescent labels, enabling measurements pivotal for uncovering the rate of EF-Tu conformational change and dissociation from the ribosome. Furthermore, to determine structural components critical for LepA's function, mutant versions of the protein were constructed and biochemically characterised.

#### **Acknowledgements**

I would like to thank my supervisor, Dr. Hans-Joachim Wieden, for all the mentoring and patience through the years. He has given me a wonderful opportunity to learn and teach others in a field that is challenging, yet rewarding. Most of all, I thank him for always pushing me to be a better in everything that I do.

Thank you to my committee members, especially Dr. Ute Kothe, who have lent helpful advice in my work, and have contributed to my knowledge.

Thank you to the Wieden lab, and all the members that have made this work possible. They have not only been my coworkers, spending long hours in the lab, but are life-long friends that have made an impression on my work and life.

Lastly, I would like to thank my family. I would especially like to thank my mother, father and sister, for supporting me and guiding me in all my decisions.

# **Table of Contents**

List of	f Tables	vii
List of	f Figures	ix
List of	f Abbreviations	x
Chapt	er 1 - Translation in bacteria	1
1.1	Introduction to translation in bacteria	1
1.2	The ribosome	4
1.3	Translation initiation	9
1.4	The elongation cycle	. 12
1.5	Translation termination and recycling	. 19
Obj	jectives	. 21
Chapt	er 2 – Elongation Factor Tu (EF-Tu)	. 23
2.1	Introduction to EF-Tu	. <b>2</b> 3
2.2	Material and Methods	.33
2	2.2.1 Molecular biology	. 34
2	2.2.2 Protein expression	. 37
2	2.2.3 Protein purification	.38
2	2.2.4 Preparation of nucleotide free EF-Tu	.38
2	2.2.5 Preparation of EF-Tu•mant-GTP/mant-GDP	.39
	2.2.6 Rapid kinetic measurement	
2	2.2.7 Preparation of [ <sup>14</sup> C]Phe-tRNA <sup>Phe</sup>	.40
	2.2.8 Hydrolysis protection of the aminoacyl-ester bond	
	2.2.9 Ribosome preparation	
	2.2.10 Ternary complex binding to the 70S ribosome	
	2.2.11 Fluorescent labelling of EF-Tu L264C	
_	2.2.12 Analysis of fluorescently labelled EF-Tu	. 45

2.3 Results	45
2.3.1 Activity of cysless EF-Tu	45
2.3.2 Fluorescent labelling of EF-Tu L264C using 1,5-IAEDANS	50
2.3.3 Analysis of fluorescently labelled EF-Tu L264C	53
2.3.4 Mutagenesis performed on EF-Tu	56
2.4 Discussion and future directions	57
2.5 Conclusion	61
Chapter 3 - LepA	62
3.1 Introduction to LepA	62
3.2 Materials and Methods	67
3.2.1 LepA Cloning	67
3.2.2 Mutagenesis	70
3.2.3 Protein expression	72
3.2.4 LepA Protein purification	73
3.2.5 Protein purification of LepA mutants	74
3.2.6 Nucleotide hydrolysis assay	74
3.2.7 Equilibrium binding constants for guanine nucleotide binding to LepA	75
3.2.8 Retro/forward translocation of tRNA on the ribosome	77
3.2.9 Ribosomal subunit dissociation	78
3.3 Results	79
3.3.1 Guanine nucleotide binding properties of LepA	79
3.3.2 GTPase activity of LepA in the presence of 70S ribosomes	81
3.3.3 Retro/Forward-translocation in the presence of LepA	84
3.3.4 Ribosomal subunit dissociation	92
3.4 Discussion and future directions	93
3.5 Conclusion	97

References	98
Appendix	
, p p =	

## **List of Tables**

Table 2.1: EF-Tu mutagenesis primers
Table 2.2: Quickchange mutagenesis PCR protocol for engineering EF-Tu C81M, C81A and C81S on a two-cysless background
Table 2.3: Components used for mutagenesis of EF-Tu
Table 2.4: Quickchange mutagenesis protocol for generating L264C and T361C EF-Tu mutants. 37
Table 2.5: Quickchange mutagenesis protocol for generating L264C/T34C EF-Tu mutant37
Table 2.6: Association and dissociation constants of mant guanine nucleotides to EF-Tu 46
Table 3.1: Components used to isolated and amplify the <i>lepA</i> gene in <i>E. coli</i>
Table 3.2: PCR protocol used to isolate and amplify the <i>lepA</i> gene in <i>E. coli</i>
Table 3.3: Primers used to generate <i>lepA</i> mutants
Table 3.4: PCR protocol used to engineer the CTD truncation mutants ( $\Delta$ A494, $\Delta$ P520, $\Delta$ G555).71
Table 3.5: PCR components used to engineer the CTD truncation mutants ( $\Delta A494$ , $\Delta P520$ , $\Delta G555$ )
Table 3.6: Quickchange mutagenesis protocol used to generate the H81A LepA substitution mutant
Table 3.7: Quickchange mutagenesis components for generating the H81A LepA substitution72
Table 3.8: Equilibrium binding constants of mant-GTP/GDP for LepA and LepA mutations81
Table 3.9: Retro-Translocation assay in the presence and absence of LepA, various guanine nucleotides and LepA mutants

# **List of Figures**

Figure 1.1: Secondary structure of tRNA	2
Figure 1.2: Tertiary structure of tRNA <sup>Phe</sup> from yeast	3
Figure 1.3: The three tRNA binding sites on ribosome	5
Figure 1.4: 30S ribosomal subunit from <i>Thermus thermophilus</i>	7
Figure 1.5: 50S ribosomal subunit from <i>E. coli</i> .	9
Figure 1.6: Translation initiation in bacteria	. 12
Figure 1.7: The Elongation cycle in bacteria.	. 13
Figure 1.8: Kinetic scheme of EF-Tu dependent A-site binding	. 15
Figure 1.9: Peptide bond formation	. 17
Figure 1.10: Translocation of tRNAs and mRNA within the ribosome	. 18
Figure 1.11: Translation termination and ribosome recycling	. 20
Figure 2.1: Nucleotide dependent changes in the tertiary structure of EF-Tu	. 24
Figure 2.2: Ternary complex of EF-Tu•GTP•aa-tRNA	. 25
Figure 2.3: EF-Tu in complex with EF-Ts	. 27
Figure 2.4: Efficiency of fluorescence resonance energy transfer as a function of distance	. 29
Figure 2.5: Reaction scheme for the covalent labelling of proteins with thiol reactive fluorescendyes	
Figure 2.6: Cysteines present in <i>E. coli</i> EF-Tu	.31
Figure 2.7: EF-Tu multiple sequence alignment.	.33
Figure 2.8: Hydrolysis protection assay of the aminoacyl-ester bond in [14C]Phe-tRNAPhe	.47
Figure 2.9: Percentage of [ <sup>14</sup> C]Phe-tRNA <sup>Phe</sup> delivered to the ribosomal A-site by EF-Tu•GTP	.49
Figure 2.10: Percentage of pre-translocation complex in the presence of EF-Tu determined by nitrocellulose filtration.	
Figure 2.11: Chemical structure of 1.5-IAFDANS	51

Figure 2.12: SEC purification elution profile of fluorescently labelled 1,5-IAEDANS EF-Tu L264C
Figure 2.13: Distance changes between Leu 264 and Trp 185 in <i>E. coli</i> EF-Tu in the GDP or GTP bound conformation
Figure 2.14: Fluorescence spectrum of 1,5-IAEDANS labelled L264C EF-Tu54
Figure 2.15: Fluorescence spectra of 1,5-IAEDANS labelled EF-Tu L264C with GTP or GDP bound.
Figure 2.16: Distance changes upon EF-Tu conformational change between Leu 264 and Thr 34 on domain I of EF-Tu
Figure 2.17: Residue Thr 361 in domain III of EF-Tu.
Figure 2.18: Cys 81 is in close proximity to the acceptor stem of aa-tRNA59
Figure 2.19: Leu 264 in EF-Tu is in close proximity to the 30S subunit during A-site binding 61
Figure 3.1: Domain alignment of LepA, EF-Tu and EF-G
Figure 3.2: Comparison of LepA and EF-G structures64
Figure 3.3: Secondary structure LepA CTD64
Figure 3.4: Retro-translocation of tRNA-mRNA within the ribosome
Figure 3.5: Mant-GTP76
Figure 3.6: Equilibrium dissociation constants of mant-GTP/GDP to LepA81
Figure 3.7: Ribosome stimulated GTPase activity of LepA and LepA mutants83
Figure 3.8: Michaelis–Menten analysis of LepA and EF-G ribosome stimulated GTP hydrolysis. 84
Figure 3.9: Retro-translocation of [ <sup>3</sup> H]fMet[ <sup>14</sup> C]Phe-tRNA <sup>Phe</sup> in the presence and absence of LepA and guanine nucleotides
Figure 3.10: Retro-translocation of [ <sup>3</sup> H]fMet[ <sup>14</sup> C]Val-tRNA <sup>Val</sup> in the presence and absence of LepA and guanine nucleotides
Figure 3.11: Forward translocation in the presence and absence of LepA90
Figure 3.12: Retro-translocation in the presence of LepA mutants
Figure 3.13: 70S dissociation measured by light scattering93

### **List of Abbreviations**

1,5-IAEDANS 5-((2-[(iodoacetyl)amino]ethyl)amino)naphthalene-1-sulfonic acid

aa-tRNA Aminoacyl-transfer ribonucleic acid

Abs Absorbance

ALS Alkaline lysis solution

AMP Adenosine monophosphate

Cryo-EM Cryo-electron microscopy

CTD C-terminal domain

DNA Deoxyribonucleic acid

dpm Decays per minute

EDTA Ethylenediaminetetraacetic acid

EF Elongation factor

fMet Formylmethionine

FRET Fluorescence Resonance Energy Transfer

GAF GTPase-activating factor

GDP Guanosine-5'-diphosphate

GEF Guanine nucleotide exchange factor

GTP Guanosine-5'-triphosphate

IF Initiation factor

IPTG Isopropyl β-D-1-thiogalactopyranoside

K<sub>D</sub> Equilibrium dissociation constant

LepA Leader peptidase A

mRNA Messenger ribonucleic acid

MWCO Molecular weight cut-off

nt Nucleotide

OAc Acetate

OD Optical density

PDB Protein Data Bank

PEP Phospho-enol-pyruvate

P<sub>i</sub> Phosphate

PK Pyruvate Kinase

PP<sub>i</sub> Pyrophosphate

PTC Peptide transferase center

PMSF Phenylmethanesulphonylfluoride

RF Recycling factor

RNase Ribonuclease

RNP Ribonucleoprotein

RRF Ribosome recycling factor

rRNA Ribosomal ribonucleic acid

SD Shine Dalgarno

SDS PAGE Sodium dodecyl sulfate polyacrylamide gel electrophoresis

SEC Size exclusion chromatography

TCA Trichloroacetic acid

tRNA Transfer ribonucleic acid

#### Chapter 1 - Translation in bacteria

#### 1.1 Introduction to translation in bacteria

Protein synthesis is one of the key processes in all living cells. It is part of the central dogma of gene expression, which was discussed in 1961 by Jacob and Monod (1). They showed that genes are expressed in two stages: i) Transcription - DNA is transcribed into messenger RNA (mRNA) and (ii) Translation - mRNA directed synthesis of the protein polypeptide chain, which utilizes a message containing triple nucleotide (triplet) codons specific for a single amino acid (1). In prokaryotes the transcribed mRNA is used directly as a message for subsequent protein synthesis (2).

The process of gene expression is facilitated by intermediate steps and many key players. In 1966, Crick hypothesized that there are RNA adaptor molecules that recognize a specific mRNA codon and contain the corresponding amino acid subsequently used in polypeptide chain synthesis (3). In this way, the molecule bridges the gap between the mRNA and the protein polypeptide chain (3). Around the same time of Crick's hypothesis, Zamecnik and Hoagland found that [14C] labelled amino acids attached to a small RNA were transferred to a growing polypeptide chain (4). There are approximately 30 different transfer RNAs (tRNAs) within prokaryotes (5) which are amino acid specific and have been studied extensively over the last 50 years in terms of processing, dynamics and structure.

Each tRNA contains between 75 to 90 RNA nucleotides (6) and forms a cloverleaf secondary structure (7, 8) (Figure 1.1). While diverse in sequence, determination of the structure of tRNA revealed a number of common elements between various tRNAs. These are (i) a 5'-terminal phosphate, (ii) a 3' acceptor stem, (iii) the so called D loop, containing a modified dihydrouridine

base, (iv) the anticodon loop, which can base pair with the mRNA triplet codon, (v) the T $\Psi$ C loop, which contains a pseudouridine and (vi) a variable loop which varies in length between tRNAs (8, 9).

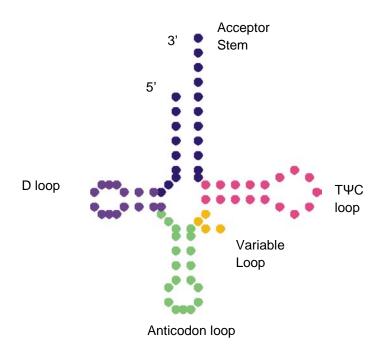


**Figure 1.1: Secondary structure of tRNA.** The cloverleaf structure of a typical tRNA showing the 3' acceptor stem (blue), TΨC loop (pink), anticodon loop (green), D loop (purple), variable loop (yellow).

The elements of the secondary structure fold into an L-shaped tertiary conformation (8, 9). At opposite ends of the tRNA are the anticodon loop and the acceptor stem, approximately 76 Å apart, whereas the D and T loops form the elbow region of the tRNA (Figure 1.2) (8, 9). The L-shape of the tRNA facilitates the contacts made during protein synthesis. For example, the anticodon loop of the tRNA can interact with the mRNA, while the amino acid on the acceptor stem can make contacts near the polypeptide chain.

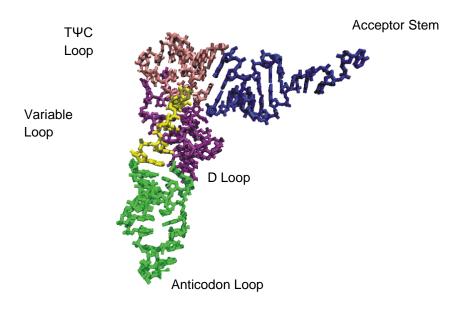


Figure 1.2: Tertiary structure of tRNA<sup>Phe</sup> from yeast. The crystal structure was determined by Sussman *et al.* (1978), PDB: 6TNA (8). The anticodon loop (green), the D loop (purple), the variable loop (yellow), the TΨC loop (pink) and the acceptor stem (blue) are shown above.

Not only do tRNAs differ in their anticodon loop but other so called discriminator bases (10, 11) help to distinguish them from each other during for example aminoacylation. Aminoacylation of tRNA requires tRNA synthetases specific for individual tRNAs and takes place in a two-step process (12, 13). First, the amino acid is activated with ATP on the tRNA synthetase, forming amino acid-adenosine monophosphate (AMP). In the second step, the activated amino acid is then transferred from the AMP to the tRNA (12, 13), resulting in the following overall aminoacylation reaction:

Amino acid + tRNA + ATP  $\leftrightarrow$  aminoacyl-tRNA + AMP + PP<sub>i</sub>.

Errors introduced by mis-aminoacylation can have severe downstream effects, such as cell growth and protein function (14). Therefore, aa-tRNA synthetases use a double-sieve mechanism to help prevent errors which may propagate into all synthesized proteins. The first strategy aminoacyl-tRNA (aa-tRNA) synthetases use to ensure correct aminoacylation is by restricting the size of the binding pocket for the specific amino acid. However, many amino acids are very similar in size to one another or smaller and cannot be excluded by this mechanism alone. Therefore, extra proofreading is needed to ensure translational fidelity. Proofreading of the aa-tRNA occurs through binding of the 3' end of aa-tRNA to a specific editing domain of the tRNA synthetase (15). The editing domain makes additional interactions with the R group of the amino acid (15), allowing for discrimination of similar sized amino acids.

Following the aminoacylation of tRNA, elongation factor Tu (EF-Tu) binds to the formed aa-tRNA and facilitates its delivery to the translating ribosome (16).

### 1.2 The ribosome

Protein synthesis takes place on the ribosome, which is a ribonucleoprotein (RNP) (17). It contains three tRNA binding sites, the A-site for aa-tRNA, the P-site for peptidyl-tRNA and the E-site for deacyl-tRNA (Figure 1.3) (18, 19).

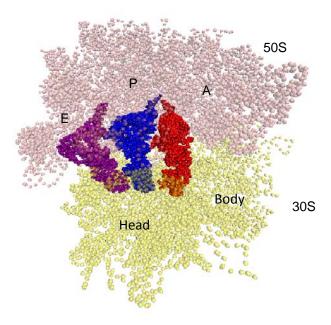


**Figure 1.3:** The three tRNA binding sites on ribosome. The 70S ribosome with three occupied tRNA binding sites was solved through cryo-electron microscopy (cryo-EM) from *Thermus thermophilus* by Yusupov *et al.* (2001), PDB 1GIX and 1GIY (20). tRNA binding sites are shown with respective tRNAs bound to the ribosome, A-site tRNA (red), P-site tRNA (blue) and E-site tRNA (purple). The 30S subunit is represented in yellow and the 50S subunit is represented in pink.

The ribosome is essential for the cell and encompasses 30% of the cellular mass in bacteria and approximately 5% in eukaryotes (21). In *Escherichia coli*, the ribosome has a mass of 2.5 MDa and a sedimentation coefficient of 70S (22). It is composed of a large and a small subunit, each made of approximately two-thirds ribosomal RNA (rRNA) and one-third protein (23). The small 30S subunit in *E. coli* contains a 1542 nucleotide 16S rRNA and 21 ribosomal proteins, the large 50S subunit consists of a 2904 nucleotide 23S rRNA, a 115 nucleotide 5S rRNA and 34 proteins (reviewed in (24)). Prior to ribosome assembly 16S and 23S rRNA are processed by RNase III (25),

RNase E, RNase G (26) and RNase T (27), to form a mature 16S and 23S rRNA. To ensure an active ribosome, all rRNA and ribosomal proteins must assemble in the correct manner (28). Self-assembly can occur *in vitro* in the absence of co-factors, but the required conditions are not physiologically relevant and self-assembly does not occur at a rate fast enough to sustain life (29). Further evidence suggests that several additional ribosomal biogenesis factors monitor the assembly of the ribosome, such as EngA (30) and ObgA (31), which are required for the fast and efficient assembly observed *in vivo*.

Electron microscopic studies on the structure of the ribosome have been available since the 1970s; however, it was not until 1999 that X-Ray crystallographic structures of the ribosome became available (32). The overall structure of the small ribosomal subunit is largely determined by the 16S rRNA and forms three domains (5' domain, central domain and 3' major domain) which form the body, platform and head of the 30S subunit (Figure 1.4) (33).

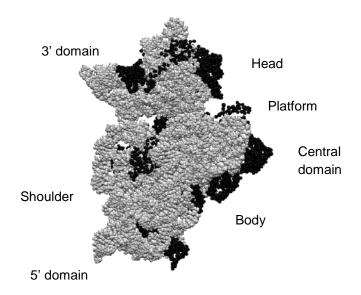


**Figure 1.4: 30S ribosomal subunit from** *Thermus thermophilus.* The small ribosome subunit in *T. thermophilus*, adapted from Schluenzen *et al.* (2000) (*33*), PDB 1FKA. 16S rRNA is shown in white rendered in space fill and all small ribosomal subunit proteins are represented in black rendered in space fill. The three main domains forming the head, platform and body of the 30S are labelled.

The proteins of the 30S subunit range in size from approximately 4 kDa to 61 kDa and are named S1 to S21 (S for small subunit) (34). The main role of the 30S ribosomal proteins are to stabilize the ribosomal subunit (33). However a number of these proteins are required for efficient proteins synthesis *in vivo*. Generally, a single protein can make several contacts with RNA to help stabilize the 30S subunit (28, 33). Interestingly, the 30S ribosomal proteins are found only on the solvent accessible regions (33).

mRNA enters the small ribosomal subunit through the 30S shoulder and exits behind the platform (35) (Figure 1.4). Once the mRNA is bound to the 30S small subunit of the ribosome, it

is anchored by proteins S3, S4 and S5 (36). The 30S ribosomal subunit also plays an important role in maintaining accuracy of translation (37). Nucleotides A1492, A1493 and G530 of the 16S rRNA interact with the codon-anticodon helix in the ribosomal A-site (38). Cognate Watson-Crick base pairing results in a short double helix which is stabilized by the conserved nucleotides A1492, A1493 and G530 (38). This is critical during the decoding process, where the cognate codon-anticodon interactions are discriminated against the near-cognate and non-cognate maintaining an error rate of around  $10^{-3}$  to  $10^{-4}$  in prokaryotes (39).

With the structure of the 30S subunit determined in 1999, the X-ray crystal structures of the 50S ribosomal subunit soon became available in 2000 (40). Like the small ribosomal subunit, the large subunit structure is mainly determined by its large rRNA (23S rRNA). 50S ribosomal proteins range from 4 kDa to 30 kDa and make contacts with rRNA to stabilize the subunit. Ribosomal proteins of the 50S subunit are named L1 to L33 (L for large subunit) (34). The overall structure of the 50S subunit consists of a large body and three protrusions (20, 40) (Figure 1.5). The L7/12 stalk forms one of the protrusions and interacts with translation factors, such as EF-Tu and EF-G (41). The central protrusion is located above the peptide exit tunnel where the polypeptide chain emerges from the ribosome. The L1 stalk forms the third protrusion, which interacts with the E-site tRNA, facilitating deacyl-tRNA dissociation from the ribosome (33, 42).

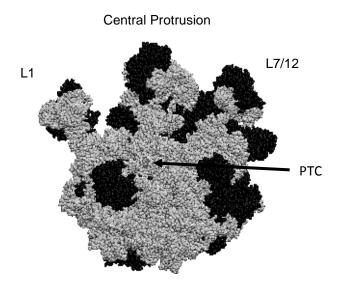


**Figure 1.5: 50S ribosomal subunit from** *E. coli.* Structure of the 50S ribosomal subunit solved by Cryo-EM (Villa *et al.* (2009) (*43*), PDB 3FIK). The L1 stalk, L7/12 stalk and Central protrusion are labelled. 23S, 5S rRNA are represented by white space fill and 50S proteins are represented with black space fill.

Structures and mutational studies of the ribosome revealed that mainly RNA is involved in key catalytic functions of the ribosome, such as peptide bond formation (reviewed in (44)). The 23S rRNA is the catalytic core of the 50S subunit, which assists in peptide bond formation between the new amino acid residue in the A-site and the growing polypeptide chain in the P-site (45). Proteins on the 50S subunit help to organize the peptidyl-transferase center (PTC) (32). Therefore, the 50S is the site of peptide bond formation enabling the growth of the polypeptide chain.

### 1.3 Translation initiation

The process of translation initiation involves the assembly of the ribosomal initiation complex.

Formation of the initiation complex is highly organized and requires three initiation factors (IF1,

IF2 and IF3) to ensure efficient and correct assembly of the 70S initiation complex (46-48) (Figure 1.6).

Prior to initiation complex assembly, mRNA binds to the 30S ribosomal subunit and is positioned within the 30S using interactions between its Shine-Dalgarno (SD) sequence AGGAGG, approximately 15 nucleotides upstream of the start codon (49), and the 16S rRNA (36). Ribosomal protein S1 then interacts with the SD sequence of the mRNA (50, 51), increasing the affinity of the mRNA for the 30S. These interactions facilitate the positioning of the AUG methionine start codon within the 30S subunit P-site (51).

The fully assembled initiation complex not only consists of bound mRNA but also contains a special tRNA positioned in the P-site of the 70S ribosome (*20, 52*). This tRNA, called initiator tRNA, has a number of unique properties to distinguish it from the so called elongator tRNAs (*53*). The initiator tRNA in bacteria caries a modified amino acid, formylmethionine (fMet), which is synthesized in a two step process. First, the tRNA body specific for fMet (tRNA<sup>fMet</sup>) is aminoacylated with methionine by methionine-tRNA synthetase, forming Met-tRNA<sup>fMet</sup> (*54*). Next, the methionine amino acid attached to the tRNA<sup>fMet</sup> is formylated by methionyl-tRNA transformylase (*55*). The formyl-amide group on the end of the methionine amino acid mimics the structure of a small peptide, and increases its affinity for the ribosomal P-site (*53*). To prevent fMet-tRNA<sup>fMet</sup> from entering the ribosomal E-site IF3 (approximately 21 kDa in *E. coli*) binds to the ribosomal E-site (*48*), forcing fMet-tRNA<sup>fMet</sup> to bind to the ribosomal P-site.

Binding of fMet-tRNA<sup>fMet</sup> to the ribosomal P-site is assisted by IF2 (approximately 93 kDa in *E. coli*) in complex with GTP (IF2•GTP), which recognizes the identity of the aldehyde of the formyl group to discriminate between initiator tRNA and elongator tRNA (53). IF2•GTP binds to fMet-

tRNA<sup>fMet</sup> and forms a ternary complex that subsequently binds to the 30S ribosomal subunit (48). Proper positioning of fMet-tRNA<sup>fMet</sup> is critical for initiation and maintenance of the reading frame. IF2 positions fMet-tRNA<sup>fMet</sup> by recognizing the SD sequence of the mRNA and the AUG methionine start codon, which base pairs to fMet-tRNA<sup>fMet</sup> (56). Subsequently, IF1 (approximately 8 kDa in *E. coli*) binds to the A-site of the 30S ribosomal subunit to help prevent premature binding of aa-tRNA in the vacant A site (57). The cryo-EM structure of the preinitiation complex was determined by Allen *et al.*, in 2005 (52) and confirmed IF1 and IF3 bind to the 30S subunit A and P sites respectively. After IF1 and IF3 dissociate from the 30S, the 50S associates to form the 70S initiation complex, which in turn stimulates IF2 to hydrolyze GTP. IF2•GDP then dissociates from the complex (58) leaving the 70S bound to mRNA and fMet-tRNA<sup>fMet</sup> in the P-site, ready for translation to begin.

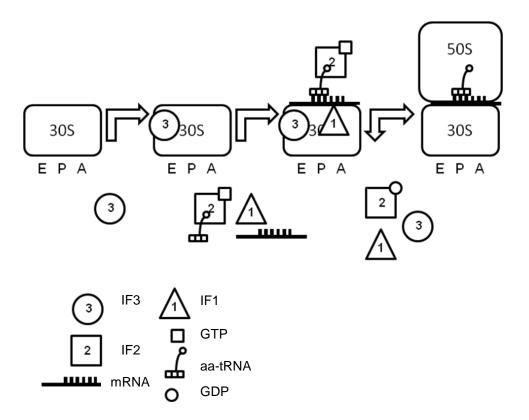


Figure 1.6: Translation initiation in bacteria. Initiation factors are indicated by their number. First IF3 binds to the E site of the 30S subunit, followed by IF2•GTP•fMet-tRNA<sup>fMet</sup>, IF1 and mRNA. Once mRNA and fMet-tRNA<sup>fMet</sup> are properly positioned on the 30S, IF2 hydrolyzes GTP and IF2•GDP, IF3 and IF1 dissociate. This allows the 50S to bind to the 30S subunit, forming the 70S initiation complex.

### 1.4 The elongation cycle

Elongation is a cyclic process that consists of three main steps: aa-tRNA binding to the ribosomal A-site, peptide bond formation and translocation (*59*) (Figure 1.7). The process of elongation in translation is universally conserved between prokaryotes and eukaryotes (*60*) and is facilitated by elongation factors (EF) EF-Tu, EF-Ts and EF-G, which catalyze various stages of the elongation process on the ribosome.

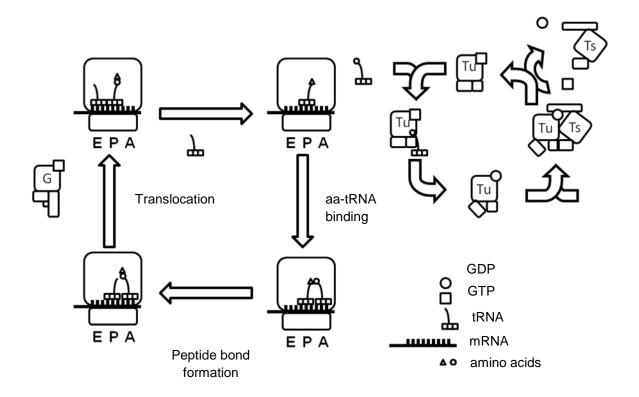
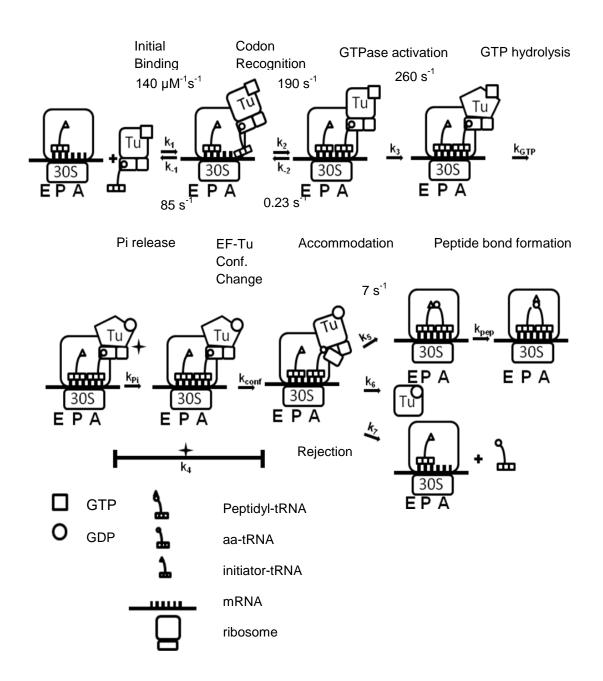


Figure 1.7: The Elongation cycle in bacteria. The cyclic process of elongation begins with the delivery of aa-tRNA by EF-Tu•GTP, followed by peptide bond formation between the amino acid in the A-site tRNA and the polypeptide chain in the P-site. EF-G•GTP catalyzes translocation of A- and P-site tRNAs to the P- and E-sites of the ribosome, along with mRNA, leaving an empty A-site with a new mRNA codon for the next round of elongation. The exchange of EF-Tu•GDP to EF-Tu•GTP is facilitated by EF-Ts.

Elongation factor Tu (EF-Tu) is a GTPase that promotes the binding of aa-tRNA to the ribosome during polypeptide elongation. In the GTP bound form, EF-Tu has a high affinity for aa-tRNA ( $K_D \approx 10^{-8}$  M (61)) and forms a ternary complex (EF-Tu•GTP•aa-tRNA) that subsequently can interact with the ribosome. A-site binding of aa-tRNA occurs through a number of intermediate steps (62) (Figure 1.8). Once aa-tRNA is delivered to the ribosome as a ternary complex (EF-Tu•GTP•aa-tRNA), the anticodon loop of aa-tRNA base pairs to the matching mRNA triplet codon in the ribosomal 30S A-site (63). Base pairing between the anticodon and the mRNA

codon induce the nucleotides A1492, A1493 and G530 of the 16S rRNA decoding site to flip out towards the anticodon-codon base pairs (38). A1492, A1493 and G530 monitor anticodon-codon base pairs one, two and three respectively (38) and stabilize cognate codon-anticodon interactions, however, these conformational changes do not occur in the presence of near-cognate and non-cognate codon-anticodon base pairs (38, 64, 65). This method of monitoring the anticodon-codon base pair contributes to the fidelity of translation.

It is not completely understood how the network of interactions from the 30S decoding site to the guanine nucleotide binding domain of EF-Tu signals the correct codon-anticodon recognition has occurred. This critical signal will cause EF-Tu to hydrolyze GTP, leading to phosphate ( $P_i$ ) (66) release and triggers a conformational change in EF-Tu. The resulting EF-Tu $\bullet$ GDP conformation has a two orders of magnitude lower affinity for aa-tRNA ( $K_D \approx 10^{-6} M$  (61)), causing EF-Tu $\bullet$ GDP to release aa-tRNA, which subsequently accommodates into the ribosomal A-site (61). However, the details of aa-tRNA release from EF-Tu and the timing of EF-Tu $\bullet$ GDP dissociation from the ribosome is unknown. Current single-molecule studies indicate that the process of accommodation proceeds via several intermediates (67). After accommodation has occurred and EF-Tu $\bullet$ GDP has dissociated from the ribosome, EF-G can bind to the ribosome.



**Figure 1.8: Kinetic scheme of EF-Tu dependent A-site binding.** During initial binding, the ternary complex binds to the ribosome, cognate codon recognition occurs followed by GTPase activation. Rates for the forward and reverse reaction of cognate anticodon are shown above. GTP hydrolysis, P<sub>i</sub> release and EF-Tu conformational change are all limited by the rate of GTPase activation. Accommodation of cognate aa-tRNA occurs following Pi release. k<sub>6</sub> is the rate constant for EF-Tu•GDP dissociation from the ribosome.

In order to maintain the rate of protein synthesis, a rapid exchange of GDP for GTP bound to EF-Tu must take place. However, EF-Tu has approximately a 10 times higher affinity for GDP ( $K_0 \approx 10^{-9}$  M) than for GTP ( $K_D \approx 10^{-8}$  M) (68) and spontaneous release of GDP from EF-Tu occurs on a minute time scale, which is too slow for the fast translation rates observed *in vivo* (57). Therefore, this exchange must be assisted in some way to ensure rapid turnover of EF-Tu $\bullet$ GDP during elongation. Elongation factor Ts (EF-Ts) binds to EF-Tu $\bullet$ GDP, and enhances the rate of GDP dissociation from EF-Tu approximately  $10^6$  fold by disrupting interactions within the nucleotide binding pocket in EF-Tu, weakening the affinity of EF-Tu for GDP (69). Subsequently, GTP binding to EF-Tu is facilitated by its higher concentration in the cell compared to GDP (69). GTP binding induces EF-Ts to dissociate from EF-Tu, enabling a new aa-tRNA to bind to EF-Tu and to be delivered to the ribosomal A-site.

Following aa-tRNA accommodation into the A-site, peptide bond formation occurs rapidly and is catalyzed by the ribosome (70). This is facilitated through positioning of aa-tRNA in the A-site towards the PTC (71), allowing the  $\alpha$ -amino group of the A-site bound aa-tRNA to attack the carbonyl carbon of the ester in the peptidyl-tRNA in the P site (Figure 1.9). This results in the formation of a peptidyl-tRNA that is elongated by one amino acid and bound to the ribosomal A site.

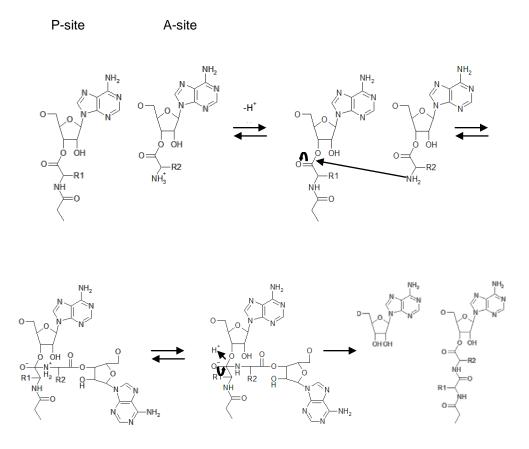


**Figure 1.9: Peptide bond formation**. The 3' ends of the P-site peptidyl-tRNA (left) and the A-site aa-tRNA (right) are shown. First, the amino group (-NH<sub>3</sub><sup>+</sup>) of the A-site aa-tRNA is deprotonated. Next, nucleophilc attack by the NH<sub>2</sub> on the ester carbonyl carbon leads to a zwitterionic intermediate. Deprotonation of the zwitterionic intermediate yields an anion, which eliminates the deacyl-tRNA in formation of the peptide bond.

In order for elongation to proceed, the peptidyl-tRNA and deacyl-tRNA in the A- and P-sites need to shift to the P- and E-sites along with the mRNA, leaving the A-site available for another round of elongation. Concomitant tRNA•mRNA movement within the ribosome occurs in two steps (72). First, the acceptor stems of the tRNAs in the A- and P-sites of the 50S move to the P- and E-sites respectively, forming a hybrid state (Figure 1.10). Second, the tRNA's anticodon stem in the

30S move from the A- and P-sites to the P- and E-sites, along with the mRNA. Under cellular conditions, EF-G helps catalyze this process (73) by inducing a structural rearrangement of the ribosome between the subunits (74, 75), L1 and L7/L12 stalk and in the 30S, which allows the simultaneous movement of tRNAs within the ribosome, along with the mRNA. EF-G also prevents sliding back of the translocated tRNAs by inserting domain IV into the A-site of the ribosome (75-78).

Recently, the highly conserved GTPase LepA was shown to be structurally similar to EF-G and to catalyze retro-translocation (79) (Figure 1.10). In retro-translocation the translocated E- and P-site tRNAs, along with the mRNA, move back to the P- and A-sites of the ribosome. However, not much is known about LepA and the function of retro-translocation.

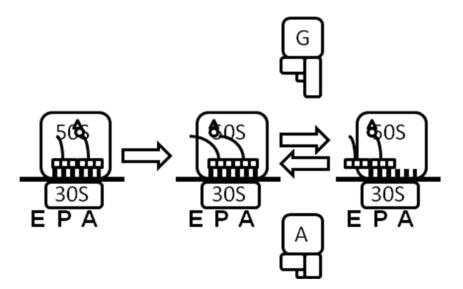


**Figure 1.10:** Translocation of tRNAs and mRNA within the ribosome. Translocation occurs in two distinct steps. First a hybrid state is achieved by the movement of the A- and P-site tRNAs acceptor stems to the P- and E-site of the 50S subunit. Next, the rest of the tRNA, along with the mRNA translocate from the A- and P-site to the P- and E-sites of the 30S. LepA (labelled with A) catalyzes retro-translocation, where EF-G is shown (labelled with G) catalyzes forward translocation.

Following translocation, the deacyl-tRNA in the E-site has a low affinity for this site and dissociates from the ribosome. This process leaves a vacant E-site, a new mRNA codon in the A-site, and the peptidyl-tRNA in the P-site ready for another round of elongation.

#### 1.5 Translation termination and recycling

Three codons, UAA, UGA and UAG, have been identified in *E. coli* and serve as 'stop' codons. When these codons are displayed in the A-site of a translating ribosome, release factors (RF) bind to the A-site (80). While UGA is only recognized by RF1 and UAG is recognized by RF2 (81), the stop codon UAA is recognized by both RF1 and RF2 (81). Binding of RF1 or RF2 to the ribosomal A-site induces the transfer of the polypeptide chain on the peptidyl-tRNA in the P-site to a water molecule in the A-site, facilitating the release of the polypeptide chain (82) (Figure 1.11). Subsequently, RF3 in complex with GTP, binds to the ribosome and hydrolyzes GTP to GDP + P<sub>i</sub>, which induces the release of RF1 or RF2. Ribosome recycling factor (RRF) binds to the ribosomal A-site, followed by EF-G•GTP (83) binding to the termination complex advancing the translocation of RRF to the ribosomal P-site, promoting the dissociation of the ribosomal subunits (80). IF3 then binds to the 30S ribosomal subunit E-site through two RNA binding domains, preventing the re-association of the two ribosomal subunits (84). After the ribosome is recycled into two separate subunits, a new mRNA can bind to the 30S subunit re-initiating the process of translation.

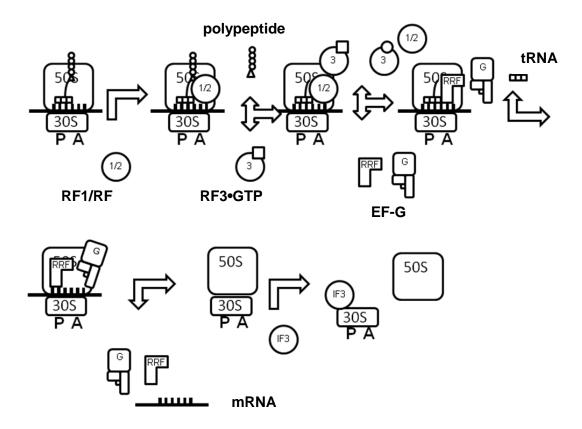


**Figure 1.11: Translation termination and ribosome recycling.** First RF1 or RF2 bind to promote the release of the polypeptide chain, followed by RF3 in complex with GTP facilitating RF1/RF2 dissociation from the ribosome. RRF and EF-G in complex with GTP, translocate deacyl- tRNA to the E-site, which dissociates from the ribosome. Following EF-G, RRF and mRNA dissociation, ribosomal subunits dissociate from each other and remain separate by IF3, which binds to the 30S subunit E-site.

### **Objectives**

The tRNA molecule is essential in the process of ribosome dependent protein synthesis (3). Throughout its functional cycle, tRNA makes contacts with several proteins; EF-Tu binds aa-tRNA and delivers it to the translating ribosome (85), EF-G catalyzes translocation and LepA catalyzes retro-translocation of tRNA•mRNA complexes within the ribosome (79). Studying the structural and functional dynamics of tRNA interactions is critical for our detailed understanding of its vital role in the living cell. Here I focus on EF-Tu and LepA as key interaction partners that modulate the dynamics of tRNA during the elongation cycle of protein synthesis by addressing the following questions.

- 1. Are there intermediate steps involved in aa-tRNA accommodation?
- 2. What is the rate of EF-Tu conformational change?
- 3. When does EF-Tu dissociate from the ribosome following aa-tRNA accommodation?

I will use fluorescence resonance energy transfer as a fast and sensitive technique to study structural transitions involving tRNA on the ribosome. This will involve the construction of a modified EF-Tu which will allow for the incorporation of fluorescent dyes at specific locations on its molecular surface. Since this approach will use cysteine specific fluorescent dyes a cysteine free EF-Tu that fully functional in terms of binding guanine nucleotides, binding aa-tRNA and ternary complex delivery to the ribosome must be constructed.

4. What are the structural requirements for retro-translocation and forward translocation in the presence of LepA?

To dissect this process I have constructed several mutant versions of LepA focusing on structural elements within LepA likely to be critical for its function.

#### **Chapter 2 – Elongation Factor Tu (EF-Tu)**

#### 2.1 Introduction to EF-Tu

Guanine nucleotide binding proteins (GTPases) are molecular switches involved in facilitating several key cellular processes, such as protein synthesis and signal transduction (reviewed in (86)). These proteins are generally active when bound to GTP and inactive when bound to GDP. Most GTPases undergo the same functional cycle, including binding and hydrolysis of GTP, typically resulting in a conformational change in the GTPase (86). GTPases also share a common guanine nucleotide binding domain, which is characterized by several similar sequence motifs and structural features. These similarities can be summarized by 5 common sequence motifs G1  $(GX_4GK(T/S) (87)$  (also known as the walker A motif), G2 (T) (88), G3 (DxxG), G4 (NKXD) and G5 (EXSA) (86) which facilitate nucleotide interactions and are conserved between the different GTPases. Similar structural features include switch regions I and II (89), which change conformation upon GTP hydrolysis and subsequent P<sub>i</sub> release. Translational GTPases have low intrinsic GTP hydrolysis rates and require the ribosome to act as a GTPase-activating factor (GAF) (90). Binding to the ribosome increases GTPase activity 2500 fold for translational GTPases (91), such as EF-Tu, EF-G, and IF2. They all bind to a similar region on the ribosome, L11, L7/12 and the sarcin-ricin loop of 23S rRNA (39). In addition to the GAP behaviour of the ribosome, EF-Tu also requires a guanine nucleotide exchange factor (GEF), elongation factor Ts (EF-Ts) to assist the dissociation of GDP and regenerate the active GTP bound form of EF-Tu (92).

EF-Tu is universally conserved in all domains of life and is one of the most prevalent proteins in the cytosol comprising approximately 5% of all cellular proteins (93). To ensure that EF-Tu is produced in sufficient quantities at all times within the cell, two genes, *tufA* and *tufB*, encode

Chapter 2 EF-Tu

EF-Tu in *E. coli* independently of each other (*94*). Therefore, if one of the *tufA* or *tufB* genes cannot be transcribed, EF-Tu can still be expressed in the cell.

EF-Tu is a 3 domain protein (Figure 2.1) with domain I being the guanine nucleotide binding domain (G domain) (95). Domain I consists of a 5 stranded anti-parallel β-sheet surrounded by 6  $\alpha$ -helices (95). The structures of EF-Tu in complex with GTP or GDP, determined using X-ray crystallography, revealed significant structural differences between the GTP and the GDP bound structure of EF-Tu (Figure 2.1) (95, 96). The EF-Tu residues 54-59 in the switch I region (40-62) change from an  $\alpha$ -helix to a  $\beta$ -strand, while switch II unwinds its helix at the C-terminus end and forms another helix at its N-terminus shifting the helix 42° away from its original position (95). Domain I moves away from domains II and III, forming a large gap in the GDP bound structure (95, 96).

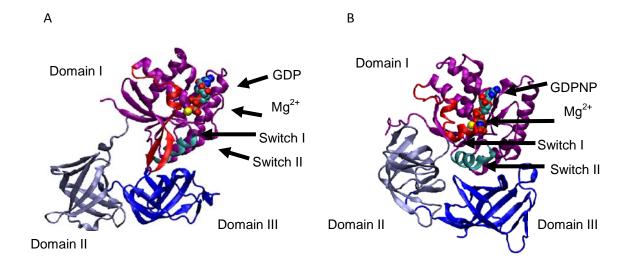


**Figure 2.1:** Nucleotide dependent changes in the tertiary structure of EF-Tu. (A) *E. coli* EF-Tu bound to GDP adapted from Song *et al.* (1999), PDB 1EFC (95) (B) *T. aquaticus* EF-Tu bound to GNPPNP, a non-hydrolysable GTP analogue, adapted from Kjeldgaard *et al.* (1993), PDB 1EFT (96). Switch I region is shown in red and switch II is in cyan. The guanine nucleotide in each structure is shown as space fill and Mg<sup>2+</sup> ion is shown as a yellow space fill.

Domain II consists of a seven-stranded antiparallel  $\beta$ -barrel and domain III is a six-stranded antiparallel  $\beta$ -barrel (95). EF-Tu in its active-state, complexed with GTP binds aa-tRNA with a high affinity ( $K_D \approx 10^{-8}$  M (61)), forming an EF-Tu $\bullet$ GTP $\bullet$ aa-tRNA ternary complex (Figure 2.2) (97) that facilitates aa-tRNA delivery to the ribosomal A-site. All three domains of EF-Tu make contact with aa-tRNA. The 3' CCA-Phe, 5' end and the T-stem of aa-tRNA are the contact sites for EF-Tu (97).

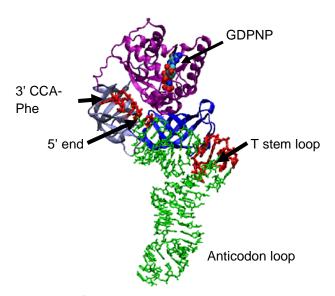


**Figure 2.2: Ternary complex of EF-Tu•GTP•aa-tRNA.** *T. aquaticus* EF-Tu with GDPNP (a non-hydrolysable form of GTP) in complex with yeast Phe-tRNA<sup>Phe</sup> shown in green adapted from Nissen *et al.* (1995), PDB 1TTT (*97*). GDPNP is shown as space fill in the G-domain of EF-Tu. Nucleotides of Phe-tRNA<sup>Phe</sup> which are contacted by EF-Tu are shown in red.

Several biochemical and kinetic studies have revealed intermediate steps taking place during the process of aa-tRNA binding to the ribosomal A-site, facilitated by EF-Tu (85, 98). The EF-Tu•GTP•aa-tRNA ternary complex, contacts the ribosome in an initial binding step (85). Cryo-EM structures reveal EF-Tu in the ternary complex prior to GTP hydrolysis, but after codon

recognition, contacting the ribosome through domains I and II (99). Domain I contacts the base of ribosomal protein L7/12 and the sarcin-ricin loop (SRL) on the 50S subunit, while domain II of EF-Tu makes contacts with the 30S ribosomal proteins S12, S5, S4 and 530 stem-loop (99). Following codon recognition, a signal is transmitted through an network of interactions, which are not completely understood, from the codon-anticodon interaction on the 30S to the G domain of EF-Tu, leading to GTPase activation (43, 100). When EF-Tu is bound to GTP, His 84 (the catalytic residue for GTP hydrolysis) on switch II points away from the y-phosphate (101). Contacts between His 84 and the y-phosphate is blocked by residues Ile 60 and Val 20, called the hydrophobic gate (101). Following codon recognition an unknown network of signals causes the SRL to anchor the phosphate binding loop (P-loop) of EF-Tu at one end of the hydrophobic gate and the 23S rRNA opens the other end of the hydrophobic gate through switch I interactions, causing Ile 60 and Val 20 to move away from each other (43). His 84 moves closer towards the acceptor end of the aa-tRNA and orientates towards the guanine nucleotide y-phosphate (43). GTP hydrolysis to GDP, followed by P<sub>i</sub> release, causes a major conformational change in EF-Tu (Figure 2.1), lowering the affinity of EF-Tu for aa-tRNA (61). The aa-tRNA is then released into the ribosomal A-site and EF-Tu dissociates from the ribosome (85).

In order for elongation to continue in a cyclic manner, EF-Tu•GDP must be regenerated into its active GTP-bound state in a quick and efficient manner. EF-Tu has a higher affinity for GDP ( $K_D \approx 10^{-9}$  M) than for GTP ( $K_D \approx 10^{-8}$  M), (68) and a very slow GDP dissociation rate (0.002 s<sup>-1</sup>) (69) preventing fast and efficient nucleotide exchange required to maintain protein synthesis rates observed *in vivo* (10 s<sup>-1</sup>) (68). GTP has a 10 times higher concentration in the cell (923  $\mu$ M) than GDP (128  $\mu$ M) (68). However, this does not compensate for the slow spontaneous dissociation

of GDP from EF-Tu (0.002 s<sup>-1</sup>) (*68*). The exchange of guanine nucleotides in EF-Tu is facilitated by the GEF, EF-Ts (*92*).

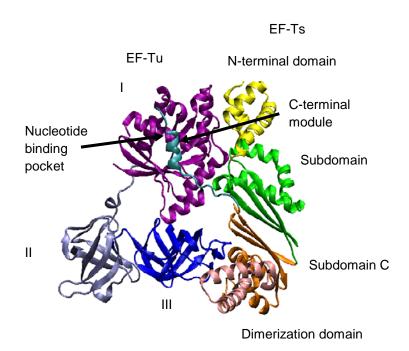


**Figure 2.3: EF-Tu in complex with EF-Ts.** *E. coli* EF-Tu in complex with EF-Ts adapted from Kawashima *et al.* (1996), PDB 1EFU (*102*). Interaction of EF-Tu and EF-Ts is seen between domain 1 of EF-Tu, which contacts the N-terminal domain (yellow), subdomain N (green) and C-terminal module (cyan) of EF-Ts. The dimerization domain (pink) and subdomain C (orange) are shown as well and are in close proximity to domain III of EF-Tu.

EF-Ts interacts with domain I and domain III of EF-Tu (Figure 2.3) (102). Interestingly, EF-Ts and ribosomal protein L7/12 make similar contacts to helix D in domain I of EF-Tu (103). Phe 81 in subdomain N of EF-Ts intrudes between His 84 and His 118 of EF-Tu, disrupting interactions between the residues that coordinate water molecules and Mg<sup>2+</sup> (102). Also, the first four residues in the phosphate loop are displaced by the interactions between EF-Tu and EF-Ts. This destabilizes GDP binding to the guanine nucleotide binding pocket in EF-Tu, allowing for GDP

release (102). The interaction between EF-Tu and EF-Ts does not disrupt all the interactions in the P-loop of EF-Tu (102). Therefore, guanine nucleotides can still bind to EF-Tu, but with a lower affinity. The EF-Tu•EF-Ts complex has a comparable affinity for GTP and GDP. Given the 10-fold excess of GTP over GDP in the cell, GTP binds to the EF-Tu•EF-Ts complex. GTP binding to EF-Tu•EF-Ts pushes the equilibrium towards the EF-Tu•GTP complex, letting EF-Ts dissociate from the complex. With the assistance of EF-Ts, the rate of GDP dissociation from EF-Tu is enhanced by a factor of 60 000, enabling the rapid turnover associated with elongation required by the cell (68).

**Objectives**: EF-Tu has been studied for many years and is probably one of the best characterized translation factors. However, questions remain about the structural dynamics of intermediate steps that may occur during the functional cycle of EF-Tu. For instance, how is aa-tRNA accommodated into the ribosomal A-site? Due to the many intermediate steps involved in aa-tRNA binding (85), accommodation seems more complex than a simple swinging-in of the aa-tRNA into the A-site. Also, the 3' end of aa-tRNA must move 70 Å from EF-Tu to the accommodated state near the PTC (62). Accommodation is fast for cognate aa-tRNA but slow for non-cognate aa-tRNA, which is rejected from the A-site (85) and will most likely require several steps to facilitate this movement and the observed discrimination between cognate and non-cognate aa-tRNA. In addition, little is known about the timing of EF-Tu dissociation from the ribosome after aa-tRNA has been released. The use of fluorescence resonance energy transfer (FRET) in conjunction with rapid kinetic measurements is ideal for answering the questions above and has been previously used successfully to address similar questions (85). However, most of the accessible data for EF-Tu has been acquired through ensemble measurements, which has numerous EF-Tu molecules in different conformational states. Therefore, ensemble

measurements are difficult to isolate intermediate conformational changes that may occur. In addition, ensemble measurements cannot measure the rate of EF-Tu conformational change unless all molecules are synchronized to have the same starting point. Therefore I have begun to construct and validate a mutant version of EF-Tu suitable for single-molecule FRET studies enabling the identification and characterization of novel intermediate conformations and rates of conformational change.

FRET is a distance dependent quantum dynamics process (Figure 2.4) that can occur between two fluorescence dyes (104), where excitation energy is transferred from a donor dye to an acceptor dye without the emission of a photon. Energy is only transferred if the donor emission spectrum overlaps with the acceptor absorption spectrum (104). Each dye pair has a distinct R<sub>0</sub>, which is the distance at which energy transfer is 50% efficient (Figure 2.4) (104). As the distance between the dyes increase, this transfer of energy decreases by a sigmoid function until FRET is no longer observed.

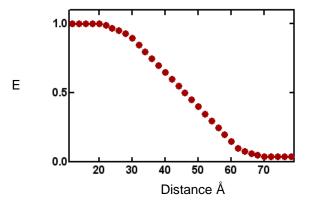


Figure 2.4: Efficiency of fluorescence resonance energy transfer as a function of distance. Efficiency (E) of energy transfer plotted against the distance between the two fluorescent dyes is distance dependent.

Typically, fluorescent dyes used are thiol reactive and therefore cysteine specific (Figure 2.5).

Figure 2.5: Reaction scheme for the covalent labelling of proteins with thiol reactive fluorescent dyes. Iodine acts as the leaving group in a substitution reaction (SN2), leaving the fluorescent dye attached to the protein through the sulphur on the cysteine side chain.

To follow the release of aa-tRNA from EF-Tu into the accommodated state, FRET can be used to observe the change in distance between the two molecules. During dissociation, the distance increase between fluorescently labelled aa-tRNA and fluorescently labelled EF-Tu results in a decrease of FRET over time. In this way, detailed distance changes and movement between EF-Tu and aa-tRNA can be uncovered.

FRET can also yield information on the time point of EF-Tu dissociation from the ribosome by using a fluorescent dye pair, one located on the ribosome and one on EF-Tu. When EF-Tu is bound to the ribosome, FRET will be high, and when dissociation occurs, FRET will decrease. This will yield precise information on how fast EF-Tu dissociates from the ribosome. In turn the rate of dissociation can be compared to the rate of aa-tRNA accommodation to understand the timing of EF-Tu dissociation from the ribosome.

Thiol specific fluorescent dyes can specifically be incorporated at cysteine residues. EF-Tu contains three intrinsic cysteines. In order to make detailed measurements using FRET, only one fluorescent dye should be placed on EF-Tu. Furthermore, the position of the dye must be optimal for the occurrence of distance dependent FRET changes. Therefore, a cysteine free

(cysless) EF-Tu must first be constructed so that a cysteine can be inserted in positions optimal for labelling and FRET measurements.

EF-Tu contains three cysteines, two of which are not conserved among 151 bacterial sequences (Figure 2.7, appendix Figure 1). One cysteine (Cys 81) however, is highly conserved throughout bacteria, and is buried near the nucleotide binding pocket. Cys 81 has previously been shown to affect aa-tRNA interactions with EF-Tu (105). These studies, however, used glycine as a substitution for cysteine, a mutation designed to have a large effect on the function of EF-Tu. The introduced glycine may have increased flexibility of the backbone of EF-Tu, leading to the observed effect on aa-tRNA binding. To circumvent this problem the side chain of Cys 81 was substituted with three different amino acid residues based on the multiple sequence alignment of 151 bacterial EF-Tu sequences (Figure 2.7, appendix Figure 1).

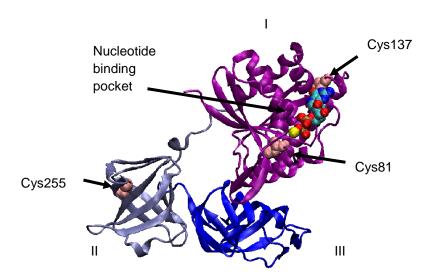


**Figure 2.6: Cysteines present in** *E. coli* **EF-Tu.** EF-Tu in complex with GDP adapted from Song et al., 1999 (95). Cysteines are shown in pink and space fill representation. Mg<sup>2+</sup> ion is shown as yellow space fill and GDP is shown in a green space fill.

To assess the affect these substitutions have on the function of EF-Tu, three key properties of EF-Tu were analyzed; guanine nucleotide binding, aa-tRNA binding and binding to the ribosome in a ternary complex. From these results and structural data, ideal positions for inserting a new cysteine for future fluorescent labelling and analysis were engineered. Leu 264 is located on domain II of EF-Tu and is not conserved. Thr 361 is located on domain III of EF-Tu, which is in close proximity to the anticodon loop of aa-tRNA when bound to EF-Tu (Figure 2.2), and is not conserved. Therefore, these sites can be used in the future to analyze the release of aa-tRNA into the ribosomal A-site during accommodation as well as the dissociation of EF-Tu from the ribosome.

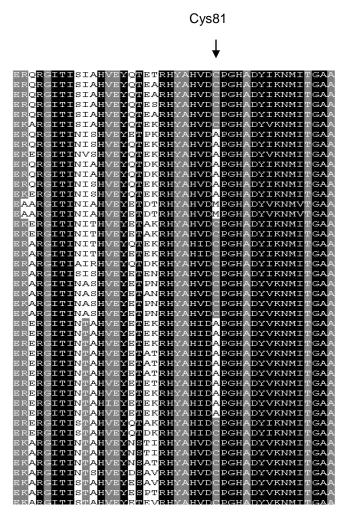


**Figure 2.7: EF-Tu multiple sequence alignment.** A segment of a multiple sequence alignment between 151 bacterial species primary protein sequences. Black represents 100% identity, grey is >80% identity, and white is <80% identity. Cys 81 is shown and is 87.5% conserved between all 151 bacterial species.

## 2.2 Material and Methods

All chemicals were obtained from VWR, Sigma-Aldrich or Invitrogen, unless stated otherwise. Fermentas restriction enzymes were used and all other enzymes were purchased as described in the respective sections. BL21-(DE3) competent cells were purchased from Novagen and DH5 $\alpha$  cells were purchased from New England Biolabs. PCR primers were purchased from Invitrogen

and Integrated DNA Technologies (IDT). Nucleotides and fluorescent nucleotide analogs were purchased from Invitrogen. Radioactive chemicals were purchased from Perkin-Elmer. Small-scale plasmid preparations were performed according to the manufacturer's specifications (EZ spin column plasmid DNA kit BioBasic). All buffers were filtered through 0.45 µm Whatman nitrocellulose membranes.

2.2.1 Molecular biology – All PCR reactions were carried out in a  $T_{Gradient}$  (Biometra) thermocycler. 6X-Histidine tagged EF-Tu was previously constructed through the insertion of the tufA gene from  $E.\ coli$  into a derivative of pET21a (pKECAHIS (106)). All subsequent mutagenesis was performed on this background.

ClustalW2 (http://www.ebi.ac.uk/Tools/clustalw2/index.html) was used to align 151 bacterial EF-Tu species sequences found in the Swiss-prot Database (www.expasy.org). Analysis of aligned sequences was performed in GeneDoc software version 2.7 (107). The non-conserved Cys 137 (34% conserved) and Cys 255 (29% conserved) were both substituted with valine. Valine was chosen because it was the most conserved residue among the 151 bacterial aligned sequences (position 137, 29% conserved, position 255, 66% conserved). The two-cysless background was then used for further mutagenesis substituting Cys81, which was found to be 87% conserved. Alanine was found in 12% and methionine in 1% of the sequences. Serine was also used to substitute Cys 81 on the two-cysless background due to their isosteric structures. Mutations substituting Cys 81 to alanine, methionine and serine were performed using site-directed Quickchange™ mutagenesis (Stratagene). Primers and PCR conditions used to generate the three different cysless tufA constructs are summarized in Tables 2.1, 2.2 and 2.3.

Table 2.1: EF-Tu mutagenesis primers.

Amino acid substitutions	Forward Primer (5'-3')	Reverse Primer (5'-3')	T <sub>m</sub>
C81A	CGCACACGTAGACGCACCGGGGCACGC C	GGCGTGCCCCGGTGCGTCTACGTGTG CG	67°C
C81S	CACTACGCACACGTAGACAGTCCGGGG CACG	AGTCGGCGTGCCCCGGACTGTCTACG TGTG	81°C
L264C	ATGTTCCGCAAATGTCTAGACGAAGGC CGTGCTGGT	ACCAGCACGGCCTTCGTCTAGACATTT GCGGAACAT	63°C
T361C	ATGGTTGTTTGCCTGATCCACCCGATCG CG	CGCGATCGGGTGGATCAGACAAACAA CCAT	61°C
T34C	GCAAT <i>CACTTGCGTG</i> CTAGCTAAAACCT AC	GTAGGTTTTAGCTAGCACGCAAGTGA T	58°C

Table 2.2: Quickchange mutagenesis PCR protocol for engineering EF-Tu C81M, C81A and C81S on a two-cysless background.

Step Number	Step	Temperature	Time	
1	Initial Denaturation	98°C	3 min	
2*	Denaturing	95°C	1 min	Cycle
3*	Annealing	64°C	1 min	18 time
4*	Extension	70°C	16 min	
5	Final Extension	70°C	15 min	

Table 2.3: Components used for mutagenesis of EF-Tu.

Component	Final Concentration
Water	-
dNTPs	0.4 mM
Forward Primer	0.4 μΜ
Reverse Primer	0.4 μΜ
Pfu buffer –MgSO <sub>4</sub>	1x
MgSO <sub>4</sub>	2 mM
Template	1 μg in 25 μL
Pfu Polymerase (Fermentas)	3 units in 25 μL

Template DNA was digested with DpnI restriction enzyme at 37°C overnight. DpnI digested PCR product containing the desired mutation was subsequently transformed into DH5 $\alpha$  *E. coli* competent cells and grown on LB agar overnight at 37°C, complemented with 100  $\mu$ g/mL ampicillin. DNA sequence and orientation was confirmed by sequencing (Macrogen).

L264C and T361C substitutions in EF-Tu were introduced into the cysless C81A *tufA* background. Primers and conditions used to generate these substitutions are listed in Tables 2.1, 2.3 and 2.4. The L264C background was further used as a template for introducing T34C, generating the T34C/L264C double mutation. Primers and conditions are listed in Tables 2.1, 2.3 and 2.5.

Table 2.4: Quickchange mutagenesis protocol for generating L264C and T361C EF-Tu mutants.

Step Number	Step	Temperature	Time	
1	Initial Denaturation	95°C	5 min	
2*	Denaturing	95°C	45 sec	Cycle
3*	Annealing	59°C	1 min	18 times
4*	Extension	72°C	15 min	
5	Final Extension	72°C	15 min	

Table 2.5: Quickchange mutagenesis protocol for generating L264C/T34C EF-Tu mutant.

Step Number	Step	Temperature	Time	
1	Initial Denaturation	95°C	5 min	
2*	Denaturing	95°C	45 sec	Cycle
3*	Annealing	47°C	1 min	18 times
4*	Extension	72°C	15 min	
5	Final Extension	72°C	15 min	

2.2.2 Protein expression - The respective mutant pEECAHIS plasmids (106) were transformed into BL21-(DE3) competent cells for expression of recombinant 6X-His tagged EF-Tu. Cells were grown in 500 mL LB with 100 µg/mL ampicillin at 37°C, starting at an optical density ( $OD_{600}$ ) value of 0.1  $OD_{600}$ . Once the  $OD_{600}$  reached a value of 0.6  $OD_{600}$ , EF-Tu overexpression was induced through the addition of a final concentration of 1 mM Isopropyl  $\beta$ -D-1-thiogalactopyranoside (IPTG). The cultures were grown for another 3 hrs and harvested by centrifugation at 5 000 xg for 10 min using a TA-10 rotor (Beckman). Cells were flash frozen and stored at -80°C prior to use.

Expression levels of EF-Tu were analyzed using time samples lysed in 8 M urea in  $TAKM_7$  (50 mM Tris-Cl pH 7.5 (20°C), 70 mM NH<sub>4</sub>Cl, 30 mM KCl and 7 mM MgCl<sub>2</sub>) and analyzed on a 12% SDS-PAGE run at 200 V for 55 min (BioRad Mini Protean 3 System). Gels were stained with Coomassie blue; all other SDS PAGEs were performed in a similar manner.

- 2.2.3 Protein purification Harvested cells containing overexpressed EF-Tu were opened in buffer A (50 mM Tris-Cl 8.0 (4°C), 60 mM NH<sub>4</sub>Cl, 7 mM MgCl<sub>2</sub>, 7 mM β-mercaptoethanol, 1 mM PMSF, 300 mM KCl, 10 mM imidazole, 15% glycerol and 50 μM GDP), supplemented with 0.1 mg/mL lysozyme and centrifuged at 30 000 xg for 45 min in a JA-16 rotor (Beckman). The cleared lysate (S-30 extract) containing the EF-Tu protein of interest was purified using affinity chromatography (7 mL column Ni-Sepharose from GE Healthcare). The column was washed with 150 mL buffer A and 200 mL buffer B (buffer A supplemented with 20 mM imidazole). Protein was then eluted in 10 column volumes of buffer C (buffer A supplemented with 250 mM imidazole) and further purified and re-buffered through size exclusion chromatography (160 mL Superdex 75 from GE healthcare) in TAKM<sub>7</sub>. Fractions containing only EF-Tu were pooled and concentrated using ultrafiltration (Vivaspin 20 MWCO 30 000 (Sartorius)). The final protein concentration was determined photometrically at 280 nm using a molar extinction coefficient 32900 M<sup>-1</sup> cm<sup>-1</sup> (calculated using ProtParam) and using the Bradford BioRad microassay.
- 2.2.4 Preparation of nucleotide free EF-Tu Since EF-Tu has a high affinity for GDP and needs to be bound to a nucleotide for stability and prevent EF-Ts association, EF-Tu was purified in the presence of GDP. To remove the bound nucleotide EF-Tu•GDP was incubated in buffer D (25 mM Tris-Cl pH 7.5 (20°C), 50 mM NH<sub>4</sub>Cl, 10 mM EDTA) for 30 min at 37°C to chelate Mg<sup>2+</sup>,

leading to GDP dissociation from EF-Tu. GDP and EF-Tu were separated using size exclusion chromatography (Superdex 75 HR 10/30 from GE healthcare) in TAKM<sub>7</sub>.

2.2.5 Preparation of EF-Tu•mant-GTP/mant-GDP – EF-Tu•GDP was incubated with a 10-fold excess of mant-GTP/GDP for 30 min at 37°C, to exchange the GDP from EF-Tu for mant-GTP/GDP (69). 3 mM phosphoenolpyruvate (PEP) and 0.1 mg/mL pyruvate kinase (PK) (Roche Diagnostic) were added to the EF-Tu•mant-GTP mixture to convert GDP present to GTP.

2.2.6 Rapid kinetic measurement - Mant-GDP/GTP dissociation rates from and association to EF-Tu were determined using a KinTek SF-2004 stopped-flow apparatus. The rate constant for the bimolecular association of mant-GTP/GDP to nucleotide free EF-Tu was determined by rapidly mixing 25  $\mu$ L of nucleotide free EF-Tu (0.3  $\mu$ M after mixing) with 25  $\mu$ L varying concentrations of mant-GTP/GDP (ranging from 0.3 to 10  $\mu$ M after mixing) at 20°C in TAKM<sub>7</sub>. The single tryptophan at position 185 of EF-Tu was excited at 280 nm and the fluorescence emission from mant was monitored through LG-400-F cut off filters (NewPort). Data was evaluated by fitting to a one-phase association (equation 1)

$$F = B^*(1-\exp(-k^*t))$$
 (Equation 1)

Where F is the fluorescence at time t, B is the fluorescence at time infinity, and k is the apparent rate constant of association. The apparent rate constants were plotted as a function of guanine nucleotide concentration, and the slope of this function yielded the rate of association.

Dissociation constants were determined by rapidly mixing 25  $\mu$ L EF-Tu•mant-GTP/GDP (0.3  $\mu$ M after mixing) with 25  $\mu$ L GTP/GDP (30  $\mu$ M after mixing) at 20°C in TAKM<sub>7.</sub> Again, the single tryptophan in position 185 was excited at 280 nm and mant fluorescence was monitored. Due to

the fact that excess unlabeled nucleotide was present the dissociation was treated as unidirectional and zero-order. Therefore, a one exponential fit (equation 2) yields k as the dissociation rate constant.

$$F = B + A*exp(-kt)$$
 (Equation 2)

2.2.7 Preparation of [ $^{14}$ C]Phe-tRNA $^{Phe}$  - [ $^{14}$ C]Phe-tRNA $^{Phe}$  was prepared through the aminoacylation of 10  $\mu$ M *E. coli* tRNA $^{Phe}$  (Sigma) with 40  $\mu$ M [ $^{14}$ C]Phe (MP-Biomedical), 5% crude synthetase (see below for preparation), 3 mM ATP (Sigma) in aminoacylation buffer (25 mM trisacetate (OAc) pH 7.5 (20°C), 8 mM Mg(OAc)<sub>2</sub>, 3 mM ATP, 100 mM NH<sub>4</sub>OAc, 30 mM KOAc, 1 mM DTT) to a final volume of 500  $\mu$ L.

The fraction of aminoacylated tRNA<sup>Phe</sup> was determined by spotting 10 µL (15 pmol) of the reaction mixture onto Whatman paper (2.5 cm<sup>2</sup> 3MM CHR) pre-soaked with 5% TCA. Any amino acid bound to tRNA<sup>Phe</sup> was precipitated together with the nucleic acid and free amino acid, which was removed using three washes with 5% TCA. Excess TCA was removed through a 30% ethanol wash. Subsequently the filter papers were dried at 80°C and added to 5 mL scintillation cocktail (MP EcoLite) in 20 mL vials (Wheaton plastic liquid scintillation vials). Decays per minute (dpm) were measured using a Tri-Carb 2800TR Perkin Elmer Liquid Scintillation Analyzer.

[<sup>14</sup>C]Phe-tRNA<sup>Phe</sup> was separated from tRNA<sup>Phe</sup> with a Jupiter 5μ C18 300A reverse phase chromatography column (Phenomenex) on an HPLC (BioCad Sprint Perfusion Chromatography system) using a linear ethanol gradient 100% buffer F (20 mM NH<sub>4</sub>OAc pH 5 (20°C), 10 mM Mg(OAc)<sub>2</sub>, 400 mM NaCl) to 100% buffer G (buffer F, 30% Ethanol).

5% crude synthetase was prepared in the following method: 14 mL of supernatant from the first 200 000 xg spin from a ribosome preparation (see ribosome preparation), was overlaid on a 9 mL 1.1 M sucrose cushion and centrifuged at 100 000 xg for 16 hrs in a Beckman Ti-45. The resulting supernatant was diluted with TAKM<sub>7</sub> supplemented with 6 mM β-mercaptoethanol. 17 g of (NH<sub>4</sub>)<sub>2</sub>SO<sub>4</sub> was added to 100 mL of crude synthetase mixture and centrifuged at 17 000 xg for 30 min. The resulting pellet was dissolved in buffer E (20 mM Tris-Cl pH 7.5 (4°C), 10 mM MgCl<sub>2</sub>, 0.3 M NaCl, 6 mM β-mercaptoethanol) and dialyzed overnight against 2 L of buffer E. Dialysis was repeated in 2 L of buffer E for 5 hrs, resulting in a final dilution of 1 in 40 000. Nucleic acids were separated from proteins by anion exchange chromatography (DE-52 cellulose Whatman), running buffer E at 6 mL/min. 70 g of (NH<sub>4</sub>)<sub>2</sub>SO<sub>4</sub>/ 100 mL was added to the eluted protein and centrifuged at 17 000 xg for 60 min.

2.2.8 Hydrolysis protection of the aminoacyl-ester bond - A hydrolysis protection assay was used to analyze the binding of EF-Tu to aa-tRNA. To form an active GTP bound form of EF-Tu, 1.5  $\mu$ M EF-Tu, 1.5  $\mu$ M GTP, 3  $\mu$ M PEP, 1% PK and 0.9  $\mu$ M EF-Ts in a total volume of 40  $\mu$ L in TAKM<sub>10</sub> was incubated for 20  $\mu$ min at 37°C. 0.5  $\mu$ M [14C]Phe-tRNA<sup>Phe</sup> in 20  $\mu$ L TAKM<sub>10</sub> was added to the EF-Tu mixture and incubated at 37°C. At various time points, from 0 to 100  $\mu$ min, aliquots of 10  $\mu$ L (15  $\mu$ mol) of the reaction mixture were spotted onto pre-soaked 5% TCA Whatman paper (2.5 cm<sup>2</sup> 3MM CHR). Free [14C]Phe liberated by spontaneous hydrolysis was washed away through three washes with 5% TCA and excess TCA was subsequently removed by washing with 30% ethanol. Filter papers were dried at 80°C for 30 min and then added to 5  $\mu$ L scintillation cocktail (MP EcoLite). Samples were analysed similar to the preparation of [14C]Phe-tRNA<sup>Phe</sup> above. The amount of [14C]Phe-tRNA<sup>Phe</sup> at a certain time was divided by the amount of [14C]Phe-tRNA<sup>Phe</sup> at the beginning and the natural logarithm (In) of this was plotted over time.

2.2.9 Ribosome preparation – 50 g of E. coli MRE600 cells were crushed in a cold mortar (20 cm diameter) at 4°C. Cold alumina (100 g) was added to the cells and the mixture was ground for 30 min. DNAse I was added to the mixture and mixed for 10 min, followed by the addition of 70 mL of opening buffer (20 mM Tris-HCl pH 7.6 (4°C), 100 mM NH<sub>4</sub>Cl, 10.5 mM MgCl<sub>2</sub>, 0.5 mM EDTA, 3 mM β-mercaptoethanol). The mixture was centrifuged at 1 000 xg for 10 min then at 10 000 xg for 30 min using a Beckman JA-14 rotor. The supernatant was centrifuged at 30 000 xg in a Beckman Ti-45 for 30 min. 40 mL aliquots of the resulting supernatant was overlaid on a 20 mL sucrose cushion (20 mM Tris-HCl pH 7.6 (4°C), 500 mM NH<sub>4</sub>Cl, 10.5 mM MgCl<sub>2</sub>, 0.5 mM EDTA, 1.1 M Sucrose, 3 mM β-mercaptoethanol) and centrifuged at 200 000 xg in a Beckman Ti-45 for 17 hrs. Pellets were dissolved in washing buffer (20 mM Tris-HCl pH 7.6 (4°C), 500 mM NH₄Cl, 10.5 mM MgCl<sub>2</sub>, 0.5 mM EDTA, 7 mM β-mercaptoethanol), then pooled and the volume was adjusted to 100 mL. 50 mL aliquots of the resulting solution was overlaid on a 4 mL sucrose cushion and centrifuged at 200 000 xg for 14.5 hrs in a Ti-45 rotor. Pellets were again dissolved in a total of 60 mL washing buffer and 10 mL aliquots of solution was overlaid on 1.5 mL sucrose cushion and centrifuged at 141 000 xg for 13 hrs using a Beckman SW28. Pellets were then resuspended in buffer for dissolving pellets (40 mL overlay buffer supplemented with 20 mM Tris-HCl, 60 mM NH<sub>4</sub>Cl, 5.25 mM Mg(OAc)<sub>2</sub>.0.25 mM EDTA, 3 mM  $\beta$ -mercaptoethanol, 5 mL 50% sucrose pH 7.6 (4°C)) and the concentration of ribosomes was determined by measuring A<sub>260nm</sub> and using the extinction coefficient 23 pmol/ $A_{260}$ .

Zonal centrifugation was used to separate the 30S, 50S and 70S ribosomal subunits from each other. First, 400 mL overlay buffer was pumped into a 217 xg spinning rotor (Beckman Ti-15), followed by the addition 22.5 mL (10 000 - 15 000  $A_{260}$  units) of ribosomes. Next, a 10-40% sucrose gradient (20 mM Tris-HCl pH 7.6 (4°C), 60 mM NH<sub>4</sub>Cl, 5.25 mM Mg(OAc)<sub>2</sub>, 0.25 mM

EDTA, 10% to 40% sucrose, 3 mM  $\beta$ -mercaptoethanol) was added until 150 mL of the overlay eluted. Finally 150 mL 50% sucrose (sucrose gradient buffer supplemented with 50% sucrose) was added and ribosomes were centrifuged at 42 000 xg for 19 hrs using a Beckman Ti-15. Fractions corresponding to 30S, 50S and 70S peaks were pooled and centrifuged at 200 000 xg for 46 hrs in a Ti-45. Resulting pellets were dissolved in a final storage buffer (20 mM Tris-HCl pH 7.6 (4°C), 50 mM NH<sub>4</sub>Cl, 5 mM MgCl<sub>2</sub>) then flash frozen and stored at -80°C.

2.2.10 Ternary complex binding to the 70S ribosome – Translation initiation complexes were prepared by incubating 0.2  $\mu$ M purified *E. coli* 70S with 0.6  $\mu$ M fMet[ $^3$ H]-tRNA $^{fMet}$  (108), 1 mM GTP, 0.6  $\mu$ M mRNA (122nt derivative of m022 sequence 5'-AUGGUU-3' (109)), and 0.3  $\mu$ M initiation factors 1, 2 and 3 in TAKM $_7$  to a final volume of 250  $\mu$ L for 40 min at 37°C. Ternary complexes were formed by first activating EF-Tu. Activation of EF-Tu was performed by incubating 3  $\mu$ M EF-Tu, 1 mM GTP, 1% PK, and 3 mM PEP in TAKM $_7$  at 37°C for 15 min and then adding 1  $\mu$ M [ $^{14}$ C]Phe-tRNA $^{Phe}$  to activated EF-Tu mixture and incubating for 1 min at 37°C (final volume of ternary complex mixture 75  $\mu$ L).

The ternary complex solution was then mixed with the initiation complex solution and incubated for 1 min at 37°C. The extent of ribosomal A-site binding for [ $^{14}$ C]Phe-tRNAPhe was measured by reacting 65  $\mu$ L (10 pmol) of mixture with excess puromycin, which is a small aa-tRNA analogue that binds to the A-site of the 50S when it is vacant.

Stability of the complex was measured using nitrocellulose filtration (65  $\mu$ L (10 pmol) aliquots of the mixture were filtered through 0.2  $\mu$ m Whatman nitrocellulose filter paper and washed with TAKM<sub>7</sub>). The amount of fMet[<sup>3</sup>H]-tRNA<sup>fMet</sup> and [<sup>14</sup>C]Phe-tRNA<sup>Phe</sup> still bound to the ribosome over time was assessed by comparing [<sup>3</sup>H] and [<sup>14</sup>C] counts to initial [<sup>3</sup>H] present.

2.2.11 Fluorescent labelling of EF-Tu L264C - Fluorescent labelling of EF-Tu L264C with 5-((2-[(iodoacetyl)amino]ethyl)amino)naphthalene-1-sulfonic acid (1,5-IAEDANS) (Invitrogen) was done using three different methods to optimize the labelling efficiency.

Method I - 12 000 pmol of previously purified 6X-His tagged EF-Tu L264C was incubated on a 2.5 mL Ni-Sepharose affinity chromatography batch column (GE healthcare) for 2 hrs in equilibration buffer (50 mM Tris-Cl pH 7.5, 70 mM NH<sub>4</sub>Cl, 30 mM KCl, 7 mM MgCl<sub>2</sub>, 10 mM β-mercaptoethanol) at 4°C. Excess protein was removed through centrifugation at 500 xg and the resulting supernatant was re-buffered in labelling buffer (25 mM Tris-Cl pH 7.5, 7 mM MgCl<sub>2</sub>, 30 mM KCl, 20% glycerol). A 20 fold molar excess of 1,5-IAEDANS over EF-Tu was added drop wise to the resin and incubated for 2 hrs at room temperature, in the dark, with mixing. Excess dye was removed by washing the column 4 times with labelling buffer. The labelled protein was then eluted by adding 10 column volumes of elution buffer (25 mM Tris-Cl pH 7.5 (4°C), 7 mM MgCl<sub>2</sub>, 300 mM KCl, 250 mM imidazole, 20% glycerol). Elution fractions containing EF-Tu were pooled and concentrated through ultrafiltration (Vivaspin 20 MWCO 30 000 (Sartorius)).

Method II - 12 000 pmol of EF-Tu L264C was diluted in labelling buffer and a 20-fold excess of 1,5-IAEDANS was added drop wise to EF-Tu in a 50 mL falcon tube. The mixture was incubated at room temperature for 3 hrs in the dark, with continuous mixing. Excess dye was removed by dialyzing the mixture in 32 mm dialysis tubing (Sigma) against 350 times excess labelling buffer for 16 hrs at 4°C, in the dark. Dialysis was repeated, giving a final dilution factor of 1 in 122 500 and EF-Tu was concentrated using ultrafiltration as in Method I above.

Method III – 20-fold molar excess of 1,5-IAEDANS was added drop-wise to 12 000 pmol of EF-Tu L264C in labelling buffer in a 50 mL falcon tube, followed by an incubation for 3 hrs at room

temperature, in the dark with continuous mixing. The excess dye was removed by gel filtration using a 30 mL size exclusion chromatography column (G-25 Sephadex (GE Healthcare)) equilibrated in labelling buffer. Fractions containing labelled EF-Tu were pooled and concentrated as above.

2.2.12 Analysis of fluorescently labelled EF-Tu - Fluorescence measurements were performed using a Varian Cary Eclipse Fluorescence Spectrophotometer, in a 0.3 x 0.3 cm quartz cuvette (Starna), at room temperature. EF-Tu contains one intrinsic tryptophan residue, which has a maximum absorbance at 280 nm and a maximum fluorescence emission at 340 nm. 1,5-IAEDANS has an excitation maximum at 336 nm and emits at a maximum of 490 nm. FRET measurements between Trp 185 (donor) and 1,5-IAEDAN labelled L264C (acceptor) were done by exciting tryptophan at 280 nm and measuring the fluorescence emission from 300 to 550 nm through 5 nm slits.

## 2.3 Results

2.3.1 Activity of cysless EF-Tu – EF-Tu contains three intrinsic cysteines, two of which are not conserved and one (Cys 81) is highly conserved and in close proximity to the guanine nucleotide binding pocket. Therefore, mutating Cys 81 may affect the function of EF-Tu. In an effort to construct a cysless version of EF-Tu which retains wild type activity, three conservative mutations (C81S, C81A and C81M) were introduced based on the multiple sequence alignment (Figure 2.7, appendix Figure 1). All Cys 81 mutations were performed on a two-cysless EF-Tu background.

Once the cysless EF-Tu mutants were generated, their ability to bind guanine nucleotides GTP and GDP were analyzed. The association and dissociation constants for GTP and GDP to EF-Tu

mutants were determined, using rapid-kinetics (experimental procedures 2.2.6). EF-Tu C81A and C81M were shown to have association and dissociation rates for GTP and GDP similar to wild type EF-Tu (Table 2.6). However, C81S was found to be more than 10 times slower than wild type for GTP dissociation and 1000 times slower for GDP association (Table 2.6).

Table 2.6: Association and dissociation constants of mant guanine nucleotides to EF-Tu.

Mutants are compared to wild type EF-Tu. C81A and C81M are similar to wild type, however,

C81S is not comparable to wild type EF-Tu.

EF-Tu	k <sub>association</sub> (GTP)	k <sub>dissociation</sub> (GTP)	k <sub>association</sub> (GDP)	k <sub>dissociation</sub> (GDP)
Wild Type	$4.29 \times 10^5 \pm 0.72 \text{M}^{-1} \text{s}^{-1}$	0.029 ± 0.0003 s <sup>-1</sup>	2.18x10 <sup>6</sup> ± 0.12M <sup>-1</sup> s <sup>-1</sup>	$0.003 \pm 2.782 \times 10^{-5} \text{ s}^{-1}$
Wild Type (69)	5x10 <sup>5</sup> M <sup>-1</sup> s <sup>-1</sup>	0.03 s <sup>-1</sup>	2x10 <sup>6</sup> M <sup>-1</sup> s <sup>-1</sup>	0.002 s <sup>-1</sup>
C81S	6.57x10 <sup>5</sup> ± 1.01 M <sup>-1</sup> s <sup>-1</sup>	0.001 ± 1.221X10 <sup>-5</sup> s <sup>-1</sup>	$6.86 \times 10^2 \pm 1.31 \mathrm{M}^{-1} \mathrm{s}^{-1}$	$0.002 \pm 1.221 \times 10^{-5} \text{ s}^{-1}$
C81M	3.87x10 <sup>5</sup> ± 0.28 M <sup>-1</sup> s <sup>-1</sup>	0.022 ± 0.0002 s <sup>-1</sup>	3.92x10 <sup>6</sup> ± 0.26 M <sup>-1</sup> s <sup>-1</sup>	0.002 ± 1.704x10 <sup>-5</sup> s <sup>-1</sup>
C81A	$1.79 \times 10^5 \pm 0.08 \mathrm{M}^{-1} \mathrm{s}^{-1}$	0.063 ± 0.0008 s <sup>-1</sup>	1.5x10 <sup>6</sup> ± 0.2 M <sup>-1</sup> s <sup>-1</sup>	0.007 ± 2.706x10 <sup>-5</sup> s <sup>-1</sup>

Next, the ability of all mutants to bind [14C]Phe-tRNAPhe in the presence of GTP were compared to wild type. A hydrolysis protection assay was used to assess the formation of the ternary complex (see experimental procedures 2.2.8) using the fact that EF-Tu binding will protect the labile aminoacyl ester bond against spontaneous hydrolysis. The natural logarithm (In) of [14C]Phe-tRNAPhe over the original amount of [14C]Phe-tRNAPhe was plotted as a function of time (Figure 2.8). The half-life of [14C]Phe-tRNAPhe in the presence of each mutant was calculated and compared to wild type in order to assess the ability of the mutants to bind to [14C]Phe-tRNAPhe (Figure 2.8). Results indicate that the half-life of [14C]Phe-tRNAPhe in the presence of EF-Tu wild type and EF-Tu C81A is 145 min, whereas the half-life of [14C]Phe-tRNAPhe in the presence of EF-Tu C81M is 23 min and EF-Tu C81S is 26 min (Figure 2.8). This indicates that only the mutation

EF-Tu C81A protects the aminoacyl ester bond as efficient as the wild type, indicating the efficient formation of the ternary complex. Although C81M and C81S do not protect the aminoacyl-ester bond from cleavage like wild type EF-Tu both mutants protect the aminoacyl ester bond against cleavage compared to the spontaneous hydrolysis in the absence of EF-Tu (Figure 2.8) which has a half life of 12 min. This indicates that a ternary complex also forms in the presence of these mutants. However, the C81M and C81S were 10 times less efficient at protecting the aminoacyl-ester bond than wild type and C81A.

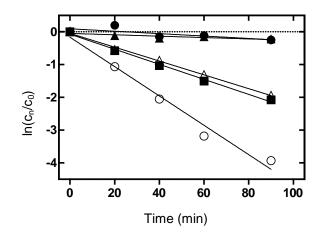


**Figure 2.8:** Hydrolysis protection assay of the aminoacyl-ester bond in [ $^{14}$ C]Phe-tRNA $^{Phe}$ . [ $^{14}$ C]Phe-tRNA $^{Phe}$  incubated in the presence of EF-Tu (filled circles) EF-Tu C81A (filled triangles) EF-Tu C81S (open triangles) EF-Tu C81M (filled squares) and no EF-Tu (open circles).  $ln(c_n/c_0)$  is plotted over time, where the slope indicates the rate of aminoacyl-ester bond cleavage.  $c_n$  is the concentration of [ $^{14}$ C]Phe-tRNA $^{Phe}$  at that time point and  $c_0$  is the concentration of [ $^{14}$ C]Phe-tRNA $^{Phe}$  at time 0.

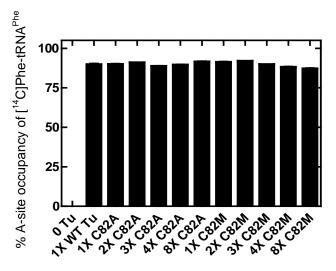
Based on the guanine nucleotide binding and Phe-tRNA<sup>Phe</sup> binding results, the C81S cysless mutant was not comparable to wild type and was not used in any further analysis or further mutagenesis.

Next, the ability of EF-Tu C81A and C81M to bind to the ribosome as a ternary complex were compared to wild type. Various amounts of C81A and C81M were used to assess the ability of the cysless EF-Tu mutants to promote Phe-tRNA<sup>Phe</sup> binding to 70S initiation complexes (see experimental procedures 2.2.10). This was done using puromycin reactivity, which binds to the 50S A-site when unoccupied, and forms a peptide bond with [<sup>3</sup>H]fMet in the P-site. After a 1 min incubation with the initiation complex, both mutants (C81A and C81M) promoted [<sup>14</sup>C]Phe-tRNA<sup>Phe</sup> binding to the ribosomal A-site, with comparable efficiency to wild type EF-Tu (Figure 2.9). In the absence of protein no [<sup>14</sup>C]Phe-tRNA<sup>Phe</sup> was bound to the ribosome. In addition, increasing amounts of C81A or C81M did not affect the overall amount of Phe-tRNA<sup>Phe</sup> delivered to the A-site (Figure 2.9). These results indicate that the C81A and C81M mutants are capable of [<sup>14</sup>C]Phe-tRNA<sup>Phe</sup> delivery to the ribosomal A-site at levels similar to wild type protein.

To ensure that the delivery of [<sup>14</sup>C]Phe-tRNA<sup>Phe</sup> seen in the presence of the C81A and C81M mutants was in a fully accommodated state, the stability of the [<sup>14</sup>C]Phe-tRNA<sup>Phe</sup> in the A-site was assessed through nitrocellulose filtration (experimental procedures 2.2.10). A ternary complex consisting of wild type or mutant EF-Tu, GTP and [<sup>14</sup>C]Phe-tRNA<sup>Phe</sup> was mixed with an initiation complex containing [<sup>3</sup>H]fMet-tRNA<sup>fMet</sup> in the P-site of the ribosome, then incubated and filtered through nitrocellulose (experimental procedures) (Figure 2.10). Equimolar concentrations of [<sup>14</sup>C]Phe-tRNA<sup>Phe</sup> and [<sup>3</sup>H]fMet-tRNA<sup>fMet</sup> remained bound to the programmed 70S, indicating that neither [<sup>14</sup>C]Phe-tRNA<sup>Phe</sup> nor [<sup>3</sup>H]fMet-tRNA<sup>fMet</sup> dissociated from the ribosome after 1 minute of incubation.

The above results show that substitution of Cys 81 with alanine resulted in a functional cysless EF-Tu mutant. Even though the C81M mutant was functional in binding guanine nucleotides and

delivering Phe-tRNA<sup>Phe</sup> to the ribosome as a ternary complex, C81M did not protect the aminoacyl-ester bond from cleavage like C81A or wild type. Therefore, the EF-Tu C81A background was used for further mutagenesis.



EF-Tu excess over initiation complex

Figure 2.9: Percentage of [<sup>14</sup>C]Phe-tRNA<sup>Phe</sup> delivered to the ribosomal A-site by EF-Tu•GTP. [<sup>14</sup>C]Phe-tRNA<sup>Phe</sup> bound to the ribosomal A-site in the presence of EF-Tu determined using puromycin reactivity. Up to 8 times excess of EF-Tu C81A or EF-Tu C81M over ribosomal initiation complex were analyzed in the delivery of [<sup>14</sup>C]Phe-tRNA<sup>Phe</sup> to the ribosome.

complex are also analyzed.

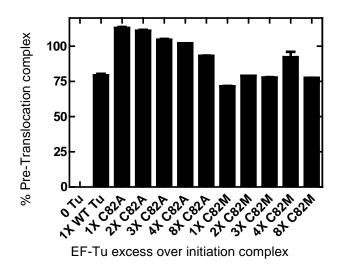


Figure 2.10: Percentage of pre-translocation complex in the presence of EF-Tu determined by nitrocellulose filtration. Percentage of the pre-translocation complex is determined by the amount of [14C]Phe-tRNAPhe and f[3H]Met-tRNAfmet bound to ribosome after 1 min compared to the amount at time 0. Up to 8 times excess EF-Tu C81A or EF-Tu C81M over ribosomal initiation

2.3.2 Fluorescent labelling of EF-Tu L264C using 1,5-IAEDANS — In order to study the rate of conformational change in EF-Tu, as well as the timing of EF-Tu dissociation from the ribosome following aa-tRNA accommodation using rapid kinetics techniques in combination with fluorescence, cysteine specific fluorescent dyes need to be conjugated to a specific cysteine in EF-Tu. Based on the construction of a fully active cysteine free EF-Tu new cysteine substitutions within EF-Tu have to be incorporated, without affecting the overall function of EF-Tu, on the molecular surface of EF-Tu in positions ideal for future FRET experiments.

omain II of EF-Tu comes into close proximity to the ribosome when it is in a ternary complex (*43*) and is an optimal location for analyzing dissociation of EF-Tu from the ribosome. Leucine 264 is a surface accessible non-conserved residue in domain II (*95, 96*) (appendix Figure 1). To enable

subsequent labelling Leu 264 was mutated to a cysteine within the cysless (C81A) EF-Tu background. Following purification EF-Tu L264C was fluorescently labelled with 5-((2-[(iodoacetyl)amino]ethyl)amino)naphthalene-1-sulfonic acid (1,5-IAEDANS) (Figure 2.11).

$$O = \begin{cases} M_w = 434.25 \text{ g/mol} \\ \lambda \text{ (Absorbance)} = 336 \text{ nm} \\ \lambda \text{ (Emission)} = 490 \text{ nm} \\ \text{Extinction coefficient (336 nm)} = 5700 \text{ M}^{-1} \text{ cm}^{-1}. \end{cases}$$

**Figure 2.11: Chemical structure of 1,5-IAEDANS.** Molecular weight, absorption maximum and emission maximum as well as the extinction coefficient for the fluorophore are listed beside the structure.

Labelling and purification of fluorescently labelled EF-Tu L264C protein was optimized using three different methods (experimental procedures 2.2.11).

In the first labelling method, L264C EF-Tu was incubated on a Ni-Sepharose column (GE healthcare) and 1,5-IAEDANS was added drop wise to the column. Only 50% of EF-Tu added to the column eluted from the column after the addition of 250 mM imidazole. Following the addition of EDTA to the Ni-Sepharose column, the other 50% of EF-Tu eluted from the column. Of the 50% that eluted from the column prior to EDTA addition, 40% was lost during ultrafiltration due to precipitation of the protein, giving an overall yield of 20%.

In the first method most of the protein precipitated on the Ni-Sepharose column. Therefore, in an effort to avoid affinity chromatography purification, EF-Tu L264C was incubated with 1,5-

IAEDANS in the absence of Ni-Sepharose resin. Following incubation of EF-Tu L264C and 1,5-IAEDANS, excess 1,5-IAEDANS was removed through dialysis against labelling buffer. The dialysis caused the formation of a white precipitate in the dialysis tubing containing the labelled protein. Contents in the dialysis tubing were collected and centrifuged. The resulting pellet and supernatant were analyzed on a 12% SDS PAGE, confirming that approximately 90% of EF-Tu was in the pellet, giving a final yield of less than 10% labelled EF-Tu L264C for this method.

In the final method for labelling EF-Tu L264C, EF-Tu L264C and 1,5-IAEDANS were incubated together and the excess dye was removed using size exclusion chromatography (Figure 2.12). EF-Tu eluted around a volume of 10 mL off the column and absorbed at 280 nm (protein) as well as 336 nm (dye), indicating that the EF-Tu L264C protein was labelled. Excess dye eluted approximately 30 mL afterwards and was confirmed by its absorbance at 336 nm. This method gave a yield of approximately 35% labelled protein with a 1:1 dye to protein ratio.

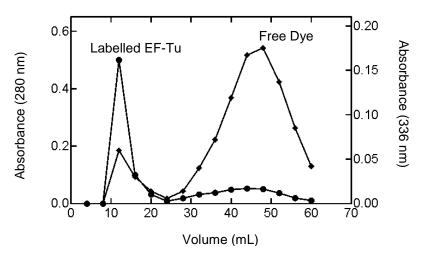
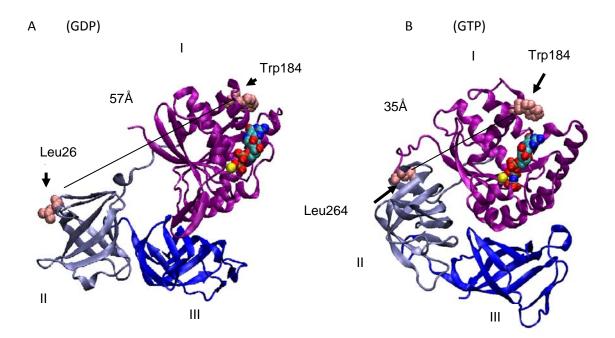


Figure 2.12: SEC purification elution profile of fluorescently labelled 1,5-IAEDANS EF-Tu L264C. Absorbance was measured at 280 nm (right) for measuring the protein and at 336 nm (left) for measuring 1,5-IAEDANS. Fluorescently labelled protein eluted after 10 mL (closed circles) and excess dye eluted at 40 mL (closed diamonds).

2.3.3 Analysis of fluorescently labelled EF-Tu L264C – A fluorescence label incorporated at position 264 in EF-Tu is not only a promising reporter for Ribosome interaction but will also enable the measurement of conformational changes within EF-Tu during nucleotide exchange or GTP hydrolysis. For example Leu 264 moves a distance of over 20 Å from Trp 185 on domain I upon GTP hydrolysis (35 Å (GTP-bound) to 57 Å (GDP-bound)) (Figure 2.13). The large distance change between Trp 185 and Leu 264 is ideal to measure the conformational changes in EF-Tu using fluorescence resonance energy transfer (FRET). Furthermore, Trp and 1,5-IAEDANS is a promising dye pair since the emission spectra of Trp (maximum of emission peak 340 nm) overlaps with the absorption spectra of 1,5-IAEDANS (maximum of absorption peak 336 nm).



**Figure 2.13: Distance changes between Leu 264 and Trp 185 in** *E. coli* **EF-Tu in the GDP or GTP bound conformation.** (A) *E. coli* EF-Tu bound to GDP adapted from Song *et al.* (1999), PDB 1EFC (95) shows a distance of 57 Å between Leu 264 and Trp 185. (B) *T. aquaticus* EF-Tu bound to GNPPNP (a non-hydrolysable GTP analogue) adapted from Kjeldgaard *et al.* (1993), PDB 1EFT (96) shows a distance of 35 Å between Leu 264 and Trp 185. The guanine nucleotide in each structure is shown in space fill and Mg<sup>2+</sup> is shown in yellow. Leu 264 and Trp 184 are shown in pink space fill.

In order to be able to measure conformational changes the occurrence of FRET between the two labels has to be confirmed. Therefore, 1,5-IAEDANS labelled EF-Tu L264C was excited at 280 nm and the resulting fluorescence emission was measured between 300 nm to 500 nm (see experimental procedures 2.2.12). Following excitation at 280 nm two peaks were observed, one with a maximum at approximately 340 nm reflecting the tryptophan emission, and another with a maximum around 490 nm for 1,5-IAEDANS emission (Figure 2.14). The spectra of free 1,5-IAEDANS however, indicated that emission of labelled protein at 490 nm can be excited directly at 280 nm but with a significant lower efficiency than observed in the labelled protein (Figure 2.14).

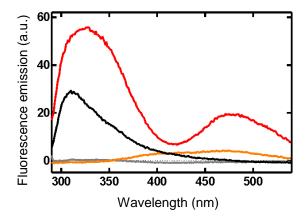


Figure 2.14: Fluorescence spectrum of 1,5-IAEDANS labelled L264C EF-Tu. Fluorescence emission scan was performed from 300 nm to 550 nm after an excitation at 280 nm. EF-Tu L264C labelled with 1,5-IAEDANS (red), EF-Tu wild type (black), 1,5-IAEDANS (orange). All spectra were recorded at a concentration of approximately 20  $\mu$ M.

Since EF-Tu L264C was purified in the presence of GDP all the previous data collected was based on the GDP-bound EF-Tu state (Figure 2.13). When EF-Tu is in complex with GTP, Leu 264 and

Trp 185 move 20 Å closer together compared to the GDP-bound state. As such, an increase in FRET efficiency is expected to be observed in the GTP-bound resulting in increased fluorescence at 490 nm. Therefore the fluorescence emission of 1,5-IAEDANS labelled EF-Tu was measured also in the presence of GTP (Figure 2.15). When the relative fluorescence at 340 nm and 490 nm were compared, no detectable difference between the fluorescence emission of EF-Tu bound to GTP or GDP was observed. Given that 35 Å is the closest distance between these two fluorescent dyes, and that tryptophan and 1,5-IAEDANS have a reported R<sub>0</sub> of approximately 20 Å (110) when attached to position 264 this dye pair is not sensitive enough to measure conformational changes. This suggest either the use of a different dye pair with an R<sub>0</sub> of approximately 40 Å to see distinct changes or to position 1,5-IAEDANS further away from the fluorescence donor.

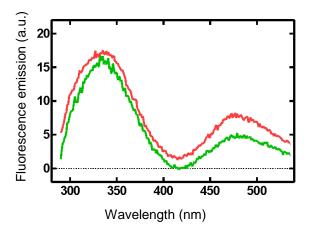
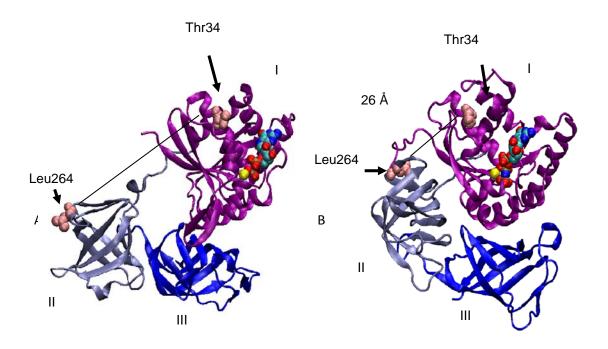


Figure 2.15: Fluorescence spectra of 1,5-IAEDANS labelled EF-Tu L264C with GTP or GDP bound. The fluorescence emission scan was performed from 300 nm to 550 nm after an excitation at 280 nm. 20  $\mu$ M EF-Tu L264C labelled with 1,5-IAEDANS in the presence of GDP (red) and EF-Tu L264C labelled with 1,5-IAEDANS in the presence of GTP (green).

2.3.4 Mutagenesis performed on EF-Tu –In order to enable the use of another dye pair another cysteine was introduced at residue Thr 34 on domain I of EF-Tu. Leu 264 and Thr 34 move approximately 20 Å away from each other after GTP hydrolysis and  $P_i$  release (Figure 2.16) and should be detectable by double labelling with a dye pair which has an  $R_0$  closer to 40 Å (Cy3 and Cy5 or CPM and fluorescein-5-malemide (111)).



**Figure 2.1**: <sup>49 Å</sup> **ice changes upon EF-Tu conformational change between Leu 264 and Thr 34 on domain I of EF-Tu.** (A) *E. coli* EF-Tu with GDP adapted from Song *et al.* (1999), PDB 1EFC (*95*) shows the distance between Leu 264 and Thr 34 on domain I to be 49 Å apart. (B) *T. aquaticus* EF-Tu with GDPNP a non hydrolysable GTP analogue adapted from Kjeldgaard *et al.* (1993), PDB 1EFT (*96*) shows a distance between Leu 264 and Thr 34 on domain I to be 26 Å apart. The guanine nucleotide and Mg<sup>2+</sup> ion is also shown in space fill. Residues Leu 264 and Thr 34 are shown in pink and space fill.

In order to measure the structural details of aa-tRNA release into the ribosomal A-site and uncover likely intermediate steps between aa-tRNA delivery to the ribosome and

accommodation (85), another single cysteine mutant of EF-Tu was engineered substituting Thr 361 on domain III (Figure 2.17) with cysteine in the C81A cysless EF-Tu background. Thr 361 is not conserved (appendix Figure 1) and is in close proximity to the aa-tRNA when bound (Figure 2.17).

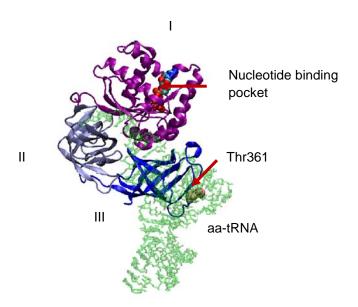


**Figure 2.17: Residue Thr 361 in domain III of EF-Tu.** Thr 361 shown in pink on domain III of EF-Tu in the ternary complex of EF-Tu•GTP•aa-tRNA. *T. aquaticus* EF-Tu with GDPNP in complex with yeast Phe-tRNA<sup>Phe</sup> (green) adapted from Nissen *et al.* (1995), PDB 1TTT (*97*). GDPNP is shown as a space fill structure.

## 2.4 Discussion and future directions

I have successfully engineered a fully functional cysless EF-Tu . Furthermore, I have inserted cysteines in this cysless background for future fluorescent labelling. In addition, I have generated an efficient method for fluorescently labelling and purifying EF-Tu for fluorescent analysis. Previously published studies on the substitution of Cys 81 with a glycine (105) as well as chemical modification of the side chain of Cys 81 (112) have suggested that this residue is important for EF-Tu interactions with aa-tRNA. These studies used glycine as a substitution for

Cys 81 (105), which may dramatically increase the flexibility of the peptide backbone, ultimately altering the conformation in this region of the protein. Consistent with the previous study, the motivation here is to understand the functional role of Cys 81, which when alkylated inactivates EF-Tu (105). However, Parmaggiani and coworkers (105) were not interested in replacing the cysteine residue with a side chain that retained the activity of EF-Tu and therefore are consistent with our finding that a serine substitution in position 81 significantly affects the activity of EF-Tu. Furthermore, only little information regarding the amino acid sequences of different bacterial EF-Tu species were available for Parmaggiani and coworkers (105), preventing an evolutionary analysis of Cys 81. Here, an extensive multiple sequence alignment was performed using 151 bacterial EF-Tu sequences to identify amino acid residues that evolutionarily can be tolerated. Results presented in this study reveal that alanine as a substitution for Cys 81 is not only the most abundant substitution in nature (12%), but does not show any effect on mant-GTP/GDP binding, binding to Phe-tRNA Phe to form a ternary complex or delivering Phe-tRNA<sup>Phe</sup> to the ribosome in a ternary complex. The results for the EF-Tu mutants (C81M and C81S) binding to mant-GTP and mant-GDP were not surprising, since methionine is found as a natural Cys 81 substitutions in some bacterial species (1%). Interestingly for the C81S mutant, the GTP dissociation rate is identical to the GDP dissociation rate, and because the GTP concentration in the cell is 10-fold higher than that of GDP, the C81S mutation may spend more time in the GTP-bound form than in the GDP. Furthermore, the C81S mutation may inhibit conformational changes in EF-Tu from the GTP-bound state to the GDP-bound state. The conformation of EF-Tu C81S must be analyzed in further detail to fully answer how C81S effects EF-Tu.

For the C81M mutant, association and dissociation of guanine nucleotides are similar to wild type. Therefore, the weaker interaction between EF-Tu C81M and aa-tRNA cannot be explained by a reduced level of the GTP-bound form of EF-Tu. Even though Cys 81 has not been shown to be involved in binding aa-tRNA directly, it is near the C-terminus of the effecter loop, which is positioned above the minor groove of the acceptor stem in aa-tRNA (Figure 2.18) when bound to aa-tRNA (97). Furthermore, it is near the GTPase switch II region, which is involved in recognition of the major groove of the acceptor and the T-stem in the ternary complex. The methionine side chain has an extra methylene and methyl group than cysteine and may have an impact on nearby residues, thereby tightening the binding pocket for aa-tRNA, which may reduce the affinity for Phe-tRNA<sup>Phe</sup>.

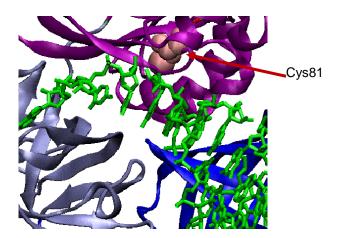


**Figure 2.18: Cys 81 is in close proximity to the acceptor stem of aa-tRNA**. *T. aquaticus* EF-Tu in complex with yeast Phe-tRNA<sup>Phe</sup> shown in green adapted from Nissen *et al.* (1995), PDB 1TTT (97). Cys 81 is shown in space fill and coloured pink.

Furthermore, the results demonstrate that C81A and C81M deliver Phe-tRNA<sup>Phe</sup> to the ribosome in a ternary complex, similar to wild type. Combining the results for guanine nucleotide association/dissociation, ternary complex formation and delivery of Phe-tRNA<sup>Phe</sup> to the

ribosome for the C81A mutation, it can concluded that Cys 81 can be substituted for alanine without affecting the function of EF-Tu. Therefore, the cysless C81A mutant can be used as a promising background in subsequent mutagenesis and fluorescent labelling experiments for future FRET studies.

Mutagenesis and fluorescent labelling of EF-Tu L264C with 1,5-IAEDANS revealed the conformation change in EF-Tu resulting in a distance change between Trp 185 and 1,5-IAEDANS labelled L264C (35 Å (GTP bound) to 57 Å (GDP bound)) did not result in a detectable change in FRET efficiency. This is was surprising since the  $R_0$  of this dye pair is approximately 20 Å (110).

Based on this observation a double mutant (L264C/T34C) was constructed enabling fluorescent labelling with a dye pair that has an  $R_0$  closer to 40 Å (such as Cy3 and Cy5 or CPM and fluorescene-5-malemide) (111). This mutant has the potential to be a powerful tool to measure EF-Tu conformational changes on a single-molecule level as well as to measure rates for EF-Tu conformational change and identify novel intermediates steps during A-site delivery of aa-tRNA.

Due to the fact that domain II of EF-Tu also comes into close contact to the 30S subunit and Leu 264 is in close proximity to 16S rRNA (Figure 2.19) (43) a mutant EF-Tu carrying a fluorescent label in this position can be used to study the interaction with the ribosome. Successful random labelling of whole ribosomes has been reported in Peske *et al.*, (80) providing a novel way of determining the timing of EF-Tu dissociation from the ribosome subsequent to aa-tRNA release.

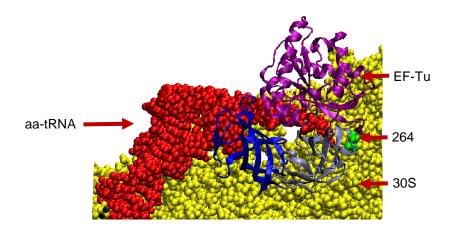


Figure 2.19: Leu 264 in EF-Tu is in close proximity to the 30S subunit during A-site binding. EF-Tu from *E. coli* (domain I (purple), domain II (ice blue) and domain III (blue)) is shown in complex with aa-tRNA (red space fill) bound to the ribosome (30S subunit (yellow space fill)), 50S subunit not shown here. It can be seen that all three domains of EF-Tu come into close contact with the ribosome. Leu 264 is shown in green and in close proximity to the ribosome. Cryo-EM structure is adapted from Villa *et al.* (2008) (43).

## 2.5 Conclusion

A cysless EF-Tu mutant has been obtained that is not compromised with respect to binding guanine nucleotides, binding Phe-tRNA<sup>Phe</sup> or delivery of Phe-tRNA<sup>Phe</sup> to the ribosome as a ternary complex. Based on this, mutant versions of EF-Tu were generated by introducing additional cysteines, enabling subsequent fluorescent labelling. Efficient fluorescent labelling of cysless L264C and a method for purifying this labelled EF-Tu has been shown. Furthermore, this provides a powerful tool for creating double fluorescently labelled EF-Tus and to measure the rate of conformational changes in EF-Tu using single-molecule FRET.

# Chapter 3 - LepA

# 3.1 Introduction to LepA

Only recently has the gene product of *lepA* been suggested to be a novel translation factor (79). The *lep* gene (<u>leader peptidase</u>) in *E. coli* encodes for signal peptidase I (113). The function of signal peptidase I is to cleave 15 to 30 residues of the N-terminal signal peptide of secreted proteins, which are generally membrane bound proteins (113). The *lep* promoter is located approximately 2 kb upstream of the *lep* gene (113). Between the *lep* promoter and the *lep* gene there is an open reading frame encoding for a 599 amino acid residue protein, which has been termed *lepA* (113).

The lepA gene is found in all bacteria, mitochondria and chloroplasts (79). LepA is one of the most conserved proteins having 55-68% identity in bacteria (79). The conservation of LepA is less than EF-Tu (70-82%) and similar to EF-G (58-70%), but higher than the essential translation factors IF2 (35-49%), IF3 (43-69%) and EF-Ts (33-50%). However, knockout of the lepA gene produces no visible phenotypic effect on cellular growth under optimal conditions (114). This raises the question of what is the function of LepA and why is it so highly conserved?

The primary sequence of LepA was shown to be homologous to those of translation factors EF-Tu and EF-G (Figure 3.1) (113). Due to sequence similarity with translation factors, it was speculated that LepA may be a translational GTPase (113). Previous studies have demonstrated that LepA binds GTP and interacts with the ribosome (115-117).

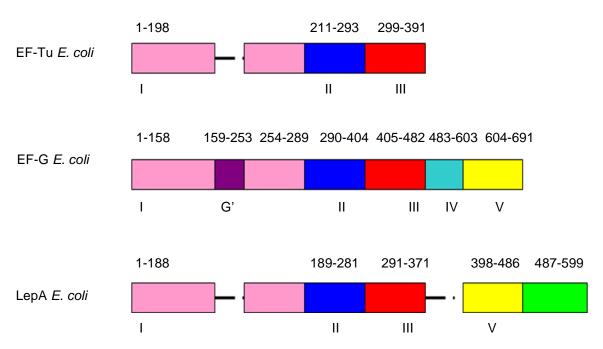


**Figure 3.1: Domain alignment of LepA, EF-Tu and EF-G.** LepA sequence from *E. coli*, EF-G is from *E. coli* and EF-Tu is taken from *E. coli*. Domains are aligned according to their similarity and are coloured accordingly. Domain I (pink), domain II (blue), domain III (red) and domain V (yellow) of LepA is homologous to these domains on EF-Tu and EF-G.

LepA is structurally similar to EF-G (Figure 3.2) (118). Domains I, II, III and V of LepA correspond to domains I, II, III and V of EF-G. However, LepA lacks domains similar to domains IV and G' of EF-G, but contains a unique C-terminal domain (CTD). Little is known about the function of the CTD, which was investigated through truncation mutations in this study (Figure 3.3). Three different truncation mutations were constructed based on the predicted secondary structure changes of LepA. The predicted secondary structure was later confirmed through the crystal structure of LepA (118). Residues 555 to 599 were not resolved in the crystal structure however, in the predicted secondary structure it is thought to form a  $\beta$  sheet.

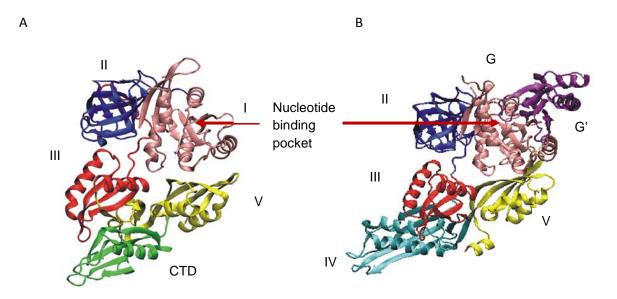


Figure 3.2: Comparison of LepA and EF-G structures. (A) LepA from *E. coli* PDB: 3CB4 (118). (B) EF-G from *T. thermophilus* PDB: 1FNM (119). Domain I (pink), II (blue), III (red), V (yellow), CTD (green) of LepA are labelled and domain G (pink), G' (purple), II (blue), III (red), IV (cyan), V (yellow) of EF-G are labelled.

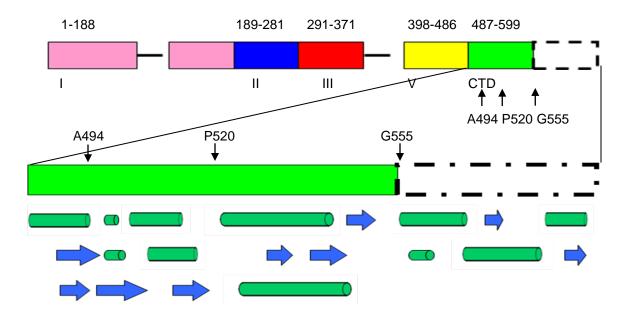
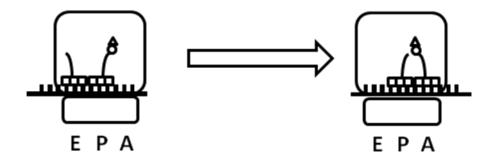


Figure 3.3: Secondary structure LepA CTD. Arrows on C-terminal domain indicate primer positions. Green cylinders indicate  $\beta$ -sheets, and blue arrows indicate  $\alpha$ -helices.

Chapter 3 LepA

The structural similarity of LepA to translational GTPases, such as EF-G, is a strong indication for the potential involvement of LepA in translation. A recent investigation into the involvement of LepA in translation has lead to the discovery that LepA might catalyze a process called retrotranslocation (79).

Retro-translocation is the movement of the translocated deacyl-tRNA and peptidyl-tRNA from the ribosomal E- and P-sites back to the P- and A-sites respectively (Figure 3.4).



**Figure 3.4: Retro-translocation of tRNA-mRNA within the ribosome.** P-site peptidyl-tRNA and E-site tRNA, move to the A- and P-sites of the ribosome during the process of retro-translocation. mRNA is also retro-translocated in this process by one triplet codon.

In the presence of deacyl-tRNA and absence of EF-G, retro-translocation can occur spontaneously (109). However, this process is prevented in the presence of EF-G. EF-G inhibits retro-translocation through the insertion of its domain IV into the ribosomal A-site (120). Also, retro-translocation requires deacyl-tRNA in the E-site, which is unstable and dissociates rapidly from the ribosome. In the presence of polyamines, such as spermine, deacyl-tRNA is stabilized in the E-site and retro-translocation may occur (109).

The rate and extent of spontaneous tRNA movement within the ribosome is dependent upon the affinity of the peptidyl-tRNA and tRNA for the respective ribosomal sites (109). In the

absence of competitors, all tRNAs and peptidyl-tRNAs will bind to the ribosomal P-site. However, the spontaneous movement of peptidyl-tRNA and deacyl-tRNA is dependent on their respective affinities for the P-site, reflecting their greatest thermodynamic stability (109). Therefore, the equilibrium between the forward and retro-translocated complex varies based on the peptidyl-tRNA (109). Many questions involving LepA and retro-translocation arise, such as: What does retro-translocation consist of? How does LepA catalyze retro-translocation? What is the function of LepA's CTD? What is the active state of LepA?

Although LepA has been suggested to be a translational GTPase (79), little is known about the guanine nucleotide bound state which is required for LepA activity in retro-translocation. Therefore, the rate and extent of retro-translocation in the presence of various guanine nucleotides (GTP, GDP, GDPNP) was studied. In order to identify different ribosomal substrates of LepA, the substrate specificity of LepA for two different ribosomal complexes, which differ in their peptidyl-tRNA was analyzed.

Similar to other translational GTPases, the Cryo-EM structure shows that LepA contacts the ribosome within the translation factor binding site (117). This structure also showed LepA in contact with the retro-translocated A-site tRNA through its CTD, and contacts the acceptor stem, D-loop and the T $\Psi$ C-loop of the A-site tRNA. To address the function of the CTD, three different truncation mutations of the CTD in LepA were constructed and their function was compared with the function of full-length protein.

Forward translocation in the presence of EF-G has been shown to occur in the presence and absence of GTP (75). EF-G seems to promote an unlocked conformation of the ribosome (121), which enables tRNA, along with mRNA, to translocate. However, translocation does not require

GTP hydrolysis but does require GTP hydrolysis to release EF-G from the ribosome (75). LepA is structurally similar to EF-G and may not require GTP hydrolysis to catalyze the process of retrotranslocation. To address this the putative catalytic residue for GTP hydrolysis (His81), based upon sequence similarity to EF-Tu (101), was substituted with alanine to generate a GTPase inactive mutant of LepA. Lastly, the structural similarity of LepA to EF-G prompted the analysis of a potential role of LepA in catalyzing the dissociation of the 70S ribosome into 30S and 50S subunits during ribosome recycling.

# 3.2 Materials and Methods

All chemicals were obtained from VWR, Sigma or Invitrogen, unless otherwise specified. Restriction enzymes were from Fermentas; enzymes purchased from other sources will be indicated. BL21-(DE3) competent cells were purchased from Novagen and DH5α cells were purchased from New England Biolabs. PCR primers, nucleotides and fluorescent nucleotide analogs were purchased from Invitrogen. Radioactive chemicals were purchased from Perkin-Elmer. Small-scale plasmid preparations were performed according to the manufacturer's specifications (BioBasic EZ spin column plasmid DNA kit). All buffers were filtered through 0.45 μm Whatman nitrocellulose membranes.

3.2.1 LepA Cloning - Genomic DNA was isolated from an overnight culture of *E. coli* DH5 $\alpha$  cells grown at 37°C in 25 mL of LB media overnight. The overnight culture was spun at 5 000 xg and the pellet was re-suspended in TES buffer (50 mM Tris-Cl pH 7.5, 10 mM NaCl, 10 mM EDTA). 10 mg/mL of lysozyme and proteinase K were added to the re-suspended solution, followed by a 1 hour incubation at 37°C. 4 M NH<sub>4</sub>OAc was added to the solution, followed by a10 min incubation at room temperature. A 1:1 phenol: chloroform extraction of the DNA was performed, then

spun down for 2 min at 5 000 xg. This was followed by a wash with chloroform to wash away the phenol. The extracted aqueous phase containing the DNA was precipitated with 2.5 volumes of isopropanol and incubated for 10 min at -20°C. After a precipitate formed, the solution was centrifuged and the pellet was re-suspended in 0.1 mL 0.1 M NH<sub>4</sub>OAc. 70% ethanol was added to re-precipitate the DNA and incubated for 10 min at -20°C. Precipitate was spun down for 10 min at 5 000 xg and the pellet was re-suspended in TES buffer. Isolated genomic DNA was used as a template to amplify the *lepA* open reading frame using PCR. Primers used were 5′-AATCATACCATATGAAGAATATACG-3′ and 5′-CTCCTAAGCTTTATTTGTTGTCTT-3′. Pfu DNA polymerase (Fermentas) was used in a Biometra T<sub>Gradient</sub> thermocycler using the conditions outlined in Tables 3.1 and 3.2.

Table 3.1: Components used to isolated and amplify the lepA gene in E. coli.

Component	Final Concentration
Template	8 ng/mL
Primers	1 μM each
Pfu buffer 5X	1 X
10 mM dNTPs	0.3 μΜ
Pfu Polymerase	0.3 U/ μL
Distilled water	-

Chapter 3 LepA

Table 3.2: PCR protocol used to isolate and amplify the *lepA* gene in *E. coli*.

Step Number	Step	Temperature	Time	
1	Initial Denaturation	95 °C	3 min	
2*	Denaturing	95 °C	1 min	Cycle
3*	Annealing	65 °C	1 min	30 times
4*	Extension	72 °C	14 min	Limes
5	Final Extension	72 °C	15 min	

A restriction digestion of amplified *lepA* DNA was performed with Scal (Fermentas) then ligated into a pBR322 vector using T4 DNA ligase. The resulting plasmid was transformed into *E. coli* DH5α cells and grown on LB agar plates supplemented with 50 μg/mL of kanamycin. A maxiprep was performed to extract the transformed DNA in the following method. ALS1 (50 mM glucose, 25 mM Tris-Cl pH 8 (20°C), 10 mM EDTA), ALS2 (0.2 M NaOH, 1% SDS), and ALS3 (5 M K-acetate, glacial acetic acid) were added to the pellet of the overnight culture. This was centrifuged at 5 000 xg for 10 min. A 1:1 phenol: chloroform extraction was performed on the resulting supernatant. The mixture was centrifuged at 5 000 xg for 15 min. A 1:1 phenol: chloroform was repeated on the upper aqueous layer followed by a final chloroform extraction. The resulting aqueous layer was ethanol precipitated overnight. Precipitate was pelleted and re-suspended in RNase A. Following an overnight incubation at 37°C with RNase A another ethanol precipitation was performed. The resulting pellet was re-suspended in water. *lepA* was excised with HindIII and Ndel (Fermentas) and ligated into a pET28a vector containing a 6X-Histidine-tag using T4 DNA ligase, resulting in pET28-*lepA*. Sequence and orientation were confirmed by sequencing (Macrogen).

3.2.2 Mutagenesis - All PCR reactions were carried out in a T<sub>Gradient</sub> (Biometra) thermocycler. C-terminal deletion mutations were generated based on a secondary structure prediction using Jpred http://www.compbio.dundee.ac.uk/www-jpred/ (Figure 3.3).

Deletion mutants of LepA ( $\Delta$ A494,  $\Delta$ P520,  $\Delta$ G555) were constructed via PCR using pET28a *lepA* as a template. A single stop primer was used for the construction of all three deletion mutants (5'-TAAGGCTTGCGGCCGCACTCGA-3'), which had a  $T_m$  of 63.9°C. The forward primers used in construction of the truncation mutants differed depending on which deletion was being constructed. The sequences of the forward primers were 26 nucleotides long and correspond to the coding region of *lepA* and the 5' terminal nucleotides correspond to the terminal amino acid in the resulting deletion mutant. The product of each PCR was a linear DNA fragment with the desired C-terminal LepA codon at one terminus, and the AUG start codon at the other. Blunt end ligations of the products produced circular plasmids encoding LepA deletion mutants in pET28a vectors. Forward primers for each CTD deletion mutant are listed in Table 3.3. Conditions for the PCR and the components used are listed in Tables 3.4 and 3.5.

Site directed mutagenesis to produce the LepA H81A substitution was carried out on the pET28a *lepA* template using Quickchange™ mutagenesis (Stratagene). Primers designed for this mutation also removed a Scal restriction site and are listed in Table 3.1. PCR conditions used to introduce the LepA H81A mutant are listed in Tables 3.6 and 3.7.

Table 3.3: Primers used to generate *lepA* mutants.

LepA Mutant	Forward Primer 5'-3'	Reverse Primer 5'-3'	T <sub>m</sub>
H81A	TATCGACACCCCAGGC <u>GCC</u> GTAGACT TCTCCTATG	ATAGGAGAAGTCTAC <u>GGC</u> GCCTGGGGT GTCGATA	81.5°C
ΔΑ494	<u>CGC</u> ATCAACACGTTCACCGTTGATTA	TAAGGCTTGCGGCCGCACTCGA	62.2°C
ΔΡ520	TGGGATCAGATCTTTCATCTTCCCA	TAAGGCTTGCGGCCGCACTCGA	60.6°C
ΔG555	<u>GCC</u> ATAACATTTAGCCAGTACGTTTT	TAAGGCTTGCGGCCGCACTCGA	59.9°C

Table 3.4: PCR protocol used to engineer the CTD truncation mutants ( $\Delta A494$ ,  $\Delta P520$ ,  $\Delta G555$ ).

Step Number	Step	Temperature	Time	
1	Initial Denaturation	98 °C	3 min	
2*	Denaturing	98 °C	1 min	Cycle
3*	Annealing	60 °C	45 sec	35 times
4*	Extension	72 °C	5 min	
5	Final Extension	72 °C	5 min	

Table 3.5: PCR components used to engineer the CTD truncation mutants ( $\Delta$ A494,  $\Delta$ P520,  $\Delta$ G555).

Component	Final Concentration
Template	3.2 μg/mL
Primers	13 pM each
5X HF buffer 5	1 X
	(1.5 mM MgCl2)
10 mM dNTPs	200 μΜ
Polymerase (Phusion)	0.016 U/ μL
Distilled water	-

Chapter 3 LepA

Table 3.6: Quickchange mutagenesis protocol used to generate the H81A LepA substitution mutant.

Step Number	Step	Temperature	Time	
1	Initial Denaturation	95 °C	3 min	
2*	Denaturing	95 °C	45 sec	Cycle
3*	Annealing	65 °C	60 sec	18 times
4*	Extension	72 °C	12 min	times
5	Final Extension	72 °C	20 min	

Table 3.7: Quickchange mutagenesis components for generating the H81A LepA substitution.

Component	Final Concentration
Template	3.2 μg/mL
Primers	1 μM each
10X Pfu buffer	1 X
	(1.5 mM MgCl2)
10 mM dNTPs	0.3 μΜ
Polymerase (Pfu)	0.016 U/ μL
Distilled water	-

Mutagenesis was confirmed by sequencing (Macrogen) and the mutated pET28-lepA plasmids were transformed into BL21-(DE3) *E. coli* competent cells.

3.2.3 Protein expression - BL21-(DE3) competent cells were used for the expression of recombinant 6X-Histidine tagged LepA. Cells were grown in 500 mL LB media supplemented with 50  $\mu$ g/mL of kanamycin at 37°C. Once the OD<sub>600</sub> reached 0.6 OD<sub>600</sub>, LepA overexpression was induced through the addition of 1 mM IPTG (Isopropyl  $\beta$ -D-1-thiogalactopyranoside). The

cultures were grown for another 3 hrs and harvested at 5 000 xg in a TA-10 rotor (Beckman).

Cells were flash frozen and stored at -80°C prior to use.

Expression levels of LepA were analyzed through time samples, lysed in 8 M urea in  $TAKM_7$  and analyzed on a 12% SDS-PAGE run at 200 V for 55 min (BioRad Mini Protean 3 System). Gels were stained with Coomassie blue; all other SDS PAGEs were performed in a similar manner.

3.2.4 LepA Protein purification- Harvested cells containing overexpressed LepA and the H81A LepA mutant were opened in buffer A (50 mM Tris-Cl 8.0 (4°C), 60 mM NH<sub>4</sub>Cl, 7 mM MgCl<sub>2</sub>, 7 mM β-mercaptoethanol, 1 mM PMSF, 300 mM KCl, 10 mM imidazole, 15% glycerol) with the supplement of 0.1 mg/mL of lysozyme, 12.5 mg/g sodium deoxycholate and DNase I and centrifuged at 30 000 xg for 45 min in a JA-16 rotor (Beckman). The cleared lysate (S-30 extract), containing LepA, was purified using affinity chromatography (7 mL Ni-Sepharose resin from GE healthcare) and eluted in a step gradient in buffer C (buffer A supplemented with 250 mM imidazole). The Ni-Sepharose column was washed 10 times with a column volume of buffer C and fractions containing LepA were pooled and concentrated using ultrafiltration (Vivaspin 20 MWCO 30 000 (Sartorius)). LepA was further purified using size exclusion chromatography (preparative Superdex 75 column from GE Healthcare) run in high-salt TAKM, (50 mM Tris-Cl pH 7.5, 70 mM NH<sub>4</sub>Cl, 300 mM KCl, 7 mM MgCl<sub>2</sub> and 10% glycerol). Fractions were analyzed on a 12% SDS-PAGE and fractions containing LepA were pooled and concentrated using ultrafiltration (Vivaspin 20 MWCO 30 000 (Sartorius)). The final concentration of LepA was determined photometrically, at 280 nm using the molar extinction coefficient 39 935 M<sup>-1</sup>cm<sup>-1</sup> (calculated using ProtParam) and using the BioRad microassay.

Chapter 3 LepA

3.2.5 Protein purification of LepA mutants - Harvested cells containing overexpressed LepA CTD truncation mutations were opened in buffer H (50 mM Tris-Cl 8.0 (4°C), 60 mM NH<sub>4</sub>Cl, 7 mM MgCl<sub>2</sub>, 7 mM  $\beta$ -mercaptoethanol, 1 mM PMSF, 300 mM KCl, 10 mM imidazole, 15% glycerol, 8 M urea) with the addition of 0.1 mg/mL of lysozyme, 12.5 mg/g sodium deoxycholate and DNase and centrifuged at 30 000 xg for 45 min in a JA-16 rotor (Beckman). The cleared lysate (S-30 extract) containing the LepA protein of interest was purified using batch affinity chromatography (7 mL Ni-Sepharose resin from GE Healthcare) eluting with a step gradient into buffer I (buffer H supplemented with 250 mM imidazole). The Ni-Sepharose column was washed 10 times with a column volume of buffer I and fractions containing the LepA CTD truncation mutant of interest were pooled and concentrated (Vivaspin 20 MWCO 30 000 (Sartorius)). The LepA CTD truncation mutant was further purified using size exclusion chromatography (160 mL preparative Superdex 75 from GE Healthcare) running the column in high-salt TAKM<sub>7</sub>. Fractions were analyzed on a 12% SDS-PAGE and fractions containing the LepA CTD truncation mutant of interest were pooled and concentrated as above.

3.2.6 Nucleotide hydrolysis assay – To measure ribosome stimulated GTP hydrolysis of LepA and LepA mutants, liberation of  $^{32}$ P<sub>i</sub> from [ $^{32}$ P]-GTP was determined in the following manner. 0.6  $\mu$ M 70S, 1.2  $\mu$ M [ $^{32}$ P]-GTP (specific activity approximately 3500 dpm/pmol) and 0.03  $\mu$ M LepA were incubated at 37°C in a total of 100  $\mu$ L TAKM<sub>7</sub> buffer. At various time points (0 to 45 min) 10  $\mu$ L (0.3 pmol) of LepA•70S reaction mixture was removed and quenched with GTPase quencher (1 M HClO<sub>4</sub> with 3 mM potassium phosphate). 300  $\mu$ L of 20 mM Na<sub>2</sub>Mo<sub>4</sub> and 750  $\mu$ L of ethyl acetate were added to the quenched reaction to extract free  $^{32}$ P<sub>i</sub>. Samples were vortexed for 30 sec and centrifuged at 15 800 xg for 5 min. The aqueous upper layer containing free  $^{32}$ P<sub>i</sub> was extracted and added to 2 mL of scintillation cocktail (MP EcoLite) in 7 mL polyethylene

scintillation vials (PerkinElmer). [<sup>32</sup>P<sub>i</sub>] decays per minute (dpm) were counted with a PerkinElmer TriCarb 2800TR liquid scintillation analyzer. Background radioactivity was subtracted and the percentage of GTP hydrolyzed was calculated and plotted as a function of time.

To determine the  $K_m$  and  $k_{cat}$  for the GTPase activity of LepA compared to EF-G, 0.03  $\mu$ M EF-G/LepA, 50  $\mu$ M [ $\gamma^{32}$ P]-GTP and titrating amounts of 70S (0 to 2  $\mu$ M) were mixed and incubated in TAKM<sub>7</sub> at 37°C. After 10 min the reaction was quenched as above with GTPase quencher and free  $^{32}$ P<sub>i</sub> was extracted and counted as above. The  $K_m$  was calculated as ½ Vmax and  $k_{cat}$  was calculated as the turnover number using Vmax/[protein].

3.2.7 Equilibrium binding constants for guanine nucleotide binding to LepA - To determine guanine nucleotide binding affinities to LepA and mutants of LepA, fluorescence measurements were performed using a Varian Cary Eclipse Fluorescence Spectrophotometer. *E. coli* LepA contains two intrinsic tryptophan residues (Trp 199, Trp 257), which were excited at 280 nm in a 0.3 x 0.3 cm quartz cuvette (Starna) at room temperature. The fluorescence emission was monitored from 300 nm to 500 nm through 5 nm slits. Measurements were carried out using 2  $\mu$ M LepA in TAKM<sub>7</sub> and adding increasing amounts of the respective mant-guanine nucleotide, which is a fluorescent analogue of guanine nucleotides. Mant is a small anthraniloyl aromatic group attached to the 3' or 2'-OH of the ribose on the guanine nucleotide (Figure 3.5).

**Figure 3.5: Mant-GTP.** The 2'-OH in this structure of GTP has a methylanthraniloyl (mant) group attached, however, the 3'-OH and 2'-OH are labelled with mant in an equal ratio.

Fluorescence resonance energy transfer (FRET) between tryptophan and mant was utilized to determine the equilibrium dissociation constants for mant-GTP/GDP to LepA. Changes in the fluorescence emission at 338 nm were plotted as a function of increasing nucleotide concentration. The background fluorescence signals due to the presence of protein and nucleotide were subtracted from the overall fluorescence of the system. Fluorescence changes were plotted against nucleotide concentration ([nt]) were fit with a quadratic function (Equation 1), with respect to the initial (Fl<sub>0</sub>) and maximum (Fl<sub>max</sub>) fluorescence to determine the dissociation constant ( $K_D$ ) for each nucleotide or fluorescent derivative using the software GraphPad Prism 5. Additional variables for total protein concentration ([P]) and signal amplitude (B = Fl<sub>max</sub> – Fl<sub>0</sub>) were accounted for (122).

$$\Delta FI = 0.5(B / [P]) * (K_D + [P] + [nt] - ((K_D + [P] + [nt])^2 - 4 * [P] * [nt])^{1/2})$$
 (Equation 1)

**3.2.8 Retro/forward translocation of tRNA on the ribosome** - Ribosomes (108), EF-Tu, initiation factors (123), EF-G(124), [3H]fMet-tRNA<sup>fMet</sup> (125), [14C]Phe-tRNA<sup>Phe</sup>, and [14C]Val-tRNA<sup>Val</sup> from E. coli were purified individually as indicated (126). In brief, EF-Tu, initiation factors and EF-G were purified using affinity chromatography and size exclusion chromatography. tRNAs were aminoacylated then purified through reverse-phase chromatography, and ribosomes were purified and separated using ultracentrifugation. An initiation complex was prepared by incubating 3 μM [<sup>3</sup>H]fMet-tRNA<sup>fMet</sup>, 1 mM DTT (BioBasic), 1 mM GTP (Sigma), 2 μM 70S, 4 μM mRNA (122 nt derivative of m022 sequence 5'-AUGGUU-3' for fMet-Val and sequence 5'-AUGUUC-3' for fMet-Phe, purified by HPLC) and 3 µM initiation factors in a total volume of 3 mL in TAKM<sub>7</sub> and incubated at 37°C for 50 min. Ternary complexes were prepared by first charging EF-Tu with GTP by mixing 1 mM GTP, 1 mM DTT, 1% pyruvate kinase (PK) (Roche), 3 mM phosphoenol pyruvate (PEP) with 27 μM EF-Tu for 15 min at 37°C in TAKM<sub>7</sub>. The ternary complex was formed by adding 9 µM [14C]Phe-tRNAPhe or [14C]Val-tRNAVal in TAKM7 to the GTPbound EF-Tu complex and incubating for 1 min at 37°C. Pre-translocation complexes were formed by incubating the initiation complex with ternary complex for 1 min at 37°C. This mixture was divided into two, where one half was used to make post-translocation complexes in the following manner; 3 µM EF-G was added to the pre-translocation complex and incubated for 1 min at 37°C. The extent of peptidyl-tRNA binding was determined through nitrocellulose filtration and was found to be >80%. Aliquots of 1 mL of the above mixtures were purified through centrifugation on a 400 µL 1.1 M sucrose cushion in a Sorvall M120GX ultracentrifuge at 259 000 xg for 2 hrs. Pellets containing purified post-translocation complexes were dissolved in TAKM<sub>7</sub> and pellets containing pre-translocation complexes were dissolved in TAKM<sub>20</sub>, flash frozen and stored at -80°C.

Retro-translocation was measured using 0.1  $\mu$ M post-translocation complexes containing [ $^3$ H]fMet[ $^{14}$ C]Val-tRNA $^{Val}$  or [ $^3$ H]fMet[ $^{14}$ C]Phe-tRNA $^{Phe}$  in the P-site. Post-translocation complexes were mixed with 0.5 mM guanine nucleotide, 0.15  $\mu$ M tRNA $^{fMet}$  and 2  $\mu$ M LepA and incubated at 37°C in TAKM $_7$  buffer with 0.6 mM spermine to stabilize tRNA $^{fMet}$  in the E-site.

Forward translocation was analyzed using 0.1  $\mu$ M pre-translocation complex containing [ $^{3}$ H]fMet[ $^{14}$ C]Val-tRNA<sup>Val</sup> or [ $^{3}$ H]fMet[ $^{14}$ C]Phe-tRNA<sup>Phe</sup>. 0.5 mM guanine nucleotide and 2  $\mu$ M LepA were mixed with pre-translocation complexes and incubated at 37°C in TAKM<sub>7</sub> buffer.

In order to assess A-site occupancy on pre/post-translocation complexes, an excess of a small analogue of aa-tRNA (puromycin) was added to 15  $\mu$ L (4 pmol) of the ribosomal complexes and incubated for 15 sec at 37°C. If the A-site is unoccupied, puromycin can bind to the 50S A-site and form a peptide bond with the polypeptide in the P-site. The reaction was stopped with 1.5 M sodium acetate (pH 4.5) saturated with magnesium sulfate. Puromycin was extracted with ethyl acetate and the formation of peptidyl-puromycin was assessed through [ $^3$ H]fMet and [ $^{14}$ C]Phe radioactivity, which are attached to the extracted puromycin. Decays per minute (dpm) were counted after the addition of scintillation cocktail (LumaSafe Plus - Zinsser) in 7 mL polyethylene scintillation vials (Zinsser).

3.2.9 Ribosomal subunit dissociation - Pre-termination complexes were prepared by combining 8  $\mu$ M mRNA (UUC sequence), 4  $\mu$ M tRNA<sup>Phe</sup> from yeast (chemical block) and 2  $\mu$ M 70S in TAKM<sub>7</sub> buffer and incubating at 37°C for 20 min. Pre-termination complexes were rapidly mixed (55  $\mu$ L each) with a factor mix of 10  $\mu$ M RRF, 4  $\mu$ M IF3, 1 mM GTP and 4  $\mu$ M EF-G or 4  $\mu$ M LepA. Dissociation of ribosomal complexes was measured through light scattering at 430 nm on a SX-18MV stopped-flow (Applied Photophysics) apparatus. Measurements contained 1000 data

Chapter 3 LepA

points each. Scattering was detected through 2 photomultipliers using a KV400 cut-off filter (Schott).

Traces were fit with a two-exponential decay (equation 2) using GraphPad Prism5 software. B is the fluorescence end level where  $x\rightarrow\infty$ ,  $k_1$  is the rate constant for the fast decay and  $k_2$  is the rate constant for the slow decay. C is the amplitude for the fast decay and D is the amplitude for the slow decay.

$$Y=B+C*exp(-k_1*x)+D*exp(-k_2*x)$$
 (Equation 2)

### 3.3 Results

3.3.1 Guanine nucleotide binding properties of LepA - All GTPases bind guanine nucleotides with various affinities ranging from nM to  $\mu$ M (127). EF-Tu binds guanine nucleotides on the nM scale (69) and requires the guanine nucleotide exchange factor EF-Ts (92) for efficient exchange of guanine nucleotides to facilitate *in vivo* translation rates. However, EF-G binds guanine nucleotides with an affinity on the  $\mu$ M scale (124) and does not require an exchange factor because dissociation and exchange of guanine nucleotides is fast enough to facilitate *in vivo* translation rates. Therefore, it is important to determine the binding affinity of guanine nucleotides to LepA to assess if an exchange factor is needed.

Analysing the nucleotide binding properties will allow the assessment of whether the LepA CTD truncation mutants are properly folded. Since the LepA CTD truncation mutants were purified in 8 M urea and exchanged to high-salt TAKM<sub>7</sub>, folding of the mutants may have been inhibited by the presence of urea disrupting hydrogen bonds. However, the G-domain of LepA is a large

portion of the protein (comprising 31% of the protein) and is the site for GTP hydrolysis. Therefore, the ability of the G-domain to bind guanine nucleotides will be a strong indication on whether the LepA CTD truncation mutants are properly folded. Fluorescence spectroscopy measurements were used to study the equilibrium binding properties of guanine nucleotides to purified LepA. Increasing amounts of guanine nucleotides (mant derivatives) were titrated into a 2 μM LepA TAKM<sub>7</sub> solution and FRET was monitored (Figure 3.6). Addition of mant-guanine nucleotides resulted in a decrease of tryptophan fluorescence ( $\lambda_{emission}$  = 338 nm) and an increase in mant fluorescence ( $\lambda_{emission}$  = 440 nm) (Figure 3.6), indicating binding of the guanine nucleotide to LepA. The equilibrium dissociation constants (KD) were determined by fitting the concentration dependence of tryptophan/mant fluorescence (see experimental procedures 3.2.7). Resulting  $K_D$  values for LepA wild type for mant-GDP and mant-GTP to be 37  $\mu$ M and 65 μM respectively (Table 3.8). Similar equilibrium dissociation constants of mant-GTP/GDP were obtained for the LepA CTD truncation mutants and the mutant LepA H81A (Table 3.8), therefore, it can be assumed that the CTD truncation mutants are properly folded. Furthermore, due to the relative similar affinities for mant-GTP and mant-GDP for LepA, an exchange factor is not likely required and turnover of the nucleotide can be driven by the 10 fold higher cellular concentration of the tri-phosphate form of the nucleotide. Also, the  $K_D$  is on the  $\mu M$  scale, indicating a relatively weak interaction of LepA with guanine nucleotides.

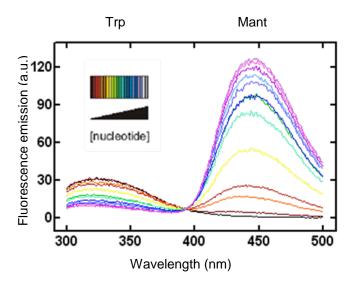


Figure 3.6: Equilibrium dissociation constants of mant-GTP/GDP to LepA. Increasing amounts of mant-nucleotide was added to a 2  $\mu$ M solution of LepA. LepAs intrinsic tryptophans were excited at 280 nm and the resulting fluorescence emission was monitored from 300 nm to 500 nm. The black trace represents LepA in TAKM<sub>7</sub> with no mant-GTP and the purple upper most trace is LepA in TAKM<sub>7</sub> with 100  $\mu$ M mant-GTP. All traces in-between are increasing concentrations of mant-GTP from 0 to 100  $\mu$ M and are shown in the side.

Table 3.8: Equilibrium binding constants of mant-GTP/GDP for LepA and LepA mutations.

Protein	K <sub>D</sub> GTP	K <sub>D</sub> GDP
LepA (Wild Type)	37 ± 3 μM	65 ± 22 μM
LepA (ΔA494)	74 ± 9 μM	88 ± 2 μM
LepA (ΔP520)	96 ± 4 μM	91 ± 5 μM
LepA (ΔG555)	95 ± 10 μM	76 ± 1 μM
LepA (H81A)	76 ± 8 μM	47 ± 4 μM
EF-G (128)	0.67 μΜ	12 μΜ

**3.3.2 GTPase activity of LepA in the presence of 70S ribosomes** – LepA is thought to be a translational GTPase with comparable activity to EF-G (79). Therefore, intrinsic GTPase activity

of LepA is expected to be low and the presence of the 70S ribosome is expected to increase the GTPase activity significantly. Furthermore, based on structural similarity of LepA to EF-Tu (79), it is likely that His 81 is the critical residue in LepA for GTP hydrolysis. Furthermore, it is unknown whether the CTD of LepA takes part in GTPase activation. Therefore, the GTPase activity of LepA, H81A, and the CTD truncation mutations in the presence of the 70S ribosome have been analyzed and compared to EF-G. A GTP hydrolysis assay described in experimental procedures 3.2.6 were used to assess the GTPase activity of LepA and LepA mutants in the presence and absence of 70S ribosomes. The GTPase activity of wild type LepA is dramatically stimulated by the ribosome (Figure 3.7) since no efficient GTP hydrolysis could be observed in the absence of 70S ribosomes. However, H81A and all the CTD truncation mutations do not show efficient hydrolysis of GTP even in the presence of the 70S ribosome (Figure 3.7). Previous studies of EF-Tu have shown that His 84 of EF-Tu helps to stabilize the transition state of GTP hydrolysis and is a critical residue for GTP hydrolysis (101), as substitution of His 84 in EF-Tu abolishes GTP hydrolysis activity in EF-Tu. These results are consistent with our hypothesis that His 81 is a critical residue in LepA required for ribosome stimulated GTPase activity. The results for the CTD truncation mutants show that they are unable to hydrolyze GTP in the presence of 70S ribosome. This suggests that the CTD of LepA may be involved in signalling GTPase activation in LepA.

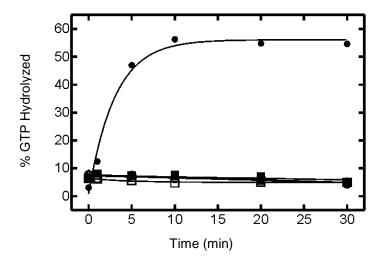


Figure 3.7: Ribosome stimulated GTPase activity of LepA and LepA mutants. GTP hydrolysis seen in the presence of LepA and 70S (closed circles), LepA (open circles), LepA  $\Delta$ A494 and 70S (closed triangle), LepA  $\Delta$ G555 and 70S (open triangle), LepA  $\Delta$ P520 and 70S (closed square), LepA H81A and 70S (open square).

The recently determined cryo-EM structure of LepA bound to the ribosome revealed several interactions of LepA with the factor binding site, similar to other translational GTPases (117). For example, domain V of LepA seems to contact the 50S ribosomal protein L11 and the 23S rRNA, similar to EF-G (117). Interestingly, residues Asn 503 - Asn 506 in LepA's unique CTD contact the 23S rRNA. The CTD of LepA also contacts the acceptor stem and the elbow region of the retrotranslocated A-site tRNA. In the absence of the CTD, the interactions between LepA's CTD and the ribosome may be lost, thereby destabilizing LepA binding to the ribosome.

In order to compare the ribosome stimulated GTPase activity of LepA to EF-G, the  $K_m$  for GTPase activation was determined (see experimental procedures 3.2.6). Rates of GTP hydrolysis were plotted as a function of increasing ribosome concentration (Figure 3.8). The  $K_m$  of LepA was

determined to be  $0.3 \pm 0.1 \,\mu\text{M}$  and  $0.14 \pm 0.01 \,\mu\text{M}$  for EF-G. To measure the catalytic efficiency of LepA compared to EF-G,  $k_{cat}/K_m$ , was also determined and was  $399 \pm 134 \,\mu\text{M}^{-1}\text{s}^{-1}$  for LepA and  $355 \pm 215 \,\mu\text{M}^{-1}\text{s}^{-1}$  for EF-G, which are comparable to each other. This strengthens the argument that the ribosome stimulated GTPase activity of LepA is similar to EF-G (129).

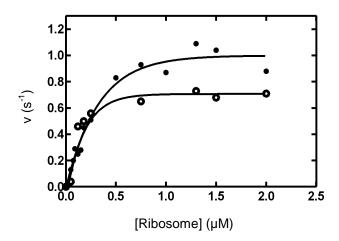


Figure 3.8: Michaelis–Menten analysis of LepA and EF-G ribosome stimulated GTP hydrolysis. A representative plot of the initial rate of GTPase activity for LepA (filled circles) and EF-G (open circles) plotted against increasing 70S ribosome concentration, give a  $K_m$  of 0.3  $\pm$  0.1  $\mu$ M and 0.14  $\pm$  0.01  $\mu$ M respectively.

3.3.3 Retro/Forward-translocation in the presence of LepA – Since LepA is a novel protein there are many questions regarding the function of it. LepA has been suggested to be involved in catalysis of retro-translocation (79). However, the mechanistic details of this process are unknown, as well as why this process may occur in the cell. Therefore, it is necessary to understand the basic mechanism by which retro-translocation is catalyzed before any details can be determined. The extent of retro-translocation in the presence of LepA was determined using two different post-translocation ribosomal complexes in order to assess whether LepA has a preference for a specific post-translocation complex (see experimental procedures 3.2.8). In

addition, various guanine nucleotides (GDP, GTP and GDPNP a non-hydrolysable form of GTP) were used to identify the catalytic functional state of LepA.

To assess the extent and rate of retro-translocation of peptidyl-tRNA within the ribosome a post-translocated ribosomal complex was used and the occupancy of the 50S ribosomal subunits A-site over time was probed with puromycin. Rates of retro-translocation for [ $^3$ H]fMet[ $^{14}$ C]PhetRNAPhe P-site occupied ribosomal complexes were measured in the presence of LepA and various guanine nucleotides (Figure 3.9). Retro-translocation can occur spontaneously in the absence of LepA at a rate of 0.04  $\pm$  0.01 min $^{-1}$ . When LepA is in complex with GDP, no catalysis of retro-translocation occurs, reflected by a rate of 0.02  $\pm$  0.01 min $^{-1}$ , which is comparable to spontaneous retro-translocation. However, in the presence of LepA•GDPNP retro-translocation seems to be catalyzed and occurs at a rate of 0.10  $\pm$  0.02 min $^{-1}$  (Table 3.9). Interestingly, LepA•GTP has an extremely lower rate of retro-translocation (0.00001 min $^{-1}$ ), i.e. this complex seems to inhibit retro-translocation.

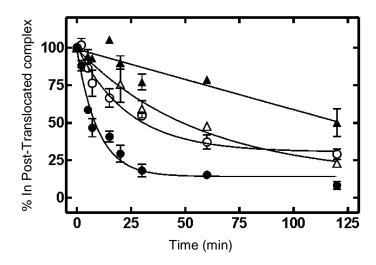


Figure 3.9: Retro-translocation of [ $^3$ H]fMet[ $^{14}$ C]Phe-tRNAPhe in the presence and absence of LepA and guanine nucleotides. Retro-translocation of 0.1  $\mu$ M Post[ $^3$ H]fMet[ $^{14}$ C]Phe-tRNAPhe ribosomal complex in TAKM $_7$ , 0.6 mM spermine buffer and 0.15  $\mu$ M tRNAPhet (open circles) in the presence of 0.1  $\mu$ M LepA wt and 0.5 mM GDPNP (closed circles), 0.1  $\mu$ M LepA wt and 0.5 mM GTP (closed triangles), 0.1  $\mu$ M LepA wt and 0.5 mM GDP (open triangles).

Similarly, the [ $^3$ H]fMet[ $^{14}$ C]Val-tRNA<sup>Val</sup> P-site occupied post-translocation complex showed that catalysis of retro-translocation occurs only in the presence of LepA•GDPNP (Figure 3.10, Table 3.9), with a rate of 0.84  $\pm$  0.07 min $^{-1}$ . Furthermore, LepA•GDP showed a similar rate of retro-translocation (0.31  $\pm$  0.06 min $^{-1}$ ) as spontaneous retro-translocation (0.45  $\pm$  0.06 min $^{-1}$ ) (Table 3.9), which is significantly faster than the [ $^3$ H]fMet[ $^{14}$ C]Phe-tRNA<sup>Phe</sup> P-site occupied complex. However, in the presence of LepA•GTP a comparable rate of retro-translocation (0.30  $\pm$  0.06 min $^{-1}$ ) to the spontaneous rate was observed.

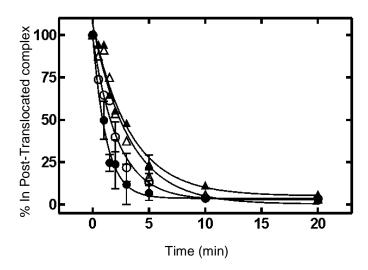


Figure 3.10: Retro-translocation of [ $^3$ H]fMet[ $^{14}$ C]Val-tRNA $^{Val}$  in the presence and absence of LepA and guanine nucleotides. Retro-translocation of 0.1  $\mu$ M Post [ $^3$ H]fMet[ $^{14}$ C]Val-tRNA $^{Val}$  ribosomal complex in TAKM $_7$ , 0.6 mM spermine buffer and 0.15  $\mu$ M tRNA $^{fMet}$  (open circle) in addition to 0.1  $\mu$ M LepA wild type (wt) and 0.5 mM GDPNP (closed circles), 0.1  $\mu$ M LepA wt and 0.5 mM GDP (open square).

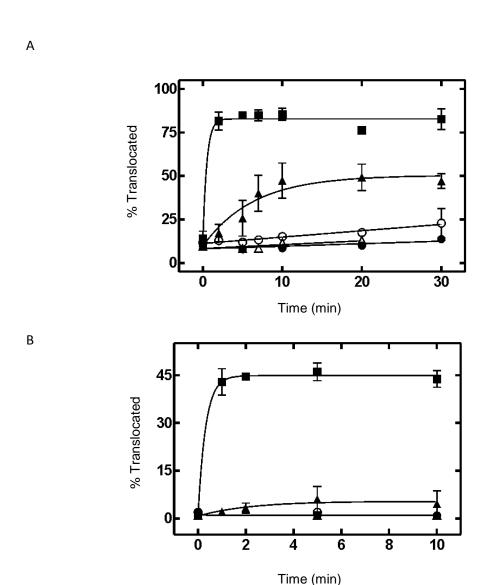
Chapter 3 LepA

Table 3.9: Retro-Translocation assay in the presence and absence of LepA, various guanine nucleotides and LepA mutants.

Component	k <sub>app</sub> [ <sup>3</sup> H]fMet[ <sup>14</sup> C]Phe-tRNA <sup>Phe</sup>	k <sub>app</sub> [ <sup>3</sup> H]fMet[ <sup>14</sup> C]Val-tRNA <sup>Val</sup>
LepA•GDPNP	0.10 ± 0.02 min <sup>-1</sup>	0.84 ± 0.07 min <sup>-1</sup>
LepA•GDP	0.02 ± 0.01 min <sup>-1</sup>	0.31 ± 0.06 min <sup>-1</sup>
LepA•GTP	0.00001 min <sup>-1</sup>	0.30 ± 0.06 min <sup>-1</sup>
Buffer	0.04 ± 0.01 min <sup>-1</sup>	0.45 ± 0.06 min <sup>-1</sup>
LepA(ΔA494)•GDPNP	0.02 ± 0.01 min <sup>-1</sup>	0.27 ± 0.01 min <sup>-1</sup>
LepA(ΔG555)•GDPNP	0.04 ± 0.01 min <sup>-1</sup>	0.51 ± 0.2 min <sup>-1</sup>
LepA(H81A)•GDPNP	0.04 ± 0.01 min <sup>-1</sup>	0.52 ± 0.06 min <sup>-1</sup>

Inhibition of retro-translocation in the presence of LepA•GTP shown here in conjunction with LepA's structural similarity to EF-G (Figure 3.2), suggested an analysis on the ability of LepA to catalyze forward translocation in the presence of guanine nucleotides. This was performed using a pre-translocation complex where the occupancy of the ribosomal A-site was analyzed over time with puromycin (see experimental procedure 3.2.8). In the pre-translocation complex with [³H]fMet[¹⁴C]Phe-tRNAPhe in the A-site of the ribosome, the absence of LepA did not show any significant forward translocation of the ribosomal complex (Figure 3.11a). Also, in the presence of LepA•GDP and LepA•GDPNP, forward translocation of the ribosomal complex was not observed. However, the presence of EF-G•GTP showed rapid translocation, indicating that translocation of this ribosomal complex can occur under certain conditions. However, forward

translocation catalyzed by LepA•GTP only reaches 50% of the extent as translocation catalyzed by EF-G•GTP. Furthermore, the rate at which forward translocation occurs in the presence of LepA•GTP is slower than in the presence of EF-G•GTP. In the pre-translocation complex with [³H]fMet[¹⁴C]Val-tRNA<sup>Val</sup> occupying the ribosomal A-site, similar results were obtained as in the [³H]fMet[¹⁴C]Phe-tRNA<sup>Phe</sup> pre-translocation complex (Figure 3.11b). However, forward translocation was only observed for the [³H]fMet[¹⁴C]Val-tRNA<sup>Val</sup> A-site occupied pre-translocation complex in the presence of EF-G•GTP and no forward translocation was detected in the presence of LepA•GTP (Figure 3.11b).



**Figure 3.11: Forward translocation in the presence and absence of LepA.** Forward translocation of 0.1 μM pre-ribosomal complex in TAKM $_7$  (a) [ $^3$ H]fMet[ $^{14}$ C]Phe-tRNA $^{Phe}$  A-site occupied pre-translocation complex in the presence of 0.6 mM spermine buffer (open circles), in addition to 0.1 μM EF-G and 0.5 mM GTP (closed squares), 0.1 μM LepA wt and 0.5 mM GTP (closed triangles), 0.1 μM LepA wt and 0.5 mM GDP (open triangles), 0.1 μM LepA wt and 0.5mM GDPNP (closed circle) (b) [ $^3$ H]fMet[ $^{14}$ C]Val-tRNA $^{Val}$  A-site occupied pre-translocation complex in TAKM $_7$  supplemented with 0.6 mM spermine buffer (open circles) in the presence of 0.1 μM EF-G and 0.5 mM GTP (closed squares), 0.1 μM LepA wt (closed triangles), 0.1 μM LepA wt and 0.5 mM GDP (open triangles), 0.1 μM LepA wt and 0.5 mM GDPNP (closed circle).

The CTD of LepA is unique and its function is unknown (*79*). To analyze its role during catalysis of retro-translocation, rates of retro-translocation of post-translocation complexes in the presence of CTD truncation mutants LepA (ΔA494, ΔG555) bound to GDPNP (Figure 3.12) were measured and compared to wild type LepA•GDPNP. For both the [³H]fMet[¹⁴C]Phe-tRNA<sup>Phe</sup> and the [³H]fMet[¹⁴C]Val-tRNA<sup>Val</sup> P-site occupied post-translocation ribosomal complexes, no catalysis of retro-translocation was observed in the presence of the LepA CTD truncation mutants and GDPNP (Table 3.9, Figure 3.12).

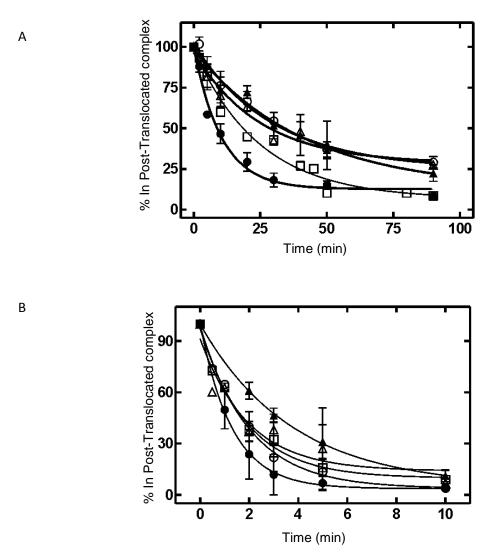


**Figure 3.12: Retro-translocation in the presence of LepA mutants.** Retro-translocation of (a) [ $^3$ H]fMet[ $^{14}$ C]Phe-tRNA $^{Phe}$  P-site occupied 70S complex in TAKM $_7$  and 0.6 mM spermine buffer (b) [ $^3$ H]fMet[ $^{14}$ C]Val-tRNA $^{Val}$  P-site occupied 70S complex in TAKM $_7$  and 0.6 mM spermine buffer in the presence of 0.5 mM GDPNP, 0.15 μM tRNA $^{fMet}$  (open circles), 0.5 mM GDPNP, 0.15 μM tRNA $^{fMet}$  and 2 μM LepA (closed circles), 0.5 mM GDPNP, 0.15 μM tRNA $^{fMet}$  and 2 μM LepA ΔG555 (open triangle), 0.5 mM GDPNP, 0.15 μM tRNA $^{fMet}$  and 2 μM LepA ΔG555 (open triangle), 0.5 mM GDPNP, 0.15 μM tRNA $^{fMet}$  and 2 μM LepA AG555 (open triangle), 0.5 mM GDPNP, 0.15 μM tRNA $^{fMet}$  and 2 μM LepA AG555 (open triangle), 0.5 mM GDPNP, 0.15 μM tRNA $^{fMet}$  and 2 μM LepA H81A (open square).

3.3.4 Ribosomal subunit dissociation - The structural similarity between LepA and EF-G are a strong indication that both proteins may share similar functions. EF-G not only catalyzes forward

translocation, but also participates in ribosome recycling (80). The ability of LepA to catalyze forward translocation as well as its similarity in structure to EF-G, suggest a role of LepA in ribosome recycling. LepAs ability to promote 70S dissociation of a pre-termination complex into the respective 30S and 50S subunits was observed using light scattering (see experimental procedure 3.2.9). In the presence of RRF, IF3 and EF-G, the rate of ribosomal subunit dissociation was determined to be  $0.608 \pm 0.037s^{-1}$  (Figure 3.13). However, no subunit dissociation could be observed in the presence of LepA under these conditions.

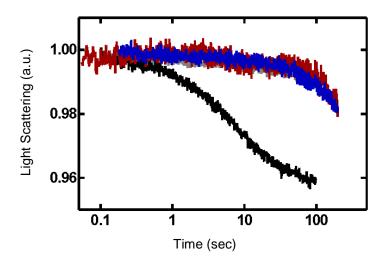


Figure 3.13: 70S dissociation measured by light scattering. The dissociation of the 70S ribosome into the 30S and 50S ribosomal subunits was measured using light scattering over time. 2  $\mu$ M 70S pre-termination complexes were rapidly mixed with 10  $\mu$ M RRF, 4  $\mu$ M IF3, 1 mM GTP and 4  $\mu$ M EF-G (black), 10  $\mu$ M RRF and 4  $\mu$ M IF3 (red), 10  $\mu$ M RRF, 4  $\mu$ M IF3 and 4  $\mu$ M LepA (blue), TAKM<sub>7</sub> (grey).

### 3.4 Discussion and future directions

The present results show that LepAs GTPase activity is stimulated by the ribosome to an extent that is comparable to EF-G, which is consistent with previous studies of the GTPase activity of LepA (79). Also, LepA binds guanine nucleotides with a weak affinity (K<sub>D</sub> of approximately 50

μM), also comparable to EF-G. Furthermore, the LepA•GDPNP complex is able to catalyze retrotranslocation in two different post-translocation ribosomal complexes ([³H]fMet[¹⁴C]Val-tRNA<sup>Val</sup> P-site occupied and [³H]fMet[¹⁴C]Phe-tRNA<sup>Phe</sup>P-site occupied). Catalysis, however, only occurs in the presence of LepA•GDPNP, deacyl-tRNA and spermine to stabilize deacyl-tRNA. This is surprising since deacyl-tRNA is only abundant in the cells when the cell is starved for amino acids (*130*). Therefore it is intriguing to speculate that catalysis of retro-translocation with LepA may only occur under stress conditions *in vivo*.

Due to misleading figures and legends in the previous literature (79), it is unclear whether GDPNP or GTP was used in those studies. GDPNP is a non-hydrolysable form of GTP, which locks LepA • GDPNP in its GTP conformation, suggesting that this is the conformation that promotes retro-translocation. Interestingly, retro-translocation was inhibited when LepA was in complex with GTP and forward translocation was promoted for the [3H]fMet[14C]Phe-tRNAPhe complex. GTP hydrolysis is required for the rapid turnover of forward translocation seen in the presence of EF-G (78). Also, domain IV of EF-G has previously been shown to be important for coupling GTP hydrolysis with forward translocation (75). Furthermore, it has been shown in previous studies that in the absence of EF-G and in the presence of deacyl-tRNA<sup>fMet</sup> spontaneous retrotranslocation of [3H]fMet[14C]Val-tRNAVal and [3H]fMet[14C]Phe-tRNAPhe P-site occupied ribosomal complex will occur in the majority and 75% of complexes respectively (109). Since LepA bound to GDPNP resembles its GTP bound form, this state may promote an open conformation of the ribosome, which leads to the formation of a thermodynamically stable state of tRNA within the ribosome, i.e. the pre-translocation state under our experimental conditions. In the case of EF-G, following unlocking of the ribosome and forward translocation, domain IV of EF-G prevents retro-translocation by inserting itself into the A-site of the ribosome

(120). LepA lacks a homologous domain to the full length of EF-G's domain IV, which may explain why retro-translocation takes place in the presence of LepA and why forward translocation in the presence of LepA•GTP is limited. However, the mechanistic details of retro-translocation are still unknown and a highly purified *E. coli* based *in vitro* translation system will be used in the future to further analyze retro-translocation. Pre-steady state kinetics will be performed along the lines of those previously used to analyze EF-G's function (120).

Role of Histidine 81 - Due to homology of LepA to EF-Tu (Figure 3.1), His 81 likely plays a functional role similar to His 84 in EF-Tu (101). Substitution of His 81 in LepA resulted in elimination of ribosome stimulated GTPase activity without effecting guanine nucleotide binding. These observations suggest that His 81 of LepA is directly involved in GTP hydrolysis and not in guanine nucleotide binding. The fact that LepA H81A does not catalyze retro-translocation suggests two possible explanations. Either this mutant does not bind to the ribosome, or H81A prevents necessary interactions between the ribosome and LepA for GTPase activation, which may be needed to catalyze retro-translocation. Therefore, binding to the ribosome must be assessed before any further conclusions can be made.

Forward translocation stimulated by LepA•GTP is only seen for the fMetPhe-tRNA<sup>Phe</sup> A-site occupied system. Furthermore, the only mechanism separating GDPNP and GTP is the fact that GTP can be hydrolyzed. GTP hydrolysis catalyzed by EF-G on the ribosome greatly accelerates the rate of ribosome rearrangement, leading to catalyzed translocation (75). LepA may function in a similar manner and it would be interesting to see how forward translocation is affected by the H81A LepA mutant.

Role of the unique CTD of LepA – When parts of the CTD were removed, no stimulation of GTPase activity was observed in the presence of the 70S ribosome. Proper folding of the truncation mutations was verified as guanine nucleotides bound to the mutants with similar K<sub>D</sub>'s as the wild type. The recent structure of LepA bound to the ribosome shows the CTD of LepA contacting the 23S rRNA of the ribosome as well as the retro-translocated A-site tRNA (117). Upon removal of the CTD, these interactions may be lost, leading to a reduced affinity of LepA for the ribosome, explaining loss of GTPase activity and retro-translocation. Therefore, the affinity of these mutants to the ribosome must be assessed. If the CTD does not affect LepA binding to the ribosome, the CTD may be essential in downstream signalling for GTP hydrolysis required for retro-translocation. However, details of the mechanism for retro-translocation need to be determined before the role of the CTD in the signalling of GTP hydrolysis can be analyzed.

Currently, the crystal structure of LepA (118) and the cryo-EM (117) of LepA on the ribosome only resolve LepA residues up to 555, leaving 43 residues at the CTD of LepA which are unresolved.

Potential role of LepA in 70S ribosome dissociation – The observation that forward translocation occurs in the presence of LepA•GTP together with LepA's structural similarity to EF-G indicate that LepA may function in more than just retro-translocation. Light scattering results, targeting a putative role of LepA in the dissociation of the 70S subunits into the 50S and 30S indicate that LepA cannot substitute EF-G in catalyzing subunit dissociation.

#### 3.5 Conclusion

The eukaryotic elongation cycle closely resembles elongation in prokaryotes. However, it is interesting that there is no homologous LepA protein in the eukaryotic cytosol, as LepA is potentially involved in a process which occurs during elongation. It has previously been shown that retro-translocation does not fix translation errors induced by antibiotics (79), but does seem to improve the activity of proteins. Perhaps improper translocation occurred more often in ancestral times, and as evolution proceeded the cell developed other regulatory methods to improve translocation and eliminate the need for retro-translocation. Therefore, if an error occurs during translocation, such as a shift of the reading frame, it may be more efficient for the cell to reverse and try again than to start over. However, the mechanistic details of retro-translocation and possible intermediates are still unknown and need to be analyzed before retro-translocation can be understood.

The fact that LepA is not found in eukaryotes makes it a promising target for antibiotics. Due to the structural similarity of LepA to EF-G, it is likely that LepA is a target for antibiotics which target EF-G, such as fusidic acid. Fusidic acid inhibits the dissociation of EF-G•GDP from the ribosome (131) and may also prevent LepA•GDP from dissociating from the ribosome. In turn this may affect retro-translocation as well.

## References

- 1. Jacob, F., and Monod, J. (1961) Genetic regulatory mechanisms in the synthesis of proteins., *Journal of Molecular Biology 3*, 318-356.
- 2. Poole, A. M., Phillips, M. J., and Penny, D. (2003) Prokaryote and eukaryote evolvability., *BioSystems 69*, 163-185.
- 3. Crick, F. H. C. (1966) Codon-anticodon pairing: the wobble hypothesis., *Journal of Molecular Biology* 19, 548-555.
- 4. Hoagland, B. M., Stephenson, M. L., Scott, J. F., Hecht, L. I., and Zamecnik, P. C. (1957) A soluble ribonucleic acid intermediate in protein synthesis., *Journal of Biological Chemistry 231*, 241-257.
- 5. Holmquist, R., Jukes, T. H., and Pangburn, S. (1973) Evolution of transfer RNA, *JMB 1973*, 91-116.
- 6. Holley, R. W., Everett, G. A., Madison, J. T., and Zamir, A. (1965) Nucleotide sequences in the yeast alanine transfer ribonucleic acid, *J. Biol Chem. 240*, 2122-2128.
- 7. Holley, R. W., Apgar, J., Everett, G. A., Madison, J. T., Marquisee, M., Merrill, S. H., Penswick, J., and Zamis, A. (1965) Structure of a ribonucleic acid., *Science 147*, 1462-1465.
- 8. Sussman, J. L., Holbrook, S. R., Warrant, R. W., Church, G. M., and Kim, S.-H. (1978) Crystal structure of yeast phenylalanine transfer RNA I. Crystallographic refinement, 1978 123, 607-630.
- 9. Kim, S. H., Quigley, G. J., Suggath, F. L., McPherson, A., Sneden, D., Kim, J. J., Weinzierl, J., and Rich, A. (1973) Three-dimensional structure of yeast phenylalanine transfer RNA: folding of the polynucleotide chain., *Science 179*, 285-288.
- 10. Hou, Y.-M. (1997) Discriminating among the discriminator bases of tRNAs., *Chemistry & Biology 4*, 93-96.
- 11. Crothers, D. M., Seno, T., and Soll, G. (1972) Is there a discriminator site in transfer RNA?, *PNAS 69*, 3063-3067.
- 12. Jakubowski, H. (1994) Energy cost of translational proofreading in vivo. The aminoacylation of transfer RNA in Escherichia coli., *Annals of the New York Academy of Sciences 30*, 4-20.
- 13. Soll, D. (1990) The accuracy of aminoacylation-ensuring the fidelity of the genetic code., *Experientia 46*, 1089-1096.
- 14. Bacher, J. M., de Crecy-Lagard, V., and Schimmel, P. R. (2004) Inhibited cell growth and protein functional changes from an editing-defective tRNA synthetase., *PNAS 102*, 1697-1701.
- 15. Fersht, A. R., and Dingwall, C. (1979) Evidence for the double-sieve editing mechanism in protein synthesis. Steric exclusion of isoleucine by valyl-tRNA synthetases., *Biochemistry* 18, 2627-2631.
- 16. Lengyel, P., and Soll, D. (1969) Mechanism of Protein Biosynthesis, *Bacteriological Reviews 33*, 264-301.
- 17. Cech, T. R. (2000) The Ribosome is a Ribozyme., *Science 289*, 878-879.
- 18. Rheinberger, H. J., Sternbach, H., and Nierhaus, K. H. (1981) Three tRNA binding sites on Escherichia coli ribosomes., *PNAS 78*, 5310-5314.

- 19. Wettstein, F., and Noll, H. (1965) Binding of transfer ribonucleic acid to ribosomes engaged in protein synthesis: number and properties of ribosomal binding sites., *J. Mol. Biol.* 11, 35-53.
- 20. Yusupov, M. M., Yusupov, G. Z., Bauchom, A., Lieberman, K., Earnest, T. N., Cate, J. H., and Noller, H. F. (2001) Crystal structure of the ribosome at 5.5A resolution., *Science* 292, 883-896.
- 21. Tissieres, A., and Watson, J. D. (1958) Ribonucleoprotein particles from Escherichia coli., *Nature 182*, 778-780.
- 22. Lovmar, M., and Ehrenberg, M. (2006) Rate, accuracy and cost of ribosomes in bacterial cells., *Biochimie 88*, 951-961.
- 23. Berk, V., and Cate, J. H. (2007) Insights into protein biosynthesis from structures of bacterial ribosomes, *Current Opinion in Structural Biology* 17, 302-309.
- 24. Al-Karadaghi, S., Kristensen, O., and Liljas, A. (2000) A decade of progress in understanding the structural basis of protein synthesis, *Progress in Biophysics and Molecular Biology* 73, 167-193.
- 25. Gegenheimer, P., and Apirion, D. (1980) Precursors to 16S and 23S ribosomal RNA from a ribonuclear III-strain of Escherichia coli contain intact RNase III processing sites., *Nucleic Acids Research 8*, 1873-1891.
- 26. Li, Z., Pandit, S., and Deutscher, M. P. (1999) RNase G and RNase E are both required for the 5' maturation of 16S ribosomal RNA., *EMBO* 18, 2878-2885.
- 27. Li, Z., Pandit, S., and Deutscher, M. P. (1999) Maturation of 23S ribosomal RNA requires the exoribonuclease RNase T., *RNA 5*, 139-146.
- 28. Spierer, P., Wang, C. C., Marsh, T. L., and Zimmermann, R. A. (1979) Cooperative interactions among protein and RNA components of the 50S ribosomal subunit of Escherichia coli., *Nucleic Acids Research 6*, 1669-1682.
- 29. Mizushima, S., and Normura, M. (1970) Assembly mapping of 30S ribosomal proteins from Escherichia coli., *Nature 226*, 1214.
- 30. Bharat, A., Jiang, M., Sullivan, S. M., Maddock, J. R., and Brown, E. D. (2006) Cooperative and critical roles for both G domains in the GTPase activity and cellular function of ribosome-associated Escherichia coli EngA., *Journal of Bacteriology* 188, 7992-7996.
- 31. Brown, E. D. (2005) Conserved P-loop GTpases of unknown function in bacteria: an emerging and vital ensemble in bacterial physiology., *Biochem Cell Biol. 83*, 738-746.
- 32. Kopylov, A. M. (2002) X-Ray Analysis of Ribosomes: the Static of the Dynamic, *Biochemistry 67*, 372-382.
- 33. Schluenzen, F., Tocilj, A., Zarivach, R., Harms, J. M., Gluehmann, M., Janell, D., Bashan, A., Bartels, H., Agmon, I., Franceschi, F., and Yonath, A. (2000) Structure of functionally activated small ribosomal subunit at 3.3 angstroms resolution., *Cell* 102, 615-623.
- 34. Kaltschmidt, E., and Wittmann, H. G. (1970) Ribosomal Proteins, XII. Number of Proteins in Small and Large ribosomal subunits of Escherichia coli as Determined by Two-dimensional gel electrophoresis., *PNAS 67*, 1276-1282.
- 35. Takyar, S., Hickerson, R. P., and Noller, H. F. (2005) mRNA Helicase Activity of the Ribosome, *Cell* 120, 49-58.
- 36. Yusupova, G. Z., Yusupov, M. M., Cate, J. H., and Noller, H. F. (2001) The path of messenger RNA through the ribosome, *Cell* 106, 233-241.

- 37. Noller, H. F. (2006) Biochemical characterization of the ribosomal decoding site, *Biochimie 2006*, 935-941.
- 38. Ogle, J. M., Brodersen, D. E., Clemons, W. M. J., Tarry, M. J., Carter, A. P., and Ramakrishnan, V. (2001) Recognition of Cognate Transfer RNA by the 30S Ribosomal Subunit., *Science* 292, 897-902.
- 39. Ramakrishnan, V. (2002) Ribosome Structure and the Mechanism of Translation, *Cell* 108, 557-572.
- 40. Ban, N., Nissen, P., Hansen, J., Capel, M., Moore, P. B., and Steitz, T. A. (1999) Placement of protein and RNA structures into a 5A-resolution map of the 50S ribosomal subunit., *Nature 400*, 841-847.
- 41. Agrawal, R. K., Penczek, P., Grassucci, R. A., and Frank, J. (1998) Visualization of elongation factor G on the Escherichia coli 70S ribosome: The mechanism of translocation., *PNAS 95*, 6134-6138.
- 42. Selmer, M., Dunham, C. M., Murphy, F. V. t., Weixlbaumer, A., Petry, S., Kelley, A. C., Weir, J. R., and Ramakrishnan, V. (2006) Structure of the 70S ribosome complexed with mRNA and tRNA., *Science 313*, 1935-1942.
- 43. Villa, E., Sengupta, J., Trabuco, L. G., LeBarron, J., Baxter, W. T., Shaikh, T. R., Grassucci, R. A., Nissen, P., Ehrenberg, M., Schulten, K., and Frank, J. (2008) Ribosome-induced changes in elongation factor Tu conformation control GTP hydrolysis., *PNAS 106*, 1063-1068.
- 44. Rodnina, M. V., Beringer, M., and Wintermeyer, W. (2007) How ribosomes make peptide bonds, *TRENDS in Biochemical Sciences 32*.
- 45. Wohlgemuth, I., Beringer, M., and Rodnina, M. V. (2006) Rapid peptide bond formation on isolated 50S ribosomal subunits., *EMBO 7*, 699-703.
- 46. Bosch, L., and Van der Hofstad, G. A. (1979) Initiation of protein synthesis in prokaryotes., *Methods in Enzymology 60*, 11-15.
- 47. Cummings, H. S., and Hershey, J. W. (1994) Translation initiation factor If1 is essential for cell viability in Escherichia coli., *J. Bacteriol.* 176, 198-205.
- 48. Carter, A. P., Clemons, W. M. J., Brodersen, D. E., R.J., M.-W., Hartsch, T., Wimberly, B. T., and Ramakrishnan, V. (2001) Crystal Structure of an initiation factor bound to the 30S ribsomal subunit, *Science 291*, 498-501.
- 49. Shine, J., and Dalgarno, L. (1975) Determinant of cistron specificity in bacterial ribosomes., *Nature 254*, 34-38.
- 50. Smit, M. H. d., and van Duin, J. (1994) Translational initiation on structured messengers. Another role for the Shine-Dalgarno interaction., *J. Mol. Biol. 235*, 173-184.
- 51. Boni, I. V., Isaeva, D., Musychenko, M. L., and Tzareva, N. V. (1991) Ribosome messenger recognition: mRNA target sites for ribosomal protein S1., *Nucleic Acids Research 19*, 155-162.
- 52. Allen, G. S., Zavialov, A., Gursky, R., Ehrenberg, M., and Frank, J. (2005) The Cryo-EM strucutre of a Translation Initiation complex from Escherichia coli, *Cell* 121, 703-712.
- 53. Mangroo, D., Wu, X.-Q., and RajBhandary, U. L. (1995) Escherichia coli initiator tRNA: structure-function relationships and interactions with the translational machinery., *Biochem & Cell Biology 73*, 1023-1031.

- 54. Meinnel, T., Mechulam, Y., Dardel, F., Schmitter, J. M., Houndtondji, C., Brunie, S., Dessen, P., Fayat, G., and Blanquet, S. (1990) Methionyl-tRNA synthetase from E. coli, *Biochimie* 72, 625-632.
- 55. Migita, L. K., and Doi, R. H. (1970) Formylation of methionly-transfer RNA from prokaryotes and eukaryotes by Bacillus subtilis transformylase., *Arch Biochem Biophys* 138, 457-463.
- Allen, G. S., and Frank, J. (2007) Structural insights on the translation initiation complex: ghosts of a universal initiation complex., *Molecular Microbiology 63*, 941-950.
- 57. Voet, D., and Voet, J. (2004) *Biochemistry*, 3rd ed., John Wiley & Sons, Inc.
- 58. Canonaco, M. A., Calogero, R. A., and Gualerzi, C. O. (1986) Mechanism of translational initiation in prokaryotes. Evidence for a direct effect of IF2 on the activity of the 30S ribosomal subunit., *FEBS Letter 207*, 198-204.
- 59. Wintermeyer, W., Peske, F., Beringer, M., Gromadski, K. B., Savelsbergh, A., and Rodnina, M. V. (2004) Mechanisms of elongation on the ribosome: dynamics of a macromolecular machine., *Biochemical Society Transactions 32*, 733-737.
- 60. Connell, S. R., and Nierhaus, K. H. (2000) Translational Termination Not Yet at its End, *ChemBiochem* 1, 250-253.
- 61. Pingoud, A., Gast, F.-U., Block, W., and Peters, F. (1983) The elongation factor Tu from Escherichia coli, aminoacyl-tRNA, and guanosine tetraphosphate form a ternary complex which is bound by programmed ribosomes, *Journal of Biological Chemistry 258*, 14200-14205.
- 62. Rodnina, M. V., Gromadski, K. B., Kothe, U., and Wieden, H.-J. (2005) Recognition and selection of tRNA in translation, *FEBS Letter 579*, 938-942.
- 63. Luhrmann, R. (1980) Dinucleotide codon-anticodon interaction as a minimum requirement for ribosomal aa-tRNA binding: stabilisation by viomycin of aa-tRNA in the A-site., *Nucleic Acids Research 8*, 5813-5824.
- 64. Moazed, D., and Noller, H. F. (1990) Binding of tRNA to the ribosomal A and P sites protects two distinct sets of nucleotides in 16S rRNA, *J. Mol. Biol. 211*, 135-145.
- 65. O'Connor, M., and Dahlberg, A. E. (1995) The involvement of two distinct regions of 23S ribosomal RNA in tRNA selection., *J. Mol. Biol. 254*, 838-847.
- 66. Kothe, U., and Rodnina, M. V. (2006) Delayed Release of Inorganic Phosphate from Elongation Factor Tu Following GTP Hydrolysis on the Ribosome, *Biochemistry*, 12767-12774.
- 67. Blanchard, S. C., Gonzales, R. L. J., Kim, H. D., Steven, C., and Puglisi, J. D. (2004) tRNA selection and kinetic proofreading in translation, *Nature Structural and Molecular Biology* 11, 1008-1014.
- 68. Schummer, T., Gromadski, K. B., and Rodnina, M. V. (2007) Mechanism of EF-Ts-catalyzed guanine nucleotide exchange in EF-Tu: contribution of interactions mediated by helix B of EF-Tu, *Biochemistry 46*, 4977-4984.
- 69. Gromadski, K. B., Wieden, H.-J., and Rodnina, M. V. (2002) Kinetic Mechanism of Elongation Factor Ts-Catalyzed Nucleotide Exchange in Elongation factor Tu, *Biochemistry* 41, 162-169.
- 70. Pape, T., Wintermeyer, W., and Rodnina, M. V. (1999) Induced fit in initial selection and proofreading of aminoacyl-tRNA on the ribosome., *EMBO 18*, 3800-3807.

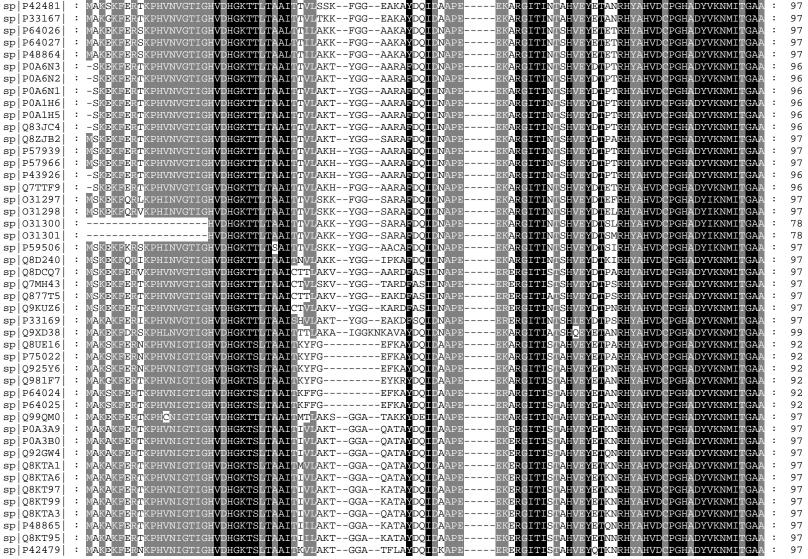
- 71. Rodnina, M. V., and Wintermeyer, W. (2003) Peptide bond formation on the ribosome: structure and mechanism, *Current opinion in Structural Biology 13*, 334-340.
- 72. Joseph, S. (2003) After the ribosome structure: How does translocation work?, *RNA 9*, 160-164.
- 73. Inoue-Yokosawa, N., Ishikawa, C., and Kaziro, Y. (1974) The role of guanosine triphosphate in translocation reaction catalyzed by elongation factor G., *J. Biol Chem.* 249, 4321-4323.
- 74. Czworkowski, J., and Moore, P. B. (1997) The conformational properties of elongation factor G and the mechanism of translocation., *Biochemistry 36*, 10327-10334.
- 75. Rodnina, M. V., Savelsbergh, A., Katunin, V. I., and Wintermeyer, W. (1997) Hydrolysis of GTP by elongation factor G drives tRNA movement on the ribosome, *Nature 385*, 37-41.
- 76. Agrawal, R. K., Penczek, P., Grassucci, R. A., and Frank, J. (1998) Visualization of elongation factor G on the Escherichia coli 70S ribosome: the mechanism of translocation., *PNAS 95*, 6134-6138.
- 77. Martemyanov, K. A., and Gudkov, A. T. (1999) Domain IV of elongation factor G from Thermus thermophilus is strictly required for translocation., *FEBS Letter 452*, 155-159.
- 78. Savelsbergh, A., Katunin, V. I., Mohr, D., Peske, F., Rodnina, M. V., and Wintermeyer, W. (2003) An Elongation Factor G-Induced Ribosome Rearrangement Precedes tRNA-mRNA Translocation, *Molecular Cell* 11, 1517-1523.
- 79. Qin, Y., Polacek, N., Vesper, O., Staub, E., Einfeldt, E., Wilson, D. N., and Nierhaus, K. H. (2006) The Highly Conserved LepA is a Ribosomal Elongation Factor that Back-Translocates the Ribosome, *Cell 4*, 721-733.
- 80. Peske, F., Rodnina, M. V., and Wintermeyer, W. (2005) Sequence of Steps in ribosome recycling as defined by kinetic analysis, *Molecular Cell* 18, 403-412.
- 81. Scolnick, E., Tompkins, R., Caskey, T., and Nirenberg, M. (1968) Release factors differing in specificity for terminator codons., *PNAS 62*, 768-774.
- 82. Wilson, K. S., Ito, K., Noller, H. F., and Nakamura, Y. (2000) Functional sites of interaction between release factor RF1 and the ribosome., *Nature Structural biology* 7, 866-870.
- 83. Kaji, A., Kiel, M. C., Hirokawa, G., Muto, A. R., Inokuchi, Y., and Kaji, H. (2001) The fourth step of protein synthesis: Disassembly of the posttermination complex is catalyzed by elongation factor G and ribosome recycling factor, a near-perfect mimic of tRNA., *Cold Spring Harb Symp Quant Biol 66*, 515-529.
- 84. Karimi, R., Pavlov, M. Y., Buckingham, R. H., and Ehrenberg, M. (1999) Novel roles for classical factors at the interface between translation termination and initiation., *Molecular Cell* 3, 601-609.
- 85. Pape, T., Wintermeyer, W., and Rodnina, M. V. (1998) Complete kinetic mechanism of elongation factor Tu-dependent binding of aminoacyl-tRNA to the A site of the E. coli ribosome., *The EMBO Journal 17*, 7490-7497.
- 86. Bourne, H. R., Sanders, D. A., and McCormick, F. (1990) The GTPase superfamily: a conserved switch for diverse cell functions., *Nature 348*, 125-132.
- 87. Walker, J. E., Saraste, M., Runswick, M. J., and Gay, N. J. (1982) Distantly related sequences in the alpha and beta subunits of ATP synthase, myosin, kinases and other ATP-requiring enzymes and a common nucleotide binding fold., *EMBO 1*, 945-951.
- 88. Bourne, H. R. (1995) GTPases: a family of molecular switches and clocks., *Phil Trans R Soc London 349*, 283-289.

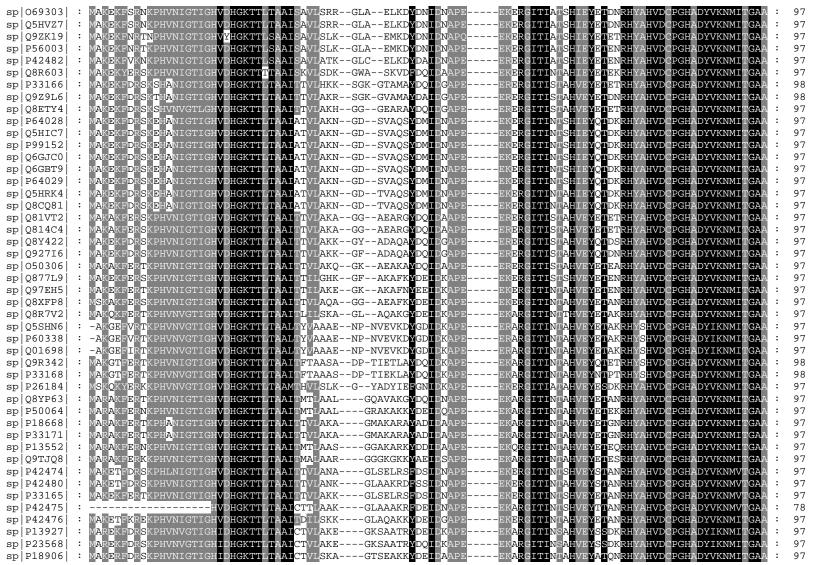
- 89. Milburn, M. V., Tong, L., deVos, A. M., Brunger, A., Yamaizumi, Z., Nishimua, S., and Kim, S. H. (1990) Molecular switch for signal transduction: structural differences between active and inactive forms of protooncogenic ras proteins., *Science 247*, 939-945.
- 90. Sander, G., Marsh, R. C., Voigt, J., and Parmeggiani, A. (1975) A comparative study of the 50S ribosomal subunit and several 50S subparticles in EF-T and EF-G dependent activities., *Biochemistry 14*, 1805-1814.
- 91. Mohr, D., Wintermeyer, W., and Rodnina, M. V. (2002) GTPase activation of elongation factors Tu and G on the ribosome., *Biochemistry 41*, 12520-12528.
- 92. Chau, V., Romero, G., and Biltonene, R. L. (1981) Kinetic studies on the interactions of Escherichia coli K12 elongation factor Tu with GDP and elongation factor Ts., *J. Biol Chem. 256*, 5591-5596.
- 93. Furano, A. V. (1977) The Elongation Factor Tu Coded by the tufA Gene of Escherichia coli K-12 is almost identical to that coded by the tufB Gene, *The Journal of Biological Chemistry* 252, 2154-2157.
- 94. Zuurmond, A. M., Rundlof, A. K., and Kraal, B. (1999) Either of the chromosomal tuf genes of E. coli K-12 can be deleted without loss of cell viability., *Mol. Gen Genet. 260*, 603-607.
- 95. Song, H., Parsons, M. R., Rowsell, S., Leonard, G., and Phillips, S. E. V. (1999) Crystal Structure of Intact Elongation Factor EF-Tu from Escherichia coli in GDP Conformation at 2.05A Resolution., *Journal of Molecular Biology 285*, 1245-1256.
- 96. Kjeldgaard, M., Nissen, P., Thirup, S., and Nyborg, J. (1993) The crystal strucutre of elongation factor EF-Tu fom Thermus aquaticus in the GTP conformation., *Structure 1*, 35-50.
- 97. Nissen, P., Kjeldgaard, M., Thirup, S., Polekhina, G., Reshetnikova, L., Clarck, B. F. C., and Nyborg, J. (1995) Crystal Structure of the Ternary Complex of Phe-tRNAPhe, EF-Tu, and a GTP analog, *Science 270*, 1464-1472.
- 98. Rodnina, M. V., Pape, T., Fricke, R., Kuhn, L., and Wintermeyer, W. (1996) Initial Binding of the Elongation Factor TuGTPAminoacyl-tRNA Complex Preceding Codon Recognition on the Ribosome, *JBC 271*, 646-652.
- 99. Stark, H., Rodnina, M. V., Rinke-Appel, J., Brimacombe, R., Wintermeyer, W., and van Heel, M. (1997) Visualization of elongation factor Tu on the Escherichia coli ribosome., *Nature 389*, 403-406.
- Stark, H., Rodnina, M. V., Wieden, H.-J., Zemlin, F., Wintermeyer, W., and van Heel, M. (2002) Ribosome interactions of aminoacyl-tRNA and elongation factor Tu in the codon-recognition complex., *Nature Structural biology* 11, 849-854.
- 101. Daviter, T., Wieden, H.-J., and Rodnina, M. V. (2003) Essential role of histidine 84 in elongation factor Tu for the chemical step of GTP hydrolysis on the ribosome, *Journal of Molecular Biology* 332, 689-699.
- 102. Kawashima, T., Berthet-Colominas, C., Wulff, M., Cusack, S., and Leberman, R. (1996) The strucuture of the Escherichia coli EF-Tu EF-Ts complex at 2.5A resolution, in *Nature* 511-518.
- 103. Wieden, H.-J., Wintermeyer, W., and Rodnina, M. V. (2001) A common structural motif in elongation factor Ts and ribosomal protein L7/12 may be involved in the interaction with elongation factor Tu, *Journal of Molecular Evolution 52*, 129-136.
- 104. Forster, T. (1948) *Ann. Physik 6*, 55.

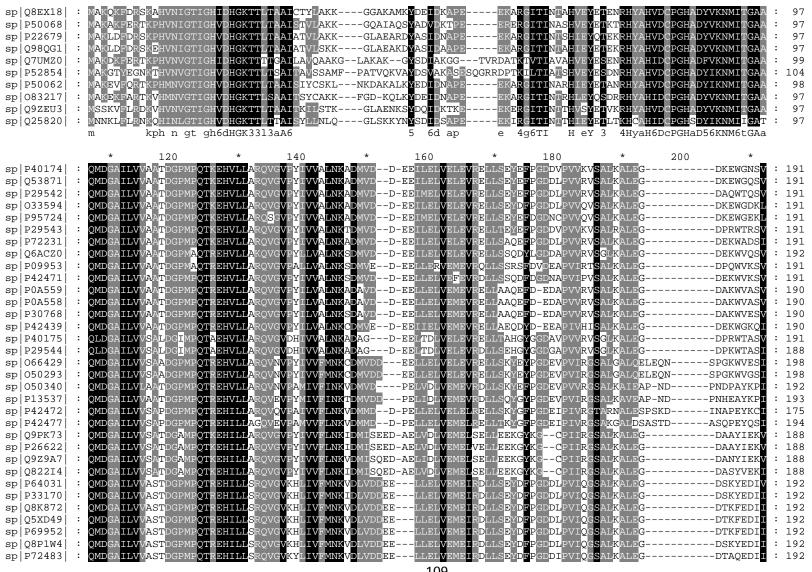
- 105. Anborgh, P. H., Parmeggiani, A., and Jonak, J. (1992) Site-directed mutagenesis of elongation factor Tu The functional and structural role of residue Cys81, *FEBS* 208, 251-257.
- 106. Boon, K., Vijgenboom, E., Madsen, L. V., Talens, A., Kraal, B., and Bosch, L. (1992) Isolation and functional analysis of histidine-tagged elongation factor Tu., *European Journal of Biochemistry 210*, 177-183.
- 107. Karl B, N., and Nicholas, H. B. J. (1997) GeneDoc: a tool for editing and annotating multiple sequence alignments.
- 108. Milon, P., Konevega, A. L., Peske, F., Fabbretti, A., Gualerzi, C. O., and Rodnina, M. V. (2007) Transient Kinetics, Fluorescence, and FRET in Studies of initiation of translation in bacteria., *Methods in Enzymology 430*.
- Konevega, A. L., Fischer, N., Semenkov, Y. P., Stark, H., Wintermeyer, W., and Rodnina, M. V. (2007) Spontaneous reverse movement of mRNA-bound tRNA through the ribosome, *Nature structural & molecular biology 14*, 318-324.
- 110. Solomaha, E., and Palfrey, H. C. (2005) Conformational changes in dynamin on GTP binding and oligomerization reported by intrinsic and extrinsic fluprescence., *Biochemi. J.* 391, 601-611.
- 111. Kaiser, C. M., Chang, H.-C., Agashe, V. R., Lakshmipathy, S. K., Etchells, S. A., Hayer-Hartl, M., Hartl, F. U., and Barral, J. M. (2006) Real-time observation of trigger factor function on translating ribosomes., *Nature 444*, 455-460.
- 112. Jonak, J., Petersen, T., Clarck, B., and Rychlik, I. (1982) N-Tosyl-L-phenylalanylchloromethane reacts with cysteine 81 in the molecule of elongation factor Tu from Escherichia coli, *FEBS Letter 50*, 485-488.
- 113. March, P. E., and Inouye, M. (1985) Characterization of the lep Operon of Escherichia coli, *The Journal of Biological Chemistry 260*, 7206-7213.
- 114. Dibb, N. J., and Wolfe, P. B. (1986) lep Operon Proximal Gene is not required for growth or secretion by Escherichia coli, *Journal of Bacteriology 166*, 83-87.
- 115. March, P. E., and Inouye, M. (1985) GTP-binding membrane protein of Escherichia coli with sequence homology to initiation factor 2 and elongation factors Tu and G., *PNAS* 82, 7500-7504.
- 116. Margus, T., Remm, M., and Tenson, T. (2007) Phylogenetic distribution of translational GTPases in bacteria., *BMC Genomics 8*, 15.
- Connell, S. R., Topf, M., Qin, Y., Wilson, D., N, Mielke, T., Fucini, P., Nierhaus, K., H, and Spahn, C., MT. (2008) A new tRNA intermediate revealed on the ribosome during EF4mediated back-translocation, *Nature Structural and Molecular Biology* 15, 910-915.
- 118. Evans, R. N., Blaha, G., Bailey, S., and Steity, T. A. (2008) The Structure of LepA, the ribosomal back translocase, *PNAS 105*, 4673-4678.
- 119. Laurberg, M., Kristensen, O., Martemyanov, K., Gudkov, A. T., Nagaev, I., Hughes, D., and Liljas, A. (2000) Structure of a mutant EF-G reveals domain III and possibly the fusidic acid binding site., *JMB 303*, 593-603.
- 120. Savelsbergh, A., Matassova, N. B., Rodnina, M. V., and Wintermeyer, W. (2000) Role of Domains 4 and 5 n Elongation Factor G Functions on the Ribosome, *JMB*, 951-961.
- 121. Xie, P. (2008) A thermal ratchet model of tRNA-mRNA translocation by the ribosome., *BioSystems 96*, 19-28.

- 122. Wilden, B., Savelsbergh, A., Rodnina, M. V., and Wintermeyer, W. (2006) Role and timing of GTP binding and hydrolysis during EF-G-dependent tRNA translocation on the ribosome, *Proceedings of the National Academy of Science 103*, 13670-13675.
- 123. Rodnina, M. V., and Wintermeyer, W. (1995) GTP consumption of elongation factor Tu during translation of heteropolymeric mRNAs, *PNAS 92*, 1945-1949.
- 124. Savelsbergh, A., Mohr, D., Wilden, B., Wintermeyer, W., and Rodnina, M. V. (2000) Stimulation of the GTPase Activity of Translation Elongation Factor G by Ribosomal Protein L7/12, *The Journal of Biological Chemistry 275*, 890-894.
- 125. Rodnina, M. V., Semenkov, Y. P., and Wintermeyer, W. (1994) Purification of fMettRNA(fMet) by fast protein liquid chromatography, *Anal. Biochem* 219, 380-381.
- 126. Rodnina, M. V., Fricke, R., and Wintermeyer, W. (1994) Transient Conformatinal States of Aminoacyl-tRNA during Ribosome Binding Catalyzed by Elongation Factor Tu, *Biochemistry*, 12267-12275.
- 127. Caldon, C. E., and March, P. E. (2003) Function of the universally conserved bacterial GTPases, *Current Opinion in Microbiology 6*, 135-139.
- 128. Arai, K., Arai, N., Nakamura, S., Oshima, T., and Kaziro, Y. (1978) Studies on polypeptide-chain-elongation factors from an extreme thermophile, Thermus thermophilus HB8.2. Catalytic properties, *Eurpean Journal of Biochemistry 92*, 521-531.
- 129. Savelsbergh, A., Mohr, D., Kothe, U., Wintermeyer, W., and Rodnin., M. V. (2005) Control of phosphate release from elongation factor G by ribosomal protein L7/12, *The EMBO Journal 24*, 4316-4323.
- 130. Rojiani, M. V., Jakubowski, H., and Goldman, Y. E. (1989) Effect of variation of charged and uncharged tRNATrp levels on ppGpp synthesis in Escherichia coli, *Journal of Bacteriology* 171, 6493-6502.
- Wang, Y., Qin, Y., Kudaravalli, R. D., Kirillov, S. V., Depsey, G. T., Pan, D., Cooperman, B.
   S., and Goldman, Y. E. (2007) Single-molecule structural dynamics of EF-G-ribosome interaction during translocation., *Biochemistry 46*, 10767-10775.

## **Appendix** 40 sp|P40174| HID<mark>HGKTT</mark>LTA<mark>AI</mark>TKVLHD-AYP-DINEASA<mark>F</mark>DQ**I**I M<mark>AKA</mark>KF<mark>ERT</mark>KPHVNIGTIGF HVDCPGHADYIKNMI KVLHD-AFP-DLNEASA<mark>F</mark>DQI sp | Q53871 sp | P29542 AHVDCPGHADYIKNMI TKVLHD-KYP-DLNAASA<mark>F</mark>DQ**T** sp | 033594 HVDC sp | P95724 HD-AIP-DLNPFTPFDET RGITI SIAHVEYQTE CPGHADYIKNMI 99 sp | P29543 HD-RFP-DLNPFTPFDQI RGITI SIAHVEYQTE. HVDCPGHADYIKNMI 99 sp | P72231 HVD APGHADYIKNMI sp Q6ACZ0 VDHGKTTLTAAI TAAT HVD sp | P09953 sp | P42471 HGKTTLTAAI TKVLAD-QYP-DLNEARAFDQV HVD. PGHADYVKNMI DHGKTTLTAAI AHVD<mark>A</mark>PGHADYIKNMITGAA sp | P0A559 IKVLHD-KFP-DLNETKA**F**DQ**I** sp | P0A558 VD<mark>HGKTT</mark>LTAAITKVLHD-KFP-NLNESRAFDQI AHVD<mark>A</mark>PGHADYIKNMITGA sp | P30768 HVD<mark>A</mark>PGHADYIKNMI sp | P42439 RGITINIAHVEYETD' PGHADYVKNMV sp P40175 sp | P29544 sp | 066429 VDHGKSTLT: RGITINITHVEYETA HVDCPGHADYIKNMI' HGKST HVDCPGHADYIKNMI sp | 050293 LTAAITKYCSF----FGWADYTPYEMI RGITINITHVEYQTEKRH HIDCPGHADYIKNMI sp | 050340 HGKTT LTAAI RGITINITHVEY<mark>ETEKRH</mark> AHIDCPGHADYIKNMITGA sp P13537 sp P42472 AHVDCPGHADYIKNMITGA*I* sp | P42477 VDHGKTTLTAAITKT AHVDCPGHADYIKNMITGAA HVDCPGHADYVKNMI RGITINASHVEYETPNRH sp Q9PK73 VDHGKTTLTAAI RGITINASHVEY: HVDCPGHADYVKNMI' sp | P26622 IVDHGKTTLTAAI sp Q9Z9A7 VDHGKTTLTAAITRALSA-AHVDCPGHADYVKNMITGA*l* sp Q822I4 VDHGKTTLTAAI RGITINTAHVEYETE HID<mark>A</mark>PGHADYVKNMI : 100: sp | P64031 HGKTTLTAAI sp|P33170| TTVLARRL-PSAVNQPKD<mark>Y</mark>AS**T** RGITINTAHVEYETE: HID<mark>APGH</mark>ADYVKNMI : 100 LTAAI sp | Q8K872 TTVLARRL-PSSVNQPKD<mark>Y</mark>AST AHIDAPGHADYVKNMITGA : 100 AHID<mark>A</mark>PGHADYVKNMITGAA TTVLARRL-PSSVNQPKD**Y**AS : 100 sp Q5XD49 AHID<mark>A</mark>PGHADYVKNMITGAA sp P69952 VD<mark>HGKTT</mark>LTAAITTVLARRL-PSSVNQPKD<mark>Y</mark>ASI : 100 HGKTTLTAAI HIDAPGHADYVKNMI : 100 sp Q8P1W4 HID<mark>A</mark>PGHADYVKNMIT sp | P72483 : 100 sp Q9CEI0 Sp Q88VE0 IVDHGKTTLTAAI TKVLAS----KGLAKEQD**F**AS RGITINTAHVEYETE: HID<mark>A</mark>PGHADYVKNMITGA RGITIS RGITIS VDHGKTTLTAAI HIDCPGHADYIKNMI sp Q8KAH0 LAK----QGMATLRE<mark>F</mark>SD**I** IVDHGKTTLTAAIT Lak----sgkaaare<mark>f</mark>gd<mark>i</mark> HIDCPGHADYIKNMI sp | P42473 AHVDCPGHADYVKNMITGAA MAKEKFORSLPHCNVGTIGHVDHGKTTLTAALTRVCSEV--FGS--ARVDFDKI sp | Q889X3 sp | P09591 HVDCPGHADYVKNMITGAA VDHGKTTLTAALTKIGAER--FGG--EFKAYDAI HVDCPGHADYVKNMITGA 97 sp Q8PC59 VD<mark>HGKTT</mark>LTAALTKIGAER--FGG--EFKA<mark>Y</mark>DAI RGITIST HVDC sp | Q8NL22 CPGHADYVKNMI 97 VDHGKTTLTAALTKVGAER--FGG--EFKAYDAI CPGHADYVKNMIT sp Q9P9Q9 : -AQDKFKRTKLHVNVGTIG ARGITI 96 IVDHGKTTLTAAIATVLSSK--FGG--EAKKYDEI sp | Q8XGZ0 |

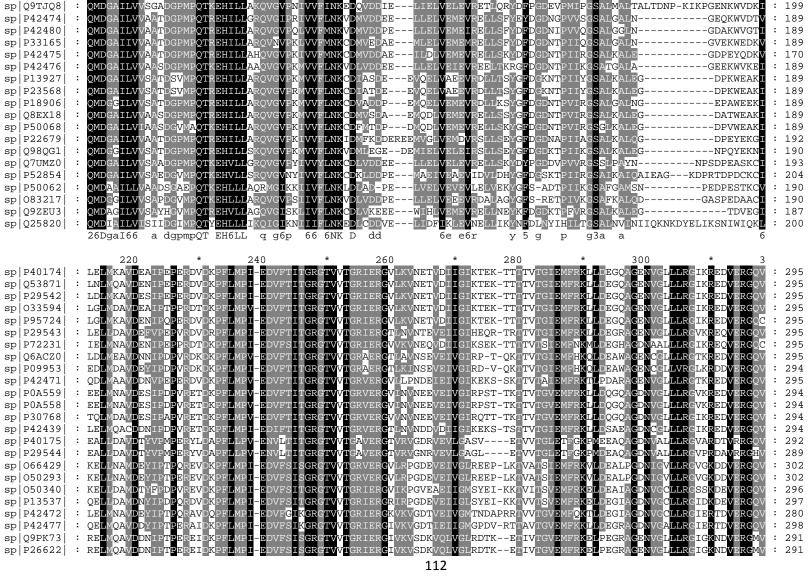


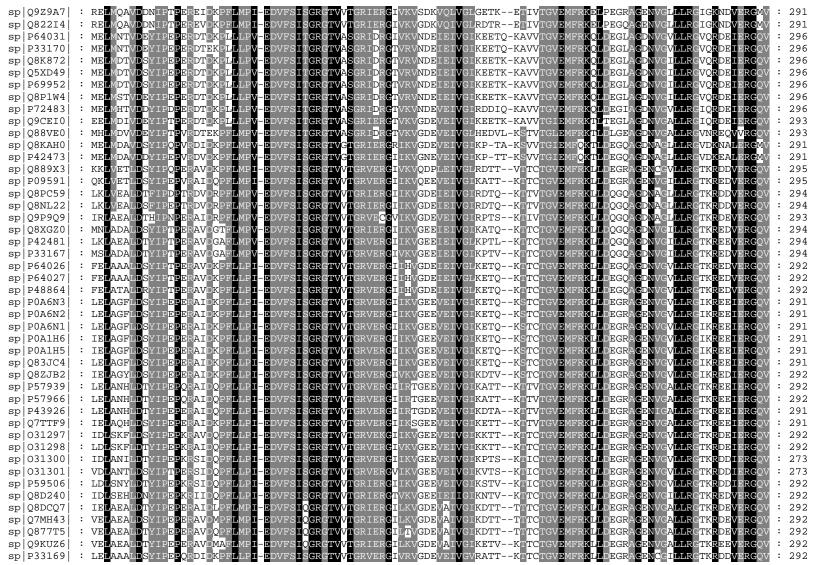


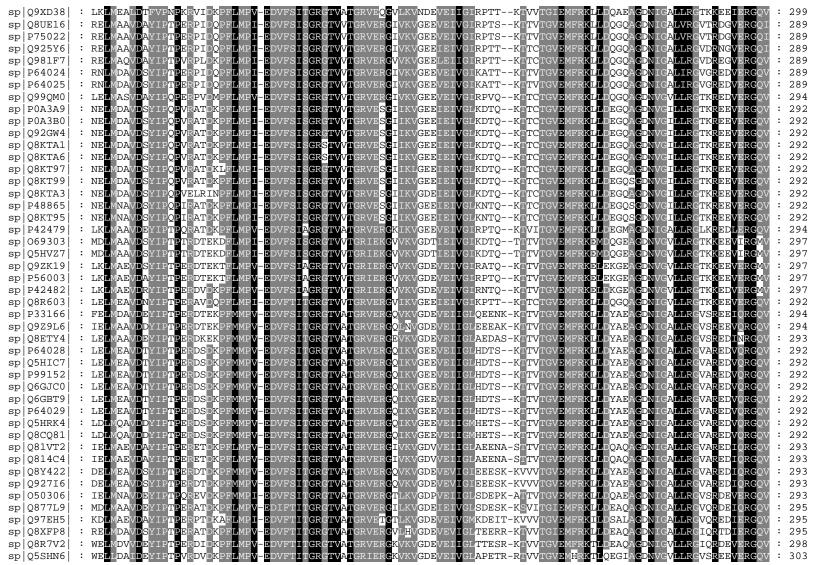


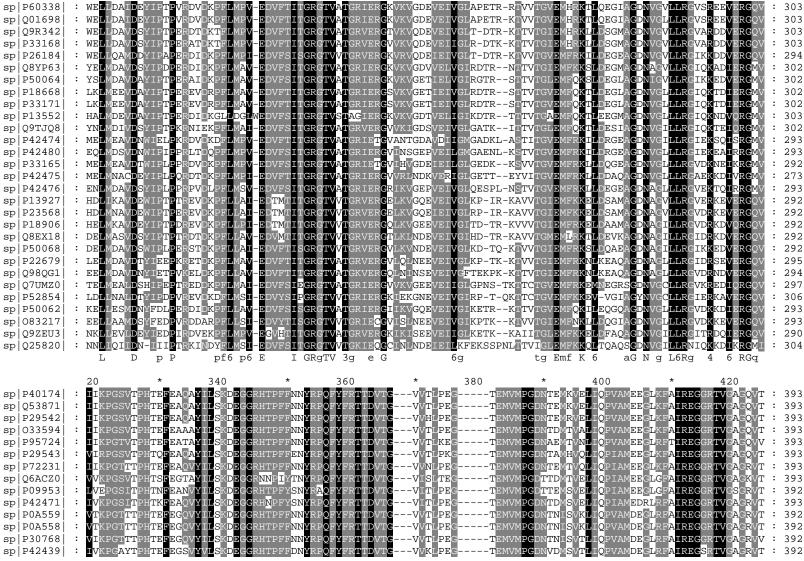
sp Q9CEI	) :	QMDGAILV	VAATDG	PMPQTREH	ILL <mark>s</mark> rqvgv	KYLIVFLNKA	DLVDDEE	-LMELVEMEV	RDLLSEY	DFPGDDIP	VIAG	ALGALNG	EPQWVAK	:	189
sp Q88VE	) i	QMDGAILV	VAATDG	PMPOTREH	ILL <mark>a</mark> rovgv	DYIVVFLNK <mark>T</mark>	DLVDDDE	-LVDLVEMEV	RELLSEY	DFPGDDIP	VIRG	ALKALEG	DPEQEKV	:	189
sp Q8KAH	) :	QMDGAILV	VAGTDG:	PMPQTREH	ILL <mark>a</mark> rqv <mark>n</mark> v	/PALVVFLNKV	DIADP-E	-LLELVEMEI	RELLTEY	GFPGDDIP	IIKGS	ALKALEG	DPEAEKQI	:	188
sp P4247	3   :	QMDGAILV	VAGTDG:	PMPQTREH	ILL <mark>a</mark> rqv <mark>n</mark> v	/PALVVFLNK	DIADP-E	-LLELVEMEI	RELLTEY	GFPGDDIP	IIKGS	ALNALNG	DPEGEKA	:	188
sp Q889X	3   :	QMDGAILV	CSAADG	PMPQTREH	ILL <mark>S</mark> RQVGV		DLVDDAE	-LLELVEMEV	RDLLS <b>T</b> Y	DFPGDDTP	IIIGS	ARMALEGKDD	NEMGTTA	:	192
sp P09591	Lİ :	QMDGAILV	CSAADG	PMPQTREH	ILL <mark>s</mark> rqvgv	/PYIVVFLNK <mark>A</mark>	ADMVDDAE	-LLELVEMEV	RDLLNTY	DFPGDDTP	IIIGS	ALMALEGKDD	NGIGVSA	:	192
sp Q8PC59		QMDGAILV	CSAADG	PMPQTREH	ILL <mark>s</mark> rqvgv	/PHIVVFLNK	ADMVDDAE	-LLELVEMEV	RELLSKY	DFPGDDTP	IIHGS	ARLALEG-DQ	SDIGVPA	:	191
sp Q8NL2	2   :	QMDGAILV	CSAADG	PMPQTREH	ILL <mark>s</mark> rqvgv	/PHIVVFLNK	ADMVDDAE	-LLELVEMEV	RELLSKY	DFPGDDTP	IIHGS	ARLALDG-DQ	SDIGVPA	:	191
sp Q9P9Q9	) :	QMDGAILV	CSAADG	PMPQTREH	ILL <mark>a</mark> rqvgv	/PYIVVFLNK <mark>A</mark>	ADMVDDAE	-LLELVEMEV	RELLSKY	DFPGDDTP	IV <mark>R</mark> G	ALKALEG-DQ	SEIGVPA	:	190
sp Q8XGZ	) :	QMDGAILV			ILL <mark>a</mark> rqvgv	/PYIIVFLNK	DMVDDAE	-LLELVEMEV	R <mark>E</mark> LLS <mark>K</mark> Y	DFPGDDTP	IIKG	AKLALEG-DK	GELGEVA	:	191
sp P42481	L  :	QMDGAILV	V <mark>S</mark> AADG	PMPQTR <mark>EH</mark>	ILL <mark>a</mark> rqvgv	/PYIIVFLNK	DMVDDAE	-LLELVEMEV	R <mark>E</mark> LLS <mark>K</mark> Y	DFPGDDTP	IIKG	AKLALEG-DK	GELGEGA	:	191
sp P3316	7   :	QMDGAILV	CSAADG	PMPQTR <mark>EH</mark>	ILL <mark>a</mark> rqvgv	/PYIIVFLNK	DSVDDAE	-LLELVEMEV	R <mark>E</mark> LLS <mark>K</mark> Y	DFPGDDTP	IV <mark>K</mark> G	AKLALEG-DT	GELGEVA	:	191
sp P64026	5 :	QMDGAILV	CSAADG	PMPQTR <mark>EH</mark>	ILL <mark>a</mark> rqvgv	/PYIIVFMNK <mark></mark> C	DMVDDAE	-LLELVEME	R <mark>D</mark> LLS <mark>S</mark> Y	DFPGDDCP	IV <mark>Q</mark> G	ALKALEG-D	AAYEEK	:	189
sp P6402	7   :	QMDGAILV	CSAADG	PMPQTR <mark>EH</mark>	ILL <mark>A</mark> RQVGV	/PYIIVFMNK	DMVDDAE	-LLELVEMEI	R <mark>D</mark> LLS <mark>S</mark> Y	D <b>F</b> PGDDCP	IV <mark>Q</mark> G	ALKALEG-D	AAYEEK	:	189
sp P4886	1 :	QMDGAILV	CSAADG	PMPQTR <mark>EH</mark>	ILL <mark>A</mark> RQVGV	/PYIIVFMNK	DMVDDAE	-LFQLVEMEI	R <mark>D</mark> LLS <mark>S</mark> Y	D <b>F</b> PGDDCP	IV <mark>Q</mark> G	ALKALEG-D	AAYEEK	:	189
sp POA6N	3   :	QMDGAILV	VAATDG	PMPQTR <mark>EH</mark>	ILL <mark>G</mark> RQVGV	/PYIIVFLNK	DMVDDEE	-LLELVEMEV	R <mark>E</mark> LLS <b>Q</b> Y	DFPGDDTP	IV <mark>R</mark> G	ALKALEG	DAEWEAK	:	188
sp POA6N2	2 :	QMDGAILV	V <mark>a</mark> a <mark>t</mark> dg	PMPQTR <mark>EH</mark>	ILL <mark>G</mark> RQVGV	/PYIIVFLNK	DMVDDEE	-LLELVEMEV	R <mark>E</mark> LLS <b>Q</b> Y	DFPGDDTP	IV <mark>R</mark> G	AL <mark>KALEG</mark>	DAEWEAK	:	188
sp POA6N	L  :	QMDGAILV	V <mark>aat</mark> dg:	PMPQTR <mark>EH</mark>	ILL <mark>G</mark> RQVGV	/PYIIVFLNK	DMVDD <mark>EE</mark>	-LLELVEMEV	R <mark>E</mark> LLS <b>Q</b> Y	DFPGDDTP	IV <mark>R</mark> G	AL <mark>KALEG</mark>	DAEWEAK	:	188
sp POA1H	5 :	QMDGAILV	V <mark>aat</mark> dg:	PMPQTR <mark>EH</mark>	ILL <mark>G</mark> RQVGV	/PYIIVFLNK	DMVDD <mark>EE</mark>	-LLELVEMEV	R <mark>E</mark> LLS <b>Q</b> Y	DFPGDDTP	IV <mark>R</mark> G	AL <mark>KALEG</mark>	DAEWEAK	:	188
sp POA1H	5   :	QMDGAILV	VAATDG:	PMPQTR <mark>EH</mark>	ILL <mark>G</mark> RQVGV	/PYIIVFLNK	DMVDDEE	-LLELVEMEV	R <mark>E</mark> LLS <b>Q</b> Y	DFPGDDTP	IV <mark>r</mark> g	AL <mark>KALEG</mark>	DAEWEAK	:	188
sp Q83JC4	1   :	QMDGAILV	VAA <mark>T</mark> DG:	PMPQTR <mark>EH</mark>	ILL <mark>G</mark> RQVGV	/PYIIVFLNK	DMVDDEE	-LLELVEMEV	R <mark>E</mark> LLS <mark>Q</mark> Y	DFPGDDTP	IV <mark>R</mark> G	SAL <mark>KALE</mark> G	DAEWEAK	:	188
sp Q8ZJB2	2 :	QMDGAILV	VAATDG:	PMPQTR <mark>EH</mark>	ILL <mark>G</mark> RQVGV	/PYIIVFMNK <mark></mark> C	DMVDDEE	-LLELVEMEV	R <mark>e</mark> lls <b>a</b> y	D <mark>F</mark> PGDDLP	vv <mark>r</mark> g	SAL <mark>KALE</mark> G	EAEWEAK	:	189
sp P57939	9 :	QMDGAILV	VAATDG:	PMPQTR <mark>EH</mark>	ILL <mark>G</mark> RQVGV	/PYIIVFLNK	DMVDDEE	-LLELVEMEV	R <mark>E</mark> LLS <b>Q</b> Y	D <mark>F</mark> PGDDTP	IV <mark>RG</mark>	ALQALNG	VAEWEEK	:	189
sp P57966		QMDGAILV	VAATDG:	PMPQTR <mark>EH</mark>	ILL <mark>G</mark> RQIGV	AYIIVFLNK	DMVDDEE	-LLELVEMEV	RELFSQY	D <mark>F</mark> PGDDTP	IV <mark>RG</mark>	ALQALNG	VAEWEEK	:	189
sp P43926	5   :	QMDGAILV	V <mark>a</mark> a <mark>t</mark> dg:	PMPQTR <mark>EH</mark>	ILL <mark>G</mark> RQVGV	/PYIIVFLNK	DMVDDEE	-LLELVEMEV	R <mark>E</mark> LLS <b>Q</b> Y	DFPGDDTP	IV <mark>R</mark> G	ALQALNG	VAEWEEK	:	188
sp Q7TTF	9 :	QMDGAILV	V <mark>a</mark> a <mark>t</mark> dg:	PMPQTR <mark>EH</mark>	ILL <mark>G</mark> RQVGV	/PYIIVFLNK	DMVDDEE	-LLELVEMEV	R <mark>E</mark> LLS <b>Q</b> Y	DFPGDDTP	IV <mark>R</mark> G	ALQAL <mark>NG</mark>	VPEWEEK	:	188
sp 03129	7   :	QMDGAILV	V <mark>a</mark> a <mark>t</mark> dg:	PMPQTR <mark>EH</mark>	ILL <mark>G</mark> RQVGV	/PYIIVFLNK	DMVDDEE	-LLELVEMEV	R <mark>D</mark> LLT <b>Q</b> Y	DFPGDDTP	IIRG	AL <mark>KALEG</mark>	DPEWESK	:	189
sp 031298		QMDGAILV	V <mark>a</mark> atdg:	~	ILL <mark>G</mark> RQVGV	* التنافي التنافي - الت	DMVDDEE	-LLELVEMEV	R <mark>D</mark> LLT <b>Q</b> Y	DEPGDDTP	IIRG	AL <mark>KALEG</mark>	DADWESK		189
sp 031300		QMDGAILV	VAATDG:	PMPQTREH	ILL <mark>G</mark> RQVGV	/PYIVVFLNK		-LLELVEMEV	RDLLTQY	DEPGDKTP	IIRG	ALKALEG	DCIWESK	:	170
sp   031301		QMDGAILV		~	ILL <mark>G</mark> RQVGV	/PYIVVFLNK		-LLELVEMEV	RDLLTQY	DEPGEKTP		ALKALEG	DAVWEEK		170
sp   P59506		QMDGAILV		PMPQTREH	ILL <mark>G</mark> RQVGV	/PYIVVFLNK		-LLELVEMEV	RDLLTQY	DEPGDSTP			DPQWEQK		189
sp Q8D240		QMDGAILV	VAATDG	~	ILL <mark>G</mark> RQVGV	/PYIVVFMNK	DMVDDEE	-LLELVEIEI	RELLSQY	DEPGDEIP	_	SALKALEK	DPIWIQK		189
sp Q8DCQ		QMDGGILV		~	ILL <mark>G</mark> RQVGI	IPYIIVFMNK C	DMVDDEE	-LLELVEMEV	RELLSEY	DEPGDDLP	~		EEQWEAK		189
sp Q7MH4	!	QMDGGILV		~	ILL <mark>G</mark> RQVGI	IPYIIVFMNKC	DMVDDEE	-LLELVEMEV	RELLSEY	DEPGDDLP	~		EEQWEAK		189
sp Q877T!		QMDGGILV		~	ILL <mark>G</mark> RQVGI	PYIIVFMNKO	DMVDDEE	-LLELVEMEV	RELLSEY	DEPGDDLP	~		EEQWEAK		189
sp Q9KUZ	!	QMDG <mark>G</mark> ILV		PMPQTREH	~	PYIIVFMNKO		-LLELVEMEV	RELLSEY	DEPGDDLP	VIQG	ALGALNG	EAQWEAK		189
sp   P33169		QMDGAILV		~	~	/PFIIVFMNKC	DMVDDEE	-LLELVEMEV	RELLSEY	DEPGDDLP	VIQG		EPEWEAK		189
sp Q9XD38	!	QMDAAILV	VSATDG.	PMPQTKEH	~	/PYVIVFINKA	ADMI AADERA	EMIEMVEMDV	RELLNKY	SEPGDTTP	I VHG:		SEIGMPA		196
sp Q8UE16		QMDGAILV	CSAADG	PMPQTREH		/PAIVVFLNK		-LLELVELE	RELLSSY	DEPGDDIP	LIKE		KKIGEDA		186
sp P75022		EMDGAILV	CSAADG	~	ILL <mark>A</mark> RQVGV	/PALVVFLNKV	DQVDDAE	-LLELVELEV	RELLSSY	DEPEDDIP	LIKE		KKIGEDA		186
sp   Q925Y6		QMDGAILV		PMPQTREH	~		DQVDDAE	-LLELVELEV	RELLSSY	EFPGDDIP	IVKG		KKIGEDA		186
sp   Q981F'	!	QMDGAILV		~	~		DQVDDAE		RELLSKN	FERGUDIP	IVKG		KTIGEDA		186
sp   P64024	!	QMDGAILV		~	ILL <mark>A</mark> RQVGV		DQVDDAE	-LLEIVELEV	RELLSKY	FREGUETA	LIKG	ALAALED CC	KELGEDA KELGEDA		186 186
sp P6402	:	QMDGAILV		PMPQTREH	~		DQVDDAE	- LLELVEVEV	RELLSKY	PERCONT.		ALAALED-SS	_		
sp Q99QM0		QMDGAILV	VSAADG	~	~	/PALVVFMNKV	DMVDDEE	-LLELVEMEV	RELLSSY	QE PGDDIP	ITKG	ALAAVEG-RD	PQIGEEK		191
sp P0A3A9	ı :	QMDGAILV	VSAADG	PMPQTREH	ILL <mark>A</mark> KQVGV	/PAMVVFLNKI	UMADDAD	-LLELVEMEV	RELLSKY	GERETE	LIKG	ALQALEG-KP	EGEKA	•	189

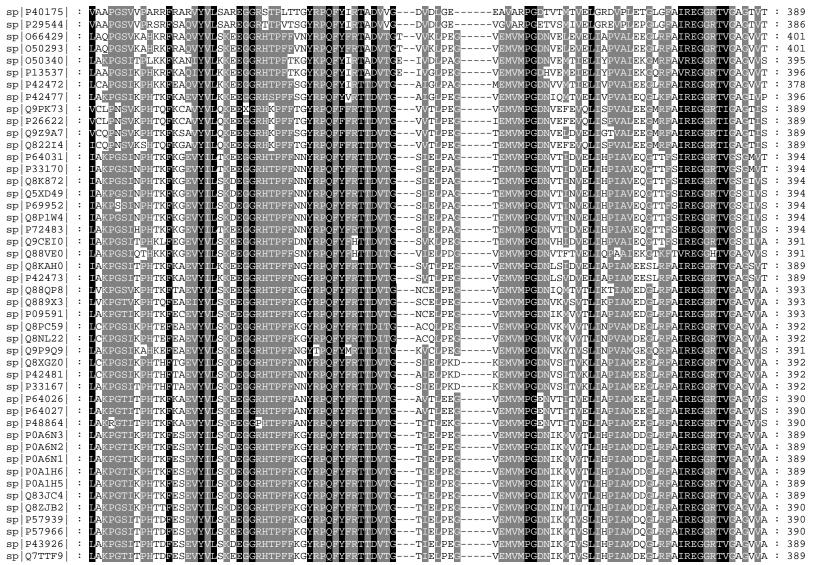
sp P0A3B0	١:	OMDGAILV	/SAADGDV	IPOTREHILI	AKOVGVE	AMVVETNKT	DMVDDPD	-I.I.EI.VEME	VRELLS	KVGEPG	DEIDIIKG	SALOALEG-KPEGEK	Δ <b>Π</b> :	189
sp   Q92GW4	:	OMDGAILV\	/SAADGPM	~	~	AMVVFLNKI	DMVDDPD	-LIELVEME				SALOALEG-KPEGEK		189
sp Q8KTA1	:	OMDGAILV\	/SAADGIN /SA <mark>A</mark> DGPM	~	AKOVGVE		DMVDDSD	-LLELVEME		_		SALQALEG-KPEGEK		189
sp Q8KTA6	:	OMDGAILV\		IPOTREHILI	AKOVGVE		DMVDDSD	-LIELVEME	VPFI.I.S	KVCHDC	DEILLIKG	SALOALEG-KPEGEK		189
sp Q8KT97	:	QMDGAILV\		IPOTREHILI	AKOVGVE	AMVVFLNKV	DMVDDPD	-I.I.FI.VEME	VPFI.I.S	KVCHDC	DEILLIKG	SALOALEG-KPEGEK		189
- 17	:	QMDGAILV\ QMDGAILV\	ZZA ADCDV	IPOTREHILI	~		DMVDDPD	TI EI VEME	VDELLC	KYGFPG	DEIBAIKS	SALOALEG-KPEGEK		189
- ! ~ .	:	QMDGAILV\ QMDGAILV\	ZCA ADCDM	~	~ ' -		ZDMVDDDD	TIELVEME	ABELLS			SALOALEG-KPEGEE		189
- 1	:	QMDGAILV\ OMDGAILV\	/SAADGPM /SAADGPM	~	~ ' -		IDMVDDPD	TIELVEME	VELLIC	KYCEDC	DEIPTIKG	SALOALEC KD E CEK		189
-	:	~	ZCA ADCDM	~	AKOVOVE		DMVDDPD	-TTETAEME	VELLE	KYCIPG	NEIPIIKG	SALOALEC KD E CEK		
sp Q8KT95	:	QMDGAILV\	/SAADGPI	IPQTREHILI IPOTREHILI	ARQVGVE	AMVVFLNKV		-LLELVEME	VRELLS	KYGEPG	DETAILE	SALQALEG-KPEGEK		189
sp P42479	:	QMDGAILV\	/SAADGPI	~	~ ' -	YIVVFLNKV	DMPDDDFF	-LRELVEME	V RDLLK	CYDERC		SALKALEG-DTSDIGEG		
sp   069303	! :	QMDGAILV		IPQTREHILI	SROVGVE	YIVVFMNKA	ADMVDDAE	-LLELVEME	TKELLS	SYDEPG		SALKALEEAKAGQDGEWSA		194
sp Q5HVZ7	! :	QMDGAILV\	/SAADGPM	~	SROVGVE	YIVVFMNKA	ADMVDDAE	-LLELVEME	TKELLS	SYDEPG	DDIPILSG	SALKALEEAKAGQDGEWSA		194
sp   P56003	! :	QMDGAILV	/SAADGPM	~	SROVGVE	HIVVFLNKÇ	DMVDDQE	-LLELVEME	VKELLS	AYERPG	DDIPIVAG	SALRALEEAKAGNVGEWGE		194
sp   P42482	:	QMDGAILV\	/SAADGPM	IPQTREHILI	SRQVGVF	YIVVFLNKE	DMVDDAE	-LLELVEME	VRELLS	NYDEPG	DDTPIVAG	SALKALEEAKTGNVGEWGE		194
sp Q8R603	١.	QMDGAILV	/SAADGPM	IPQTREHILI	SRQVGVF	YIVVYLNKS	DMVEDEE	-LTETARME	VRELLT	EYGRPG	DDIPVIRG	SSLGALNGEEKWVE		189
sp P33166	:	QMDGAILV	/SAADGPM	IPQTREHILI				-LLELVEME	VRDLLS	EYDEPG		SALKALEGDAEWEA		190
sp Q9Z9L6	:	QMDG <mark>G</mark> ILV\	/SA <mark>A</mark> DGPM	~	~ -	YLVVFLNKC	DMVDDEE	-LLELVEME	VRDLLS	EYDEPG	DDVPVIRG	SALKALEGDAEWEE		190
sp Q8ETY4	:	QMDGAILV	/ <mark>S</mark> A <mark>A</mark> DGPM	~	SRNVGVE	AFVVFLNKT	DMVDDEE	-LLELVEME	VRDLLT	EYDEPG	DDLPVIKG	SALKALEGVAEYEE		189
sp P64028	:	QMDGGILV	/SAADGPM	IPQTREHILI	SRNVGVF	ALVVFLNKV	DMVDDEE	-LLELVEME	VRDLLS	EYDEPG	DDVPVIAG	SALKALEGDAQYEE		189
sp Q5HIC7	:	QMDGGILV		IPQTREHILI		ALVVFLNKV	DMVDDEE	-LLELVEME	VRDLLS	EYDEPG	DDVPVIAG	SALKALEGDAQYEE		
sp P99152	:	QMDGGILV		IPQTREHILI			DMVDDEE	-LLELVEME	VRDLLS	EYDEPG		SALKALEGDAQYEE		189
sp Q6GJC0	:	QMDGGILV\	/SA <mark>A</mark> DGPM			ALVVFLNKV	DMVDDEE	-LLELVEME	VRDLLS	EYDEPG	DDVPVIAG	SALKALEGDAQYEE		189
sp Q6GBT9	:	QMDGGILV	/SA <mark>A</mark> DGPM	~	SRNVGVP	ALVVFLNKV	DMVDDEE	-LLELVEME	VRDLLS	EYDEPG	DDVPVIAG	SALKALEGDAQYEE		189
sp P64029	:	QMDG <mark>G</mark> ILV\	/SA <mark>A</mark> DGPM	IPQTREHILI	SRNVGVP		DMVDDEE	-LLELVEME	VRDLLS	EYDEPG	DDVPVIAG	SALKALEGDAQYEE		189
sp Q5HRK4	:	QMDG <mark>G</mark> ILV\		IPQTREHILI		PALVVFLNKV	DMVDDEE	-LLELVEME	VRDLLS	EYDEPG	DDVPVIAG	SALKALEGDAEYEQ		189
sp Q8CQ81	:	QMDGGILV	/SA <mark>A</mark> DGPM	IPQTREHILI	SRNVGVP		DMVDDEE	-LLELVEME	VRDLLS	EYDEPG	DDVPVIAG	SALKALEGDAEYEQ	KI:	189
sp Q81VT2	:	QMDG <mark>G</mark> ILV\	/ <mark>S</mark> A <mark>A</mark> DGPM	1PQTREHILI	L <mark>s</mark> rqvgvf	YIVVFLNKC	DMVDDEE	-LLELVEME	VR <mark>D</mark> LLS	EYGFPG	D <mark>DI</mark> PVI <mark>K</mark> G	SALKALQGEADWEA	KI :	189
sp Q814C4	:	QMDG <mark>G</mark> ILV\	/ <mark>S</mark> A <mark>A</mark> DGPM	IPQTREHILI	S <mark>RQVG</mark> VF	YIVVFLNKC	DMVDDEE	-LLEL <mark>V</mark> EME	VR <mark>D</mark> LLS	EYGEPG	D <mark>DI</mark> PVI <mark>k</mark> G	SALKALQGEADWEA	KI :	189
sp   Q8Y422	:	QMDGAILV\	/ <mark>S</mark> A <mark>A</mark> DGPM	IPQTREHILI	L <mark>S</mark> RQVG <b>V</b> F	YIVVFMNKC	DMVDDEE	-LLELVEME	IRDLLT	EYEFPG	D <b>DI</b> PVI <b>K</b> G	SALKALQGEADWEA	KI :	189
sp Q927I6	:	QMDGAILV	/ <mark>S</mark> A <mark>A</mark> DGPM	IPQTREHILI	S <mark>RQVG</mark> VF	YIVVFMNKC	DMVDDEE	-LLEL <mark>V</mark> EME	IRDLLT	EYEFPG	D <mark>DI</mark> PVI <mark>k</mark> G	SALKALQGEADWEA	KI :	189
sp 050306	:	QMDGAILV	/ <mark>S</mark> A <mark>A</mark> DGPM	IPQTREHILI	S <mark>RQVGV</mark> F	YIVVFLNKC	DMVDDEE	-LLEL <mark>V</mark> EME	VR <mark>D</mark> LLS	EYDFPG	D <mark>EV</mark> PVI <mark>K</mark> G	SALKALEGDPKWEE	KI :	189
sp Q877L9	:	QMDGAILV	/ <mark>S</mark> A <mark>A</mark> DGPM	IPQTREHILI	ASRVGVE	HIVVFLNKA	ADQVDDAE	-LIELVEME	VRELMN	IEYG <b>F</b> PG	d <mark>da</mark> pvv <mark>v</mark> g	SALKALENPEDDAATQ	CI :	191
sp Q97EH5	:	QMDGAILV	/ <mark>S</mark> a <mark>a</mark> dgpm	IPQTREHILI	ASRVGVE	YIVVFLNK <mark>A</mark>	AD <mark>Q</mark> VDDPE	-LI <mark>D</mark> L <mark>V</mark> EME	VRELL <mark>N</mark>	EYGEPG	D <mark>DT</mark> PIV <mark>V</mark> G	SALKALQNPDDAEAIK	P <b>I</b> :	191
sp Q8XFP8	:	QMDGAILV(	CS <mark>A</mark> ADGPM	IPQTREHILI	LSSRVGVD	HIVVFLNKA	DMVDDEE	-LLEL <mark>V</mark> EME	VRELLS	EYNEPG	D <mark>DI</mark> PVI <mark>K</mark> G	SAL <mark>V</mark> ALENPTDEAATA	CI :	191
sp Q8R7V2	:	QMDGAILV	/ <mark>S</mark> a <mark>a</mark> dgpm	IPQTREHILI	<mark>a</mark> rqvg <b>v</b> f	YIVVFLNK <mark>A</mark>	DMVDDPE	-LI <u>E</u> L <mark>V</mark> EME	<b>V</b> RDLLN	IQYEFPG	D <mark>DT</mark> PIV <mark>V</mark> G	SALKALECGCGKRECQWCG	KI:	194
sp Q5SHN6	:	QMDGAILV	/ <mark>S</mark> a <mark>a</mark> dgpm	IPQTREHILI	<mark>a</mark> rqvg <b>v</b> f	YIVVFMNK <mark>V</mark>	DMVDDPE	-LL <mark>DLV</mark> EME	<b>V</b> RDLLN	IQYEFPG	D <mark>EV</mark> PVI <mark>R</mark> G	SALLALEQMHRNP-KTRRGENEWVD	KI:	199
sp P60338	:	QMDGAILV	/ <mark>S</mark> a <mark>a</mark> dgpm	IPQTREHILI	<mark>a</mark> rqvg <b>v</b> f	YIVVFMNK <mark>V</mark>	DMVDDPE	-LL <mark>DLV</mark> EME	<b>V</b> RDLLN	IQYEFPG	D <mark>EV</mark> PVI <mark>R</mark> G	SALLALEQMHRNP-KTRRGENEWVD	KI:	199
sp Q01698	:	QMDGAILV\	/ <mark>S</mark> A <mark>A</mark> DGPM	IPQTREHILI	<mark>a</mark> rqvgvf	YIVVFMNK <mark>V</mark>	DMVDDPE	-LL <mark>dlv</mark> eme	<b>V</b> RDLLN	IQYEFPG	D <mark>EV</mark> PVI <mark>R</mark> G	SALLALEEMHKNP-KTKRGENEWVD	KI :	199
sp   Q9R342	:	QMDGAILV	/ <mark>SSA</mark> DGPM	IPQTREHILI	<mark>a</mark> rqvg <b>v</b> f	YIVVFMNKV	DMVDD <mark>EE</mark>	-LLEL <mark>V</mark> EME	VR <mark>E</mark> LLS	KYEFPG	D <mark>DL</mark> PVV <mark>K</mark> G	SALRALEALQSNP-KMARGTDKWVD	YI :	200
sp P33168	:	QMDGAILV\	/SSADGPM	IPQTREHILI	a <mark>rqvg</mark> vf	YIVVFMNKV	DMVDDEE	-LLELVEME	VRELLS	KYEFPG	D <mark>DL</mark> PVI <mark>K</mark> G	SALQALE <mark>ALQANP-KTARGEDKWVD</mark>	RI :	200
sp   P26184	:	QMDGAILV\	/ <mark>S</mark> a <mark>a</mark> dgpm	IPQTREHILI	a <mark>rqvg</mark> vf	SIVVFMNKC	DMVDDEE	-LLELVELE	IRDLLN	TYEFPG	D <mark>DI</mark> PIIKG	SALQALENAEDEE-KTK	C <b>i</b> :	191
sp Q8YP63	:	QMDGAILV\	/AA <mark>T</mark> DGPM	IPQTREHILI	akqvg <mark>v</mark> p	KLVVFLNKE	DMMEDAE	-LLEL <mark>V</mark> ELE	LRELLT	EYEFDG	DDIPIVRG	SGLQALEVMTKNP-KTQRGENPWVD	KI :	199
sp P50064	:	QMDGAILV\	/SA <mark>A</mark> DGPM	IPQTREHILI	<mark>a</mark> rqvg <b>v</b> f	NIVVFLNKK	DQLDDPE	-LLELVELE	VRELLS	KYDFPG	D <mark>DV</mark> PIV <mark>A</mark> G	SALMALEKMASEP-KLIRGKDDWVD	CI :	199
sp P18668	:	QMDGAILV\	/SA <mark>A</mark> DGPM	IPQTREHILI	a <mark>kqvg</mark> vp	NIVVFLNKE	DMVDDAE	-LLELVELE	VRELLS	SYDFPG	D <mark>DI</mark> PIV <mark>A</mark> G	SALQALE <mark>AIQGGA-SGQKGDNPWVD</mark>	KΙ :	199
sp P33171	:	QMDGAILV\	/ <mark>S</mark> A <mark>A</mark> DGPM	IPQTREHILI	a <mark>kqvg</mark> vf	NIVVFLNKE	DMVDDAE	-LLELVELE	VRELLS	SYDEPG	DDIPIVAG	SALQALE <mark>AIQGGA-SGQKGDNPWVD</mark>	KI :	199
sp P13552	:	QMDGAILV\	/SA <mark>A</mark> DGPM	IPQTREHILI	a <mark>kqvg</mark> vp	SIVVFLNKA	DMVDDEE	-LLELVELE	VRELLS	SYDFPG	D <mark>DI</mark> PIV <mark>S</mark> G	SALKALDFLTENP-KTTRGENDWVD	KΙ :	199
													_	

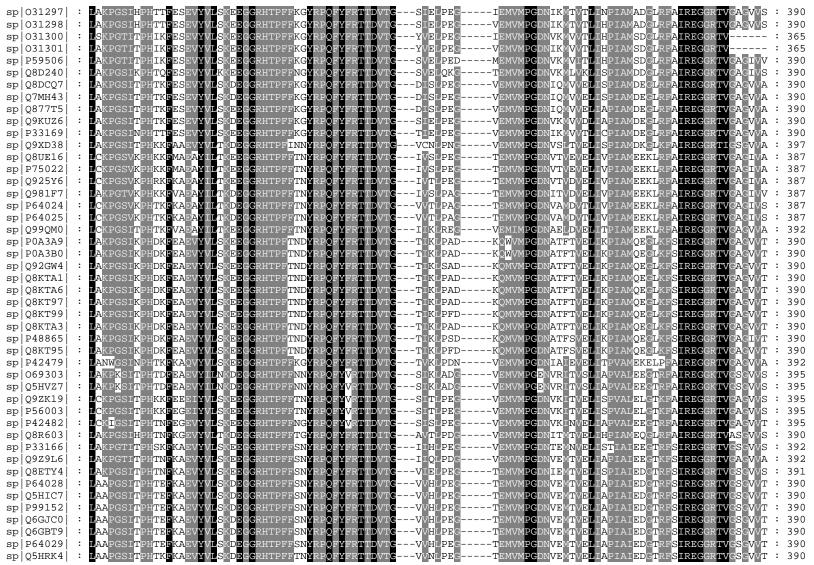


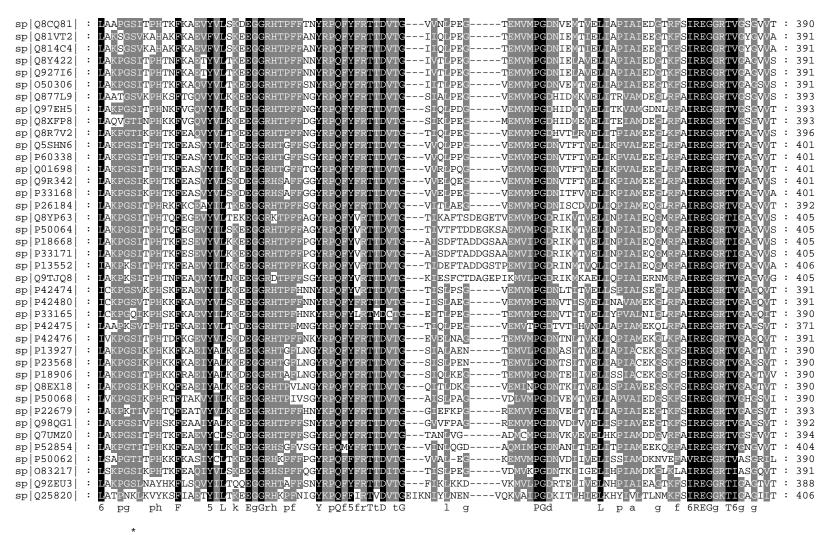












sp | P40174 | : K NK-- : 397 sp | Q53871 | : K NK-- : 397 sp | P29542 | : K VK-- : 397

```
sp|033594| : KITK-- : 397
sp|P95724| : KINK-- : 397
sp | P29543 |
           : RIVK-- : 397
           : KILK-- : 397
sp | P72231 |
sp|Q6ACZ0| : KIIN-- : 397
sp | P09953 |
           : KITK-- : 396
           : KITA-- : 397
sp | P42471 |
sp | P0A559 |
           : KIIK-- : 396
           : KIIK-- : 396
sp | P0A558 |
sp | P30768 |
           : KIIK-- : 396
sp | P42439 |
           : KIIK-- : 396
           : AVE--- : 392
sp | P40175 |
sp | P29544 |
           : ALV--- : 389
sp | 066429 |
           : KILD-- : 405
sp | 050293 |
           : KILD-- : 405
           : EIIE-- : 399
sp | 050340 |
           : EVIE-- : 400
sp|P13537|
sp|P42472| : KILD-- : 382
           : EIIA-- : 400
sp | P42477 |
sp | Q9PK73 |
           : KIIA-- : 393
           : KIIA-- : 393
sp | P26622 |
sp | Q9Z9A7 |
           : KINA-- : 393
           : KIIA-- : 393
sp|Q822I4|
sp | P64031 |
           : EIEA-- : 398
sp | P33170 |
           : EIEA-- : 398
           : EIEA-- : 398
sp | Q8K872 |
sp|Q5XD49| : EIEA-- : 398
sp|P69952|
           : EIEA-- : 398
           : EIEA-- : 398
sp Q8P1W4
           : EIEA-- : 398
sp | P72483 |
sp Q9CEI0
           : EIKA-- : 395
sp Q88VE0
           : EIDD-- : 395
sp | Q8KAH0 |
           : KIVE-- : 393
sp | P42473 |
            : KIVE-- : 393
           : KIIE-- : 397
sp | Q88QP8 |
sp | Q889X3 |
           : KIIA-- : 397
           : KIIE-- : 397
sp|P09591|
sp Q8PC59
           : KIIK-- : 396
sp | Q8NL22 |
           : KIIK-- : 396
sp | Q9P9Q9 |
           : KVIG-- : 395
sp | Q8XGZ0 |
           : KIIE-- : 396
sp|P42481|
           : KIIE-- : 396
sp | P33167 |
           : KILD-- : 396
sp P64026 : SVIA-- : 394
sp|P64027| : SVIA-- : 394
sp|P48864| : SVIA-- : 394
```

```
sp|P0A6N3| : KVLS-- : 393
sp|POA6N2|
           : KVLS-- : 393
           : KVLS-- : 393
sp | POA6N1 |
           : KVLG-- : 393
sp POA1H6
sp|POA1H5|
           : KVLG-- : 393
sp Q83JC4
           : KVLG-- : 393
           : KVIA-- : 394
sp Q8ZJB2
sp | P57939 |
           : KIIK-- : 394
           : KIIK-- : 394
sp | P57966 |
sp | P43926 |
           : KIIK-- : 393
sp Q7TTF9
           : KIIK-- : 393
           : KVLL-- : 394
sp | 031297 |
sp | 031298 |
           : KVLV-- : 394
sp | 031300 |
           : ----- : -
sp|031301|
           : ----- : -
           : KVLQ-- : 394
: KIIV-- : 394
sp|P59506|
sp | Q8D240 |
sp Q8DCQ7
           : KIFA-- : 394
           : KIFA-- : 394
sp | Q7MH43 |
sp | Q877T5 |
           : KIFE-- : 394
           : KIIA-- : 394
sp Q9KUZ6
sp|P33169|
           : KIIA-- : 394
sp|Q9XD38|
           : EITE-- : 401
sp Q8UE16
           : SIVE-- : 391
           : SIVE-- : 391
sp | P75022 |
           : SIVE-- : 391
sp | Q925Y6 |
sp|Q981F7|
           : TIKE-- : 391
sp|P64024|
           : SIIE-- : 391
           : SIIE-- : 391
sp | P64025 |
sp | Q99QM0 |
           : KIVE-- : 396
sp POA3A9
           : KINN-- : 394
sp POA3B0
           : KINN-- : 394
sp | Q92GW4 |
           : KINN-- : 394
sp | Q8KTA1 |
           : KINN-- : 394
           : KINN-- : 394
sp | Q8KTA6 |
sp Q8KT97
           : KINN-- : 394
           : KINN-- : 394
sp | Q8KT99 |
sp Q8KTA3
           : KINN-- : 394
sp|P48865|
           : KINN-- : 394
sp | Q8KT95 |
           : RINN-- : 394
sp | P42479 |
           : DIIA-- : 396
sp|069303|
           : KIIK-- : 399
           : KIIK-- : 399
sp Q5HVZ7
sp|Q9ZK19| : NIIE-- : 399
sp|P56003| : NIIE-- : 399
sp|P42482| : KITK-- : 399
```

```
sp|Q8R603| : EITK-- : 394
          : TITE-- : 396
sp|P33166|
           : SIQK-- : 396
sp | Q9Z9L6 |
          : SIQK-- : 395
sp Q8ETY4
sp|P64028|
          : EIIK-- : 394
sp Q5HIC7
           : EIIK-- : 394
           : EIIK-- : 394
sp | P99152 |
sp Q6GJC0
           : EIIK-- : 394
sp Q6GBT9
           : EIIK-- : 394
sp | P64029 |
           : EIIK-- : 394
sp Q5HRK4
           : EIFE-- : 394
           : EIFE-- : 394
sp | Q8CQ81 |
sp|Q81VT2|
           : TIVE-- : 395
sp|Q814C4|
          : TIVE-- : 395
sp | Q8Y422 |
          : NISK-- : 395
           : NISK-- : 395
sp|Q927I6|
          : EIIE-- : 395
sp|050306|
sp | Q877L9 |
          : EITE-- : 397
           : SIIE-- : 397
sp Q97EH5
sp Q8XFP8
           : SIIE-- : 397
           : AIIE-- : 400
sp | Q8R7V2 |
sp Q5SHN6
           : KILE-- : 405
           : KILE-- : 405
sp|P60338|
sp|Q01698|
           : KILE-- : 405
           : KVLE-- : 405
sp | Q9R342 |
          : KVLE-- : 405
sp|P33168|
sp|P26184|
          : EIVE-- : 396
sp|Q8YP63|
           : KIVK-- : 409
           : KILK-- : 409
sp | P50064 |
           : KILQ-- : 409
sp|P18668|
sp | P33171 |
           : KILQ-- : 409
sp | P13552 |
          : KILA-- : 410
sp|Q9TJQ8|
           : KILK-- : 409
           : KIIE-- : 395
sp | P42474 |
          : EILD-- : 395
sp|P42480|
sp|P33165| : EIID-- : 394
sp | P42475 |
          : EIK-- : 375
sp | P42476 |
           : EILK-- : 395
sp|P13927|
           : EVLE-- : 394
sp|P23568|
           : EVLE-- : 394
sp | P18906 |
          : EVLE-- : 394
sp|Q8EX18|
           : KVIK-- : 394
           : KTSN-- : 394
sp | P50068 |
sp | P22679 | : KILK-- : 397
sp|Q98QG1| : KILK-- : 396
sp|Q7UMZ0| : KILE-- : 398
```

```
sp|P52854| : KNIRII : 410
sp|P50062| : ELE-- : 394
sp|083217| : ELL-- : 395
sp|Q9ZEU3| : ELE-- : 392
sp|Q25820| : ELKN-- : 410
```

**Figure 1: Alignment of EF-Tu bacterial sequences.** 151 bacterial EF-Tu sequences aligned using GeneDoc. Black shows 100% identity, grey shows 80-100% identity and white is less than 100% identity. Species number and name are in order as they appear above below.

P40174-Streptomyces coelicolor

Q53871- Streptomyces collinus.

P29542- Streptomyces ramocissimus

O33594- Streptomyces aureofaciens

P95724- Streptomyces cinnamoneus

P29543 (EF-Tu 2)- Streptomyces ramocissimus

P72231-Planobispora rosea

Q6ACZ0- Leifsonia xyli

P09953- Micrococcus luteus

P42471- Brevibacterium linens

P0A559- Mycobacterium bovis

P0A558- Mycobacterium tuberculosis

P30768- Mycobacterium leprae

P42439- Corynebacterium glutamicum

P40175 (EF-Tu 3)- Streptomyces coelicolor

P29544 (EF-Tu 3) - Streptomyces ramocissimus

O66429- Aquifex aeolicus

O50293- Aquifex pyrophilus

O50340- Fervidobacterium islandicum

P13537- Thermotoga maritime

P42472- Chloroflexus aurantiacus

P42477- Herpetosiphon aurantiacus

Q9PK73- Chlamydia muridarum

P26622 - Chlamydia trachomatis

Q9Z9A7- Chlamydia pneumonia

Q822I4- Chlamydophila caviae

P64031- Streptococcus pneumonia

P33170- Streptococcus oralis

Q8K872- Streptococcus pyogenes serotype M3

Q5XD49- Streptococcus pyogenes serotype M6

P69952 - Streptococcus pyogenes serotype M1

Q8P1W4- Streptococcus pyogenes serotype M18

P72483- Streptococcus mutans

Q9CEIO- Lactococcus lactis subsp. Lactis

Q88VE0- Lactobacillus plantarum

Q8KAH0- Chlorobium tepidum

P42473- Chlorobium vibrioforme

Q88QP8- Pseudomonas putida

Q889X3- Pseudomonas syringae

P09591- Pseudomonas aeruginosa

Q8PC59 - Xanthomonas campestris

Q8NL22- Xanthomonas axonopodis

Q9P9Q9- Xylella fastidiosa

Q8XGZ0- Ralstonia solanacearum

P42481- Thiobacillus cuprinus

P33167- Burkholderia cepacia

P64026- Neisseria meningitidis serogroup A

P64027- Neisseria meningitidis serogroup B

P48864- Neisseria gonorrhoeae

P0A6N3- Escherichia coli O157:H7

P0A6N2 - Escherichia coli O6

POA6N1- Escherichia coli

P0A1H6- Salmonella typhi

POA1H5- Salmonella typhimurium

Q83JC4 - Shigella flexneri

Q8ZJB2- Yersinia pestis

P57939 (EF-Tu A)- Pasteurella multocida

P57966 (EF-Tu-B) - Pasteurella multocida

P43926- Haemophilus influenzae

Q7TTF9- Haemophilus ducreyi

O31297- Buchnera aphidicola subsp. Acyrthosiphon pisum

O31298- Buchnera aphidicola subsp. Schizaphis graminum

O31300- Buchnera aphidicola subsp. Melaphis rhois

O31301- Buchnera aphidicola subsp. Schlechtendalia chinensis

P59506- Buchnera aphidicola subsp. Baizongia pistaciae

Q8D240 - Wigglesworthia glossinidia brevipalpis

Q8DCQ7- Vibrio vulnificus

Q7MH43- Vibrio vulnificus (strain YJ016)

Q877T5- Vibrio parahaemolyticus

Q9KUZ6- Vibrio cholera

P33169 - Shewanella putrefaciens

Q9XD38- Leptospira interrogans

Q8UE16- Agrobacterium tumefaciens(strain C58 / ATCC 33970)

P75022- Agrobacterium tumefaciens

Q925Y6- Rhizobium meliloti

Q981F7- Rhizobium loti

P64024- Brucella melitensis

P64025- Brucella suis

Q99QM0 - Caulobacter crescentus

P0A3A9- Rickettsia rickettsii

POA3BO- Rickettsia sibirica

Q92GW - Rickettsia conorii

Q8KTA1- Rickettsia montana

Q8KTA6 - Rickettsia parkeri

Q8KT97- Rickettsia felis

Q8KT99 - Rickettsia helvetica

Q8KTA3- Rickettsia rhipicephali

P48865- Rickettsia prowazekii

Q8KT95 - Rickettsia typhi

P42479- Stigmatella aurantiaca

O69303- Campylobacter jejuni

P56003- Helicobacter pylori

P42482- Wolinella succinogenes

Q8R603- Fusobacterium nucleatum

P33166- Bacillus subtilis

Q9Z9L6- Bacillus halodurans

Q8ETY4- Oceanobacillus iheyensis

P64028- Staphylococcus aureus (strain Mu50 / ATCC 700699)

Q5HIC7- Staphylococcus aureus (strain COL)

P99152 - Staphylococcus aureus (strain N315)

Q6GJC0- Staphylococcus aureus (strain MRSA252)

Q6GBT9- Staphylococcus aureus (strain MSSA476)

P64029- Staphylococcus aureus (strain MW2)

Q5HRK4- Staphylococcus epidermidis (strain ATCC 35984 / RP62A)

Q8CQ81- Staphylococcus epidermidis (strain ATCC 12228)

Q81VT2- Bacillus anthracis

Q814C4- Bacillus cereus

Q8Y422- Listeria monocytogenes

Q927I6- Listeria innocua

O50306- Bacillus stearothermophilus

Q877L9- Clostridium tetani

Q97EH5- Clostridium acetobutylicum

Q8XFP8- Clostridium perfringens

Q8R7V2- Thermoanaerobacter tengcongensis

Q5SHN6- Thermus thermophilus (strain HB8 / ATCC 27634 / DSM 579)

P60338- Thermus thermophilus

Q01698- Thermus aquaticus

Q9R342- Deinococcus radiodurans

P33168- Deinonema sp

P26184- Flexistipes sinusarabici

Q8YP63- Anabaena sp

P50064- Gloeobacter violaceus

P18668- Synechococcus sp (strain ATCC 27144 / PCC 6301 / SAUG 1402/1)

P33171- Synechococcus sp (strain PCC 7942)

P13552- Spirulina platensis

Q9TJQ8- Prototheca wickerhamii

P42474- Cytophaga lytica

P42480- Taxeobacter ocellatus

P33165- Bacteroides fragilis

P42475- Fibrobacter succinogenes

P42476- Flavobacterium ferrugineum

P13927- Mycoplasma genitalium

P23568 - Mycoplasma pneumonia

P18906- Mycoplasma gallisepticum

Q8EX18 - Mycoplasma penetrans

P50068- Ureaplasma parvum

P22679- Mycoplasma hominis

Q98QG1 - Mycoplasma pulmonis

Q7UMZ0- Rhodopirellula baltica

P52854- Treponema hyodysenteriae

P50062 - Borrelia burgdorferi

O83217- Treponema pallidum

Q9ZEU3- Apple proliferation phytoplasma

Q25820- Plasmodium falciparum